NASA CR 135133
R77AEG222

PRELIMINARY DESIGN STUDY OF ADVANCED MULTISTAGE AXIAL FLOW CORE COMPRESSORS

Final Report

by

D.C. Wisler, C.C. Koch, L.H. Smith, Jr.

GENERAL ELECTRIC COMPANY
AIRCRAFT ENGINE GROUP
CINCINNATI, OHIO 45215

Prepared For

National Aeronautics and Space Administration

February 1977
NASA Lewis Research Center
Contract NAS3-19444

1. Report No.	2. Government Accession No.	3. Recipient's Catalog No.
NASA CR-135133		

4. Title and Subtitle	5. Report Date
Preliminary Design Study of Advanced Multistage Axial Flow Core Compressors	February 1977
	6. Performing Organization Code

7. Author(s)	8. Performing Organization Report No.
D. C. Wisler, C. C. Koch, L. H. Smith, Jr.	R77AEG222
	10. Work Unit No.

9. Performing Organization Name and Address	11. Contract or Grant No.
General Electric Company Aircraft Engine Group Cincinnati, Ohio 45215	NAS 3-19444

12. Sponsoring Agency Name and Address	13. Type of Report and Period Covered
National Aeronautics and Space Administration Washington, D.C. 20546	Final May 1975 - January 1976
	14. Sponsoring Agency Code

15. Supplementary Notes

Project Manager, Robert S. Ruggeri
NASA - Lewis Research Center
Cleveland, Ohio 44135

16. Abstract

A preliminary design study was conducted to identify an advanced core compressor for use in new high-bypass-ratio turbofan engines to be introduced into commercial service in the 1980's. An evaluation of anticipated compressor and related component 1985 state-of-the-art technology was conducted. Based on this evaluation, a parametric screening study covering a large number of compressor designs was conducted to determine the influence of the major compressor design features on efficiency, weight, cost, blade life, aircraft direct operating cost, and fuel usage. The trends observed in the parametric screening study were used to develop three high-efficiency, high-economic-payoff compressor designs. These three compressors were studied in greater detail to better evaluate their aerodynamic and mechanical feasibility. Finally, a compressor was recommended for development that yields the best overall system performance potential and good overall system economic payoff.

17. Key Words (Suggested by Author(s))	18. Distribution Statement
Compressor Core Compressor Preliminary Design Multistage Axial Flow Compressor High-Bypass-Ratio Turbofan Engines	Unclassified - Unlimited

19. Security Classif. (of this report)	20. Security Classif. (of this page)	21. No. of Pages	22. Price*
Unclassified	Unclassified	93	

* For sale by the National Technical Information Service, Springfield, Virginia 22151

FOREWORD

This report was prepared by the Aircraft Engine Group of the General Electric Company, Cincinnati, Ohio, to document the results of a preliminary design study conducted to identify appropriate design parameters for an advanced core compressor to be used in high-bypass-ratio turbofan engines of the 1985 time period. Mr. Robert S. Ruggeri, NASA-Lewis Research Center, Fluid System Components Division, was Project Manager.

The authors wish to acknowledge the valuable contributions made to this program by various supporting organizations within the General Electric Company. In particular, appreciation is extended to Messrs. R.E. Neitzel and P.W. Vinson for their assistance in conducting the economic analysis utilized in this study, and to Messrs. F. W. Tegarden and J.D. Hennessey for their efforts in accomplishing the mechanical design and analysis studies.

TABLE OF CONTENTS

LIST OF FIGURES

LIST OF TABLES

SUMMARY

A preliminary design study was conducted to identify an advanced core compressor for use in new high-bypass-ratio turbofan engines to be introduced into commercial service in the 1980's. The initial phase of the study involved a forecast of projected 1985 state-of-the-art technology in compressor and engine system aerodynamic and mechanical design areas. The turbine inlet temperature levels projected for use in 1985 vintage engines lead to optimum thermodynamic cycles that require an overall pressure ratio of the order of 40:1. To achieve this overall pressure ratio, two types of core compressor configurations were studied: boosted 14:1 pressure ratio compressors driven by single-stage turbines and unboosted 23:1 pressure ratio compressors driven by two-stage turbines. Based upon the technology projections, a parametric screening study covering a large number of compressor designs was conducted in which the influence of major compressor design features on efficiency, weight, cost, blade life, aircraft direct operating cost and fuel usage was determined. Three high-efficiency, high-economic payoff compressors were developed using the trends observed in the parametric screening studies; these were then studied in detail to better evaluate their aerodynamic and mechanical feasibility.

Finally, a compressor configuration was selected which demonstrated the best performance potential and good overall system economic payoff. The design selected for development was a 10-stage 23:1 pressure ratio compressor offering the best combination of the following advantages: high efficiency, low operating cost, low fuel usage, and acceptable development risk. It was found that this compressor with its first stage removed would also be an attractive 14:1 pressure ratio candidate for a boosted engine.

INTRODUCTION

A preliminary design study was conducted under NASA Contract NAS3-19444 to identify appropriate design parameters for an advanced core compressor for use in new high-bypass-ratio turbofan engines to be introduced into commercial service in the 1980's. Although the core compressor in a modern turbofan engine is dwarfed in size by the high bypass ratio fan component, it remains a key element in the heart of the engine and has a large impact on system performance and operating cost. The high turbine inlet temperature levels projected for use in 1985 vintage engines lead to optimum thermodynamic cycles that require high overall pressure ratios, of the order of 40:1. The high pressure compressor component must produce the majority of this pressure ratio, and must do it efficiently and reliably. The compressor must also be designed so that engine surges will not occur in the operating envelope of the engine, even after thousands of hours of operation have led to some performance deterioration due to erosion, wear, etc. Because of the performance demands placed on the core compressor and the propulsion system's overall dependence on the compressor meeting its design requirements, it was considered essential that the compressor design selection be based on an extensive preliminary design study which incorporated an assessment of the projected state-of-the-art advancements in the appropriate time period. The preliminary design study, together with its findings and resulting recommendations, are described in this report.

AERODYNAMIC STUDIES

The aerodynamic studies phase of the program was structured to provide a systematic approach to the identification and selection of an optimum configuration for an Advanced Multistage Axial Flow Compressor (AMAC compressor). The effort was divided into five phases. First, the technology levels and ground rules used in the analytical design methods were selected to represent anticipated 1985 time period state of the art. Second, parametric screening studies were conducted to determine tradeoffs between compressor efficiency, size, weight, and cost. The range of design parameters studied varied from values typical of existing compressors, termed "conservative loading" designs, to those that would be used in very highly loaded compressors, termed "maximum loading" designs. The center point of the range was termed "nominal loading" designs. Third, based on the results of the parametric study, several high efficiency compressor configurations were specified. Fourth, a more detailed study of the three most promising compressors was conducted using axisymmetric calculations and off-design performance estimating procedures. Finally, an optimum configuration was recommended for the AMAC compressor. This configuration was judged to have a high economic payoff for use in an advanced commercial engine, represented a substantial advance in the state of the art, and had acceptable development risk.

METHODS AND GROUNDRULES FOR SCREENING STUDIES

The parametric screening studies were conducted consistent with certain groundrules that relate to engine system constraints and 1985 state-of-the-art technology projections. In order to express the aerodynamic technology projections quantitatively, it is first necessary to outline the aerodynamic analysis methods that were employed.

Efficiency Prediction and Stall Correlation Model

Preliminary design studies of advanced multistage compressors at the General Electric Company rely on a computerized procedure, identified as the Compressor Unification Study, to estimate both efficiency potential and stall pressure ratio potential. The efficiency prediction model is intended to indicate the potential peak efficiency of a well-designed compressor. It attempts to account for all known sources of loss except for those due to off-design operation, blading unsuited for the aerodynamic environment, or poor hardware quality. The losses are grouped into four sources: (1) end-wall boundary layers and end-wall region secondary flows and leakage flows; (2) blade surface profile drag; (3) shocks on the blading; and, (4) part-span shrouds. End-wall losses have been determined from hub and casing boundary layer measurements made on a number of multistage, low speed, research compressor configurations. These losses are related to aspect ratio, solidity, stagger, tip clearance, blade row axial spacing, and aerodynamic loading level. Blade surface profile losses are related to suction surface diffusion,

blade maximum thickness and trailing edge thickness, Reynolds number, surface roughness, Mach number, and streamtube contraction. The shock loss model relates passage shock losses to inlet and exit Mach numbers and relates leading edge bow shock losses to inlet Mach number and leading edge thickness. The model for part-span shroud losses is based on measured shroud drag coefficients.

A detailed description of this efficiency model and some comparisons showing the capability of the model to predict the efficiency of multistage compressors is given in Reference 1. In most cases, the efficiency predicted by the model agrees with the efficiency determined from test data within one point.

The stall pressure ratio prediction method is based upon two groups of background data. The first group consists of the measured stall pressure rise capabilities of a large number of low speed repeating stages covering a wide range of stage geometries. These experimental results are expressed as a stall pressure rise coefficient, which is related to stage geometry parameters by a correlation. The second group of background data is from high speed multistage compressors. These data are presented in the form of a ratio, called effectivity, of an individual stage pressure rise coefficient measured at design speed stall to that predicted by the low speed data correlation. The average values of effectivity for multistage compressors lie generally in the range of 0.88 to 0.96. The best average effectivity ever obtained for a high pressure ratio multistage compressor is 0.99. To date, the General Electric Company is not aware of any multistage compressor data from any source to indicate that an average effectivity greater than this value has been achieved.

In applying the stall prediction method to a new design, certain stage geometry parameters and appropriate effectivities are specified, and the correlation is used to deduce the pressure rise coefficient of each stage. Other input quantities are the distributions of axial velocity and stator exit flow angle at the design speed stall point, the airflow, pitchline radii, and an estimated speed. The computer program calculates the stage pressure ratios, stacks the stages to give an overall pressure ratio, and adjusts the speed until the desired overall pressure ratio is obtained. Hub and tip radii consistent with these results and other quantities of interest are then calculated.

Technology Groundrules

The levels of technology assumed in predicting the stall margin capability and efficiency potential for advanced multistage compressors of the 1985 time period are presented in the following discussion.

Efficiency Prediction - Technology advancements leading to efficiency improvements can be classified as either aerodynamic or mechanical. Aerodynamic advancements result from the discovery of improved airfoil shapes and flowpath contours, and mechanical advancements result from such features as reduced clearances and improved surface finish. Both types of advancements were assumed for this study; the aerodynamic advancement element is described below and the mechanical advancements are described in a later section, Mechanical Design Studies.

Of the four aerodynamic loss sources previously identified, it was judged that only the end-wall loss source is likely to be reduced by any meaningful amount in the next few years. Profile losses are already quite low in well-designed and well-matched compressors that are represented by the current efficiency potential model. The shock loss model used in the study also represents the loss levels of the most efficient transonic/supersonic stages. The part-span shroud loss model is relatively unimportant because most of the configurations studied did not employ such shrouds.

For this study, it was assumed that the end-wall loss was 15 percent lower than that yielded by the model at any given tip clearance level. Research efforts currently underway and anticipated in the near future should provide the knowledge needed to achieve this loss reduction.

The efficiency model discussed so far has been concerned with losses in the compressor blading only. Since the exit Mach number is a parameter that was varied, it was necessary to predict the diffuser losses and the diffuser length needed to reduce the Mach number to the level required by the combustor. Size and performance estimates for an advanced split-flow diffuser were made as functions of the Mach number (based on an effective-area coefficient of 0.9) at the compressor outlet guide vane exit. These estimates were done as part of the compressor aerodynamic design studies in order to determine the length and performance of all compressors on the basis of the same (0.06) combustor inlet Mach number.

Inlet guide vane losses were incorporated by employing a loss coefficient (based on exit dynamic pressure) that increased with deflection angle from a value of 0.035 at zero deflection to 0.050 at 20 degree deflection. This increase was in accordance with the trend of two-dimensional cascade data. In addition to the inlet guide vane loss model, core compressor inlet duct pressure loss and length correlations were also utilized. These duct correlations were consistent with General Electric experience.

Stall Prediction - In order to carry out the study, it was necessary to establish design-point stall margin values. For many military applications, considerable stall margin is required to handle the large inlet distortions that can result from high angle-of-attack operation, off-design operation of supersonic inlets, armament firing, etc. These distortions can occur while the compressor is operating at high corrected speed, and high stall margin must therefore be provided at this operating speed. Subsonic commercial transport engines do not experience such severe distortions and, therefore, lower values of high speed stall margin may be employed. It is believed that 15 percent stall margin will be adequate for most commercial transport applications at high corrected speeds. However, part-speed stall margin requirements for commercial transport engines are similar to those of military engines for starting and rapid acceleration of the engine. In fact, commercial transport requirements may be more stringent than military requirements because the longer service life of a commercial compressor ultimately leads to its operation with deteriorated performance due to blade and casing erosion. Experience has shown that a part speed stall margin above the steady-state operating line of 25 to 30 percent is needed to assure satisfactory engine operation in the 70 percent airflow region of the compressor map. A cursory stability analysis, conducted concurrently with this study, confirmed that this stall margin level is reasonable for 1985 commercial engines.

Since the parametric screening studies were carried out at the high speed design point, it was necessary to specify sufficient stall margin at that point to assure that adequate stall margin is available for part-speed operation. A review of General Electric experience indicated that the amount of design speed stall margin specified should not be the same for all compressors. This was concluded because plots of stall pressure ratio versus percent design airflow differ for different compressors. Although many design variables affect the stall line shape on such a plot, there is a general tendency for the stall line to be higher at intermediate airflows for compressors that have low solidities, low radius ratios, increasing hub radii through the compressor, and somewhat reduced effectivities in the front stages as well as in the front stages of the fixed rear block.* Since these are similar to the characteristics of the conservative loading compressors of this study, it follows that the design point stall margin of the conservative loading compressors can be less than those of the nominal and maximum loading compressor types so that all three compressor types have the same part-speed stall margin.

In view of the foregoing discussion, and relying on past experience to aid in selecting numerical magnitudes, the following values were selected for use in the screening studies:

Parameter	Maximum Loading Compressors	Nominal Loading Compressors	Conservative Loading Compressors
Design Point Stall Margin, %	22	19	16
Average Stall Effectivity	0.975	0.950	0.925

The stall effectivity distributions through the compressors used in this study had a minimum value for the first stage and a maximum value of 0.99 for the rear stages. As the loading level was increased, the effectivity of the front stages was increased, resulting in the higher values of average stall effectivity for the maximum loading designs.

Casing treatment was considered as a possible means for increasing effectivity levels. However, at present, there is no hard evidence that casing treatment is capable of increasing the average stall effectivity of a multistage compressor beyond the levels employed in this study. Also, it seems likely that if it were found that the use of casing treatment could improve stall effectivity, it would also be found that such treatment would cause an efficiency penalty. This would probably be an unfavorable trade for the compressors of this study.

*The fixed rear block is that group of stages whose rotors are not preceded by variable stators.

Design Constraints - The compressor parametric design studies were subject to several mechanical design constraints. A minimum core compressor inlet hub radius of 16.51 cm (6.50 inches) in the 147,000 n (33,000 lb) thrust engine study size was established in order to permit the low pressure compressor (fan) drive shaft to pass through the center of the core compressor with sufficient clearance for bearings, core compressor structure, etc. A maximum physical rear stage hub speed of 381 m/sec (1250 ft/sec) was established as an upper limit for the parametric screening study. Indications are that above this speed, elaborate rotor cooling schemes of very massive structures would be required for structural integrity. This constraint was later relaxed in the detailed study phase, and the weight and cost penalties of high rim speeds were factored into the analysis. A maximum physical speed of 17,000 rpm was established as an upper limit based upon high pressure turbine stress considerations.

The ground rule used to estimate axial spacing between blade and vane rows was based on General Electric experience. The axial spacing required to avoid blade interference due to blade deflections was assumed to be a function of the rotor blade height of the stage and the stage number, as long as the axial spacing was greater than some minimum spacing. This minimum value was set to avoid blade interference caused by differential thermal growth of rotors and stators, and was made a function of compressor overall length. For compressors in the 32-45 kg/sec (70-100 lbm/sec) corrected flow size used in this study, the absolute minimum allowable spacing was assumed to be 0.635 cm (0.25 inch) in order to provide room for necessary structural details such as rotor blade retainers.

PARAMETRIC SCREENING STUDIES

A series of preliminary compressor aerodynamic designs was carried out in which key parameters were varied systematically in order to determine the trade-offs between compressor efficiency, size, weight, cost, life, etc. The parametric studies were conducted in three parts. The first part defined three compressor designs for each of two levels of total pressure ratio, 14:1 and 23:1. These three designs were a nominal loading compressor, a maximum loading compressor, and a conservative loading compressor. In the second part of the parametric study, the nominal loading 14:1 pressure ratio compressor was used as a center point. Each significant design parameter which defined the compressor was varied in two steps, one in the direction of a maximum loading configuration and the other in the direction of a conservative loading configuration. In the third part of the parametric evaluation, the trends determined from the earlier cases were used to guide the parameter selections for designs that focused on one particular characteristic, such as long life. Since compressor efficiency was found to be an important parameter affecting economics, additional studies were carried out in an attempt to maximize efficiency. These studies are presented in a later section, Further Studies of High Efficiency Compressors.

Parameters and Range of Parameters Studied

The most important design variables that define the compressor and affect its performance are aspect ratio, solidity, swirl angle (reaction), exit Mach number, inlet flow/annulus area, inlet radius ratio, flowpath shape, and number of stages. Values of these design variables selected to define maximum loading, nominal loading, and conservative loading

compressors for each of the two levels of total pressure ratio are listed in Table I. Tip speed is not listed because it is determined by the stall margin requirement rather than being a direct design specification.

The nominal values of aspect ratio, solidity, and stator exit flow angle (middle column of Table I) are generally consistent with those used previously in General Electric high-stage-loading compressors. Values in the maximum loading column were chosen as a set of extremes aimed at achieving a very high average stage pressure ratio. The conservative loading values were selected to represent compressors currently in service.

Stagewise distributions of aspect ratio, solidity, stator exit flow angle, and stalling axial velocity were established based on past experience and judgment. Generally, the trends of aspect ratio, solidity, and flow angle for the conservative loading compressors are consistent with those of the CF6 compressors, while the trends of these variables for the nominal loading compressors are consistent with those of General Electric high-stage-loading compressor designs. For each design type, the average of the rotor and stator stagewise distributions of each parameter is equal to the average value of that parameter listed in Table I for the configuration. From general considerations of structural adequacy, length and weight, the aspect ratios tend to decrease from the inlet to the outlet of a compressor, and this trend was modeled in the parametric study. Since aeromechanical considerations indicate that the first rotor aspect ratio cannot be much above 1.5 without shrouding, a part-span shroud was specified for this blade row in the conservative design and a substantially higher aspect ratio was employed. The distributions of rotor solidity generally had the highest solidities in the front stages where the relative Mach numbers were highest. The stator solidities were kept somewhat smaller than average in those front stages that were expected to be variable, and were highest in the rear stages where aerodynamic loadings were high due to axial velocity diffusion.

A stagewise distribution of stator exit flow angle that maintained a moderate level of rotor inlet Mach number and fairly low reaction ratios was chosen for the conservative loading design. The level of swirl increased to a maximum through the front half of the compressor, remained constant, and then decreased rapidly through the last few stages. The distribution for the nominal loading design had less variation and lower levels, leading to higher Mach numbers and reactions. A constant zero-level of swirl was used for the maximum loading design.

The stagewise distributions of stalling axial velocity for the maximum loading designs were characterized by an acceleration in stalling axial velocity through the first half of the compressor, estimated to provide a nearly constant axial Mach number at the design point, followed by a rapid diffusion in the last three stages. The nominal and conservative loading designs employed more moderate distributions with less average axial velocity diffusion per stage.

Results of Parametric Screening Studies

A detailed listing of key aerodynamic and mechanical design parameters and economic analysis results for all three parts of the study is given in Table II. Configurations 1-3 in Table II are the basic 14:1 pressure ratio designs, and Configurations 20-22 are the

Table I. Design Parameters for Maximum Loading, Nominal Loading and Conservative Loading Compressors.

Parameter	Maximum Loading Compressor	Nominal Loading Compressor	Conservative Loading Compressor
Number of stages			
P/P = 14	6	9	12
P/P = 23	7	10	14
Average aspect ratio	1.0	1.5	2.25
Average solidity	1.8	1.35	0.9
Flow per annulus area, kg/sec m^2 (lbm/sec ft^2)	200 (41)	186 (38)	171 (35)
Exit Mach number	0.40	0.34	0.28
Average stator exit flow angle, degrees	0	10	20
Inlet radius ratio	0.75	0.65	Min. hub radius = 16.5 cm (6.5 in)
Flowpath shape	Max. hub speed in rear stages 381 m/sec (1250 ft/sec)	Constant pitchline radius	Exit radius ratio = 0.91 (or constant hub radius)

Table II. Summary of Aerodynamic Desig

Configuration No.	Parameter Variation	Adiabatic Efficiency Incl. Diffuser Losses	Physical Speed, rpm	Corrected Tip Speed, m/sec (fps)	Rear Hub Speed (Phys.) m/sec (fps)	Lengt Rotor l to Diff Exit, m
I.	**Pressure Ratio 14:1 Configurations**					
1.	Conservative Loading 12-Stage	0.859	15,150	415 (1360)	336 (1101)	0.642 (2
2.	Maximum Loading 6-Stage	0.785	14,410	454 (1490)	381 (1250)	0.413 (
3.*	Nominal Loading 9-Stage	0.850	1?,510	385 (1263)	344 (1127)	0.554 (2
4.	Lower Aspect Ratio (1.0)	0.832	12,650	360 (1182)	321 (1053)	0.806 (
5.	Higher Aspect Ratio (2.25), 1st Stage With Part-Span Shroud	0.842	14,280	407 (1335)	363 (1191)	0.415 (1
6.	Higher Solidity (1.8)	0.845	12,810	365 (1197)	326 (1068)	0.563 (2
7.	Lower Solidity (0.9)	0.840	14,430	411 (1349)	367 (1203)	0.545 (2
8.	Lower Swirl (0°)	0.842	13,490	384 (1261)	342 (1124)	0.543 (2
9.	Higher Swirl (20°)	0.849	13,610	388 (1272)	346 (1134)	0.560 (2
10.	Higher Exit Mach. Number (0.4)	0.846	13,250	377 (1238)	338 (1109)	0.566 (
11.	Lower Exit Mach Number (0.28)	0.856	14,000	399 (1309)	354 (1160)	0.555 (2
12.	Higher Flow per Annulus Area (200 (41))	0.842	13,350	376 (1232)	339 (1113)	0.529 (2
13.	Lower Flow per Annulus Area (171 (35))	0.855	13,750	398 (1305)	350 (1147)	0.579 (
14.	Higher Inlet Radius Ratio (0.75)	0.844	11,240	369 (1210)	352 (1156)	0.461 (1
15.	Lower Inlet Radius Ratio (min. Radius Hub)	0.853	14,940	397 (1304)	337 (1106)	0.620 (2
16.	High Rear Radius Ratio (max. hub speed)	0.845	11,820	337 (1105)	359 (1179)	0.509 (2
17.	Low Rear Radius Ratio (0.91)	0.847	15,590	444 (1457)	322 (1057)	0.594 (2
18c.	Maximum Efficiency 9-Stage	0.868	15,980	437 (1435)	374 (1227)	0.536 (2
19b.	Maximum Life 9-Stage	0.849	15,030	428 (1405)	311 (1019)	0.715 (2
24.	Nominal Loading 8-Stage	0.849	14,680	419 (1375)	374 (1226)	0.484 (1
25.	Nominal Loading 10-Stage	0.847	12,520	357 (1170)	318 (1043)	).633 (2
II.	**Pressure Ratio 23:1 Configurations**					
20.	Conservative Loading 14-Stage	0.844	14,360	492 (1615)	315 (1034)	0.937 (
21.	Maximum Loading 7-Stage	0.759	11,730	491 (1610)	381 (1250)	).473 (1
22.	Nominal Loading 10-Stage	0.831	11,320	428 (1404)	357 (1171)	0.626 (2
23.	Lightly Loaded Front Stage 9-Stage	0.822	14,540	474 (1555)	370 (1213)	0.612 (2
26b2.	Maximum Efficiency 11-Stage	0.856	13,340	457 (1500)	355 (1163)	0.767 (
26d5.	Maximum Efficiency 9-Stage	0.849	14,440	480 (1575)	393 (1290)	0.630 (

*(One-Parameter Variation Center Point)

†Transcontinental trijet aircraft mission (relative to STEDLEC Baseline Engine)

Aerodynamic Design Data for Parametric Variations.

ar Hub ed (Phys.) ec (fps)	Length Rotor 1 Inlet to Diffuser Exit, m (in.)	Inlet Tip Dia. m (in.)	No. of Blades & Vanes	Average Reaction	ΔWeight† kg (lb.)	ΔPrice† %	Δ Direct Operating Cost† %	ΔFuel† Usage %
(1101)	0.642 (25.3)	0.583 (22.9)	1523	0.69	25 (56)	0.3	-0.44	-0.41
(1250)	0.413 (16.2)	0.672 (26.4)	1511	0.83	16 (35)	0.4	1.08	3.83
(1127)	0.554 (21.8)	0.607 (23.9)	1827	0.69	-1 (-2)	0	-0.37	0.17
(1053)	0.806 (31.8)	0.607 (23.9)	1265	0.64	44 (98)	2.1	0.58	2.15
(1191)	0.415 (16.3)	0.607 (23.9)	2537	0.72	-13 (-29)	-0.4	0.01	0.34
(1068)	0.563 (22.2)	0.607 (23.9)	2648	0.65	0	0.7	0	0.79
(1203)	0.545 (21.5)	0.607 (23.9)	1198	0.73	5 (12)	-0.4	-0.24	0.70
(1124)	0.543 (21.4)	0.607 (23.9)	1827	0.82	2 (5)	0.2	-0.14	0.69
(1134)	0.560 (22.1)	0.607 (23.9)	1827	0.55	2 (4)	0.1	-0.33	0.21
(1109)	0.566 (22.3)	0.607 (23.9)	1837	0.67	2 (5)	0.4	-0.16	0.59
(1160)	0.555 (21.9)	0.607 (23.9)	1620	0.71	1 (3)	-0.2	-0.56	-0.26
(1113)	0.529 (20.8)	0.607 (23.9)	1911	0.67	-5 (-11)	0	-0.20	0.56
(1147)	0.579 (22.8)	0.616 (24.3)	1698	0.71	8 (17)	0.1	-0.45	-0.11
(1156)	0.461 (18.1)	0.697 (27.5)	2707	0.69	3 (6)	0.8	-0.19	0.08
(1106)	0.620 (24.4)	0.567 (22.3)	1462	0.68	15 (33)	-0.1	-0.51	-0.11
(1179)	0.509 (20.0)	0.607 (23.9)	2419	0.69	10 (23)	0.6	-0.27	-0.11
(1057)	0.594 (23.4)	0.607 (23.9)	1379	0.69	12 (27)	-0.3	-0.35	-0.30
(1227)	0.536 (21.1)	0.583 (23.0)	1626	0.75	20 (44)	-0.5	-0.78	-0.95
(1019)	0.715 (28.2)	0.607 (23.9)	1212	0.68	32 (71)	0.6	-0.38	-0.40
(1226)	0.484 (19.1)	0.607 (23.9)	1571	0.71	-2 (-5)	-0.7	-0.52	-0.02
(1043)	0.633 (24.9)	0.607 (23.9)	2010	0.64	12 (27)	1.0	0.06	0.96
(1034)	0.937 (36.9)	0.676 (26.6)	1597	0.69	89 (197)	6.0	0.92	-1.30
(1250)	0.473 (18.6)	0.825 (32.5)	2329	0.84	68 (151)	7.7	3.22	3.74
(1171)	0.626 (24.6)	0.753 (29.7)	2592	0.72	28 (63)	6.7	1.47	-0.51
(1213)	0.612 (24.1)	0.643 (25.3)	1747	0.73	45 (99)	4.8	0.88	-0.54
(1163)	0.767 (30.2)	0.676 (26.6)	2087	0.73	45 (100)	5.5	0.33	-2.41
(1290)	0.630 (24.8)	0.656 (25.8)	1839	0.74	38 (84)	3.9	0.14	-2.27

three basic 23:1 pressure ratio cases that constituted the first part of the study. Of the other designs tabulated, Configurations 4-17, 24, and 25 are cases in which the primary compressor design parameters were varied individually to values above and below those of Configuration 3, which is the nominal loading 14:1 pressure ratio configuration. These constituted the second part of the study. The maximum efficiency, maximum life, and lightly loaded front stage Configurations 18, 19, 23, and 26 represent the third part of the study. The efficiencies presented in the table include the diffuser losses and the tabulated lengths include the diffuser length. The efficiencies have also been adjusted for stage matching effects to recognize that some compromise in design-point efficiency will usually result when a compressor is designed and developed to best match the needs of the overall engine/aircraft system for a particular mission. The adjustment to those efficiencies calculated by the efficiency potential computer model involved an adiabatic efficiency reduction of 0.7 point for the 14:1 pressure ratio compressors and a reduction of 1.0 point for the 23:1 pressure ratio compressors. The mechanical design and economic analysis study methods are described in later sections of this report. Compressor weight and cost plus overall direct operating cost and fuel usage are given as delta values relative to the engine system and compressor described in a NASA/GE study program entitled, "Study of Turbofan Engines Designed for Low Energy Consumption" (STEDLEC), Reference 2.

Discussion of Loading Level Screening Studies

Flowpaths for the three basic 14:1 pressure ratio designs defined in the first part of the parametric screening study are shown in Figures 1 through 3. The three basic 23:1 pressure ratio compressor flowpaths were similar in appearance. As indicated in Table II, a primary result of this part of the study was that compressor efficiency, direct operating cost, and fuel usage can become very unfavorable if loading is increased to an extreme. Designs having the highest loadings (Configurations 2 and 21) were found to have no weight advantage, although they were much shorter, and their slightly lower cost did not offset the large efficiency penalties incurred.*

An unforeseen result from these loading level studies was that the conservative loading designs required higher tip speeds than the nominal loading designs in order to achieve the required stall margin. This resulted from specifying parameters that gave low values of allowable stage static-pressure-rise coefficient for these designs, combined with numbers of stages that were not particularly large.

Discussion of One-Parameter Variations

For the second part of the parametric study, the 14:1 pressure ratio, nine-stage, nominal design (Configuration 3) was used as a center point, and each significant design parameter defining the compressor was varied about this center in the direction of maximum loading and in the direction of conservative loading. A total of 16 one-parameter variations was made from this nominal design in which two other levels of aspect ratio, solidity, swirl angle, exit Mach number, inlet flow/annulus area, radius ratio, flowpath shape, and number of stages were studied. The results of the one-parameter variations are presented in Table II as Configurations 4 through 17 and Configurations 24 and 25.

*Subsequent studies carried out under part three of the parametric screening study suggest that a more favorable flowpath than that shown in Figure 3 could have been found for the maximum loading cases, but the efficiency penalty would still be substantial.

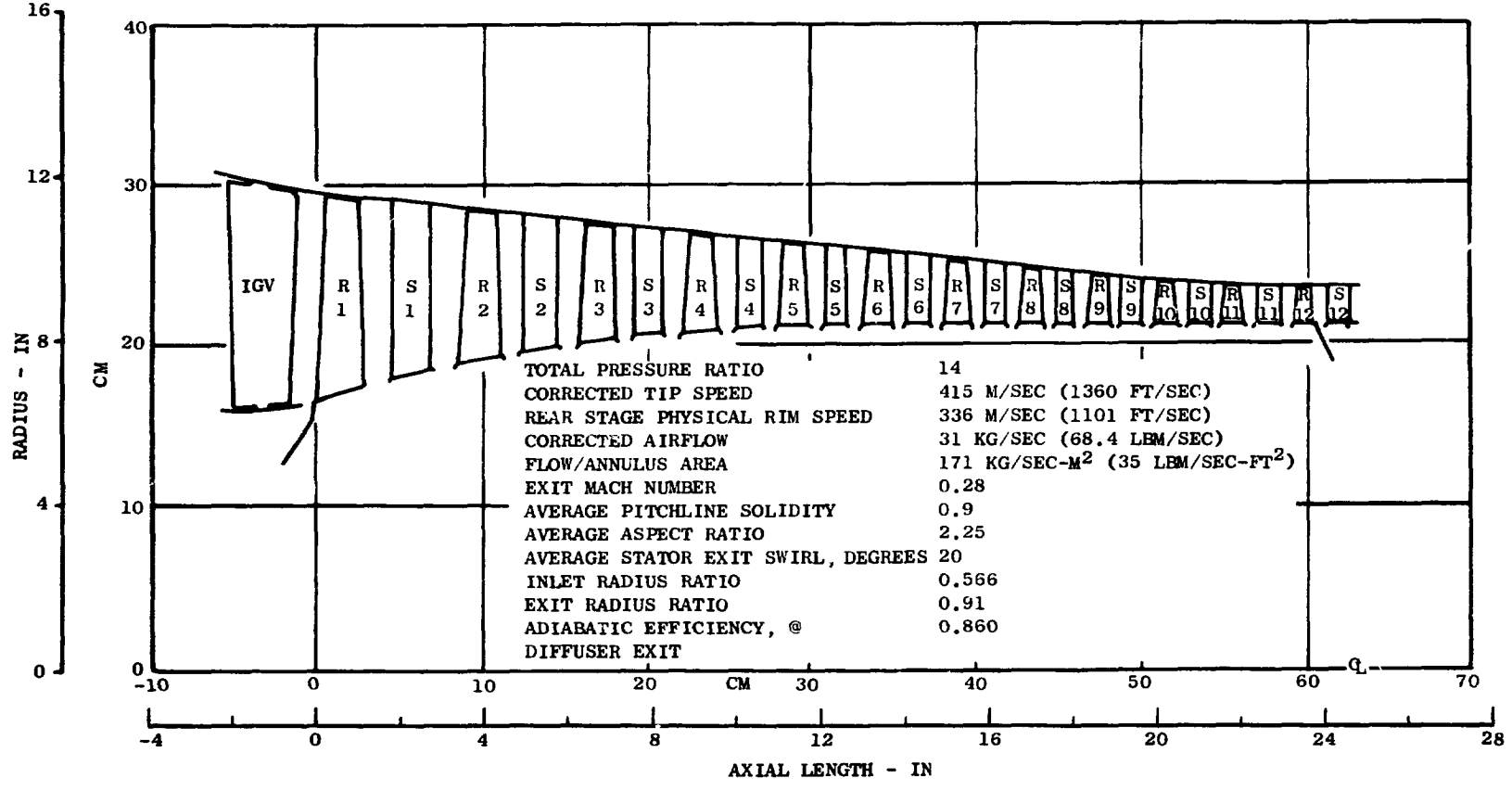

Figure 1 Conservative Loading Compressor Design, 14:1 Total-Pressure Ratio, Configuration No. 1

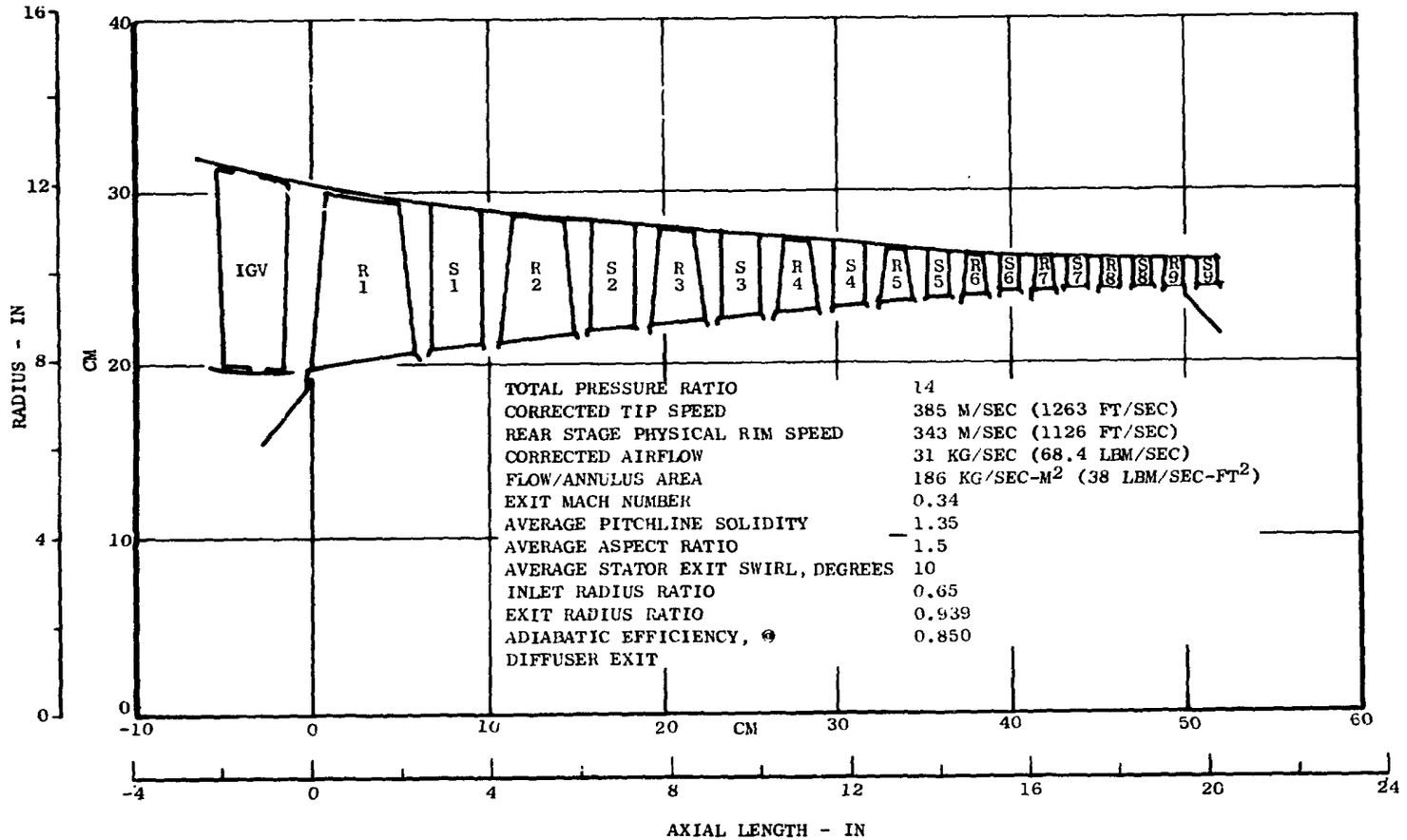

Figure 2 Nominal Loading Compressor Design, 14:1 Total-Pressure Ratio, Configuration No. 3

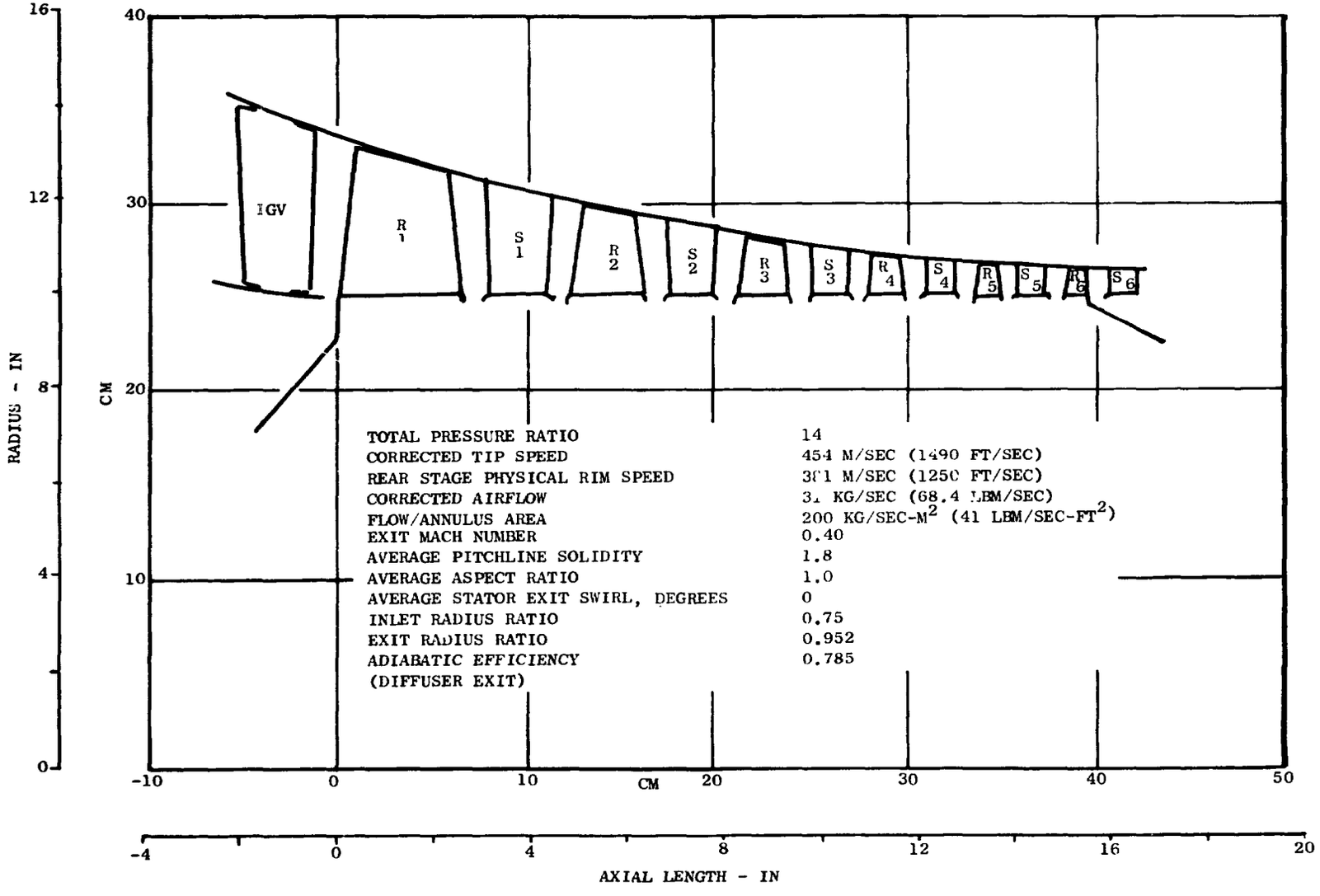

Figure 3 Maximum Loading Compressor Design, 14:1 Total-Pressure Ratio, Configuration No. 2

The results of varying the average aspect ratio (Figure 4) show that the best efficiency is obtained with average aspect ratios in the range from 1.3 to 2.0. Aspect ratios below and above this range lead to decreased efficiencies. As aspect ratio is increased, a corresponding increase in corrected tip speed is required to maintain stall margin. This raises Mach numbers, which causes the cascade losses to increase. At the same time, however, the higher blade speed leads to high-stagger blading which increases the passage aspect ratios* and decreases the end-wall losses. However, the improvement in end-wall losses at higher average aspect ratios is more than offset by declining cascade efficiencies. At low average aspect ratios, the increase in end-wall losses is sufficiently rapid as to more than offset a reduction in Mach-number-related losses at the lower tip speed. In addition, the low aspect ratio compressor is longer with increased weight and cost compared to the nominal design. All of these factors, when combined, indicate that the low aspect ratio compressor has a one percent higher direct operating cost and a two percent higher fuel usage than the nominal aspect ratio compressor.

The solidity variation results shown in Figure 5 suggest that near-nominal average solidities, ranging from 1.2 to 1.5, provide the best efficiency. As solidity is increased, the passage aspect ratio increases and end-wall losses are reduced. However, the resulting greater number of blades, with their associated wakes, decreases cascade efficiency. This occurs despite a reduction in tip speed. It appears that when the first stage rotor tip inlet relative Mach number is less than about 1.4, shock losses in the first stage have only a small effect on overall efficiency. For the remaining stages, cascade losses do not appear to be a strong function of tip speed. For solidities increasing from 0.9 to 1.2, the end-wall losses decrease faster than the cascade losses increase, which results in an overall efficiency improvement. For solidities larger than 1.5, the end-wall losses do not decrease so rapidly. Thus, the cascade losses increase faster than the end-wall losses decrease, which results in a decrease in overall efficiency. The reduced efficiency for both the low and high average solidity compressor designs is reflected in higher fuel usage and higher direct operating costs.

Swirl angle variation results are shown in Figure 6. The low swirl (high reaction) case suffers in efficiency with no other clear benefit. This reduced efficiency results from the higher rotor Mach numbers at the low swirl angles. Efficiency and the economic parameters appear to be best when average swirl angles from 9 to 20 degrees (reactions from 0.7 to 0.5) are used. The corrected tip speed, rear rim speed, length of the compressor, and total number of airfoils remained essentially unchanged as the average swirl angle was varied.

The results shown in Figure 7 indicate that a low value of compressor exit Mach number is desirable. As exit Mach number is increased from 0.28 to 0.4, the efficiency based on diffuser exit conditions continuously decreases. This results partly from higher diffuser losses. Also, as exit Mach number is increased, the blade height decreases, which increases end-wall losses by increasing the tip clearance/blade height ratio. Furthermore, the relatively high axial velocity/blade speed ratio associated with higher exit Mach numbers leads to somewhat reduced cascade efficiencies for the rear stages. Again, the consequences of lower efficiency are higher fuel usage and higher direct operating cost.

* Passage aspect ratio is defined as the blade height divided by the pitchline staggered spacing between blades.

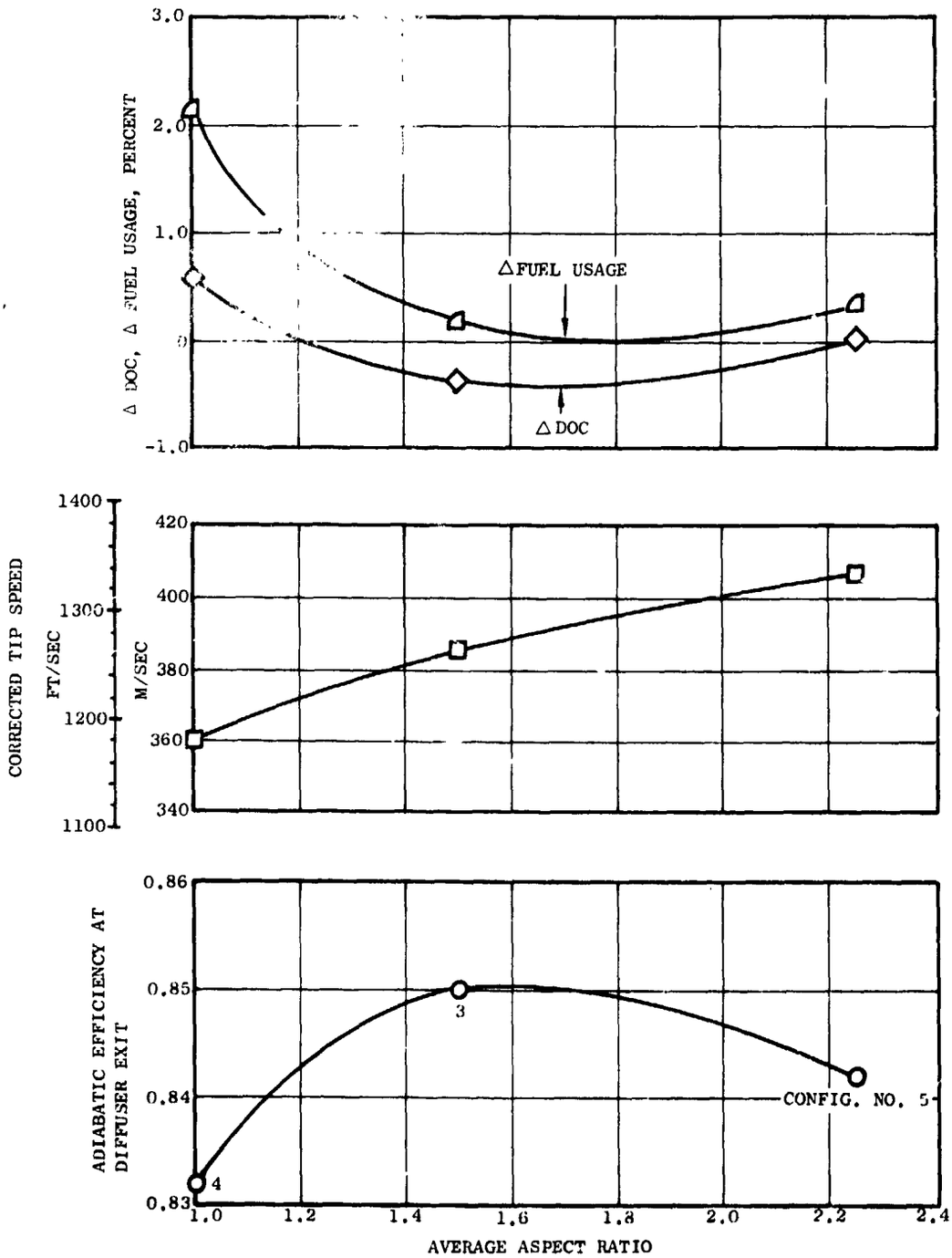

Figure 4 Variation in Direct Operating Cost, Fuel Usage, Tip Speed, and Compressor Efficiency with Aspect Ratio

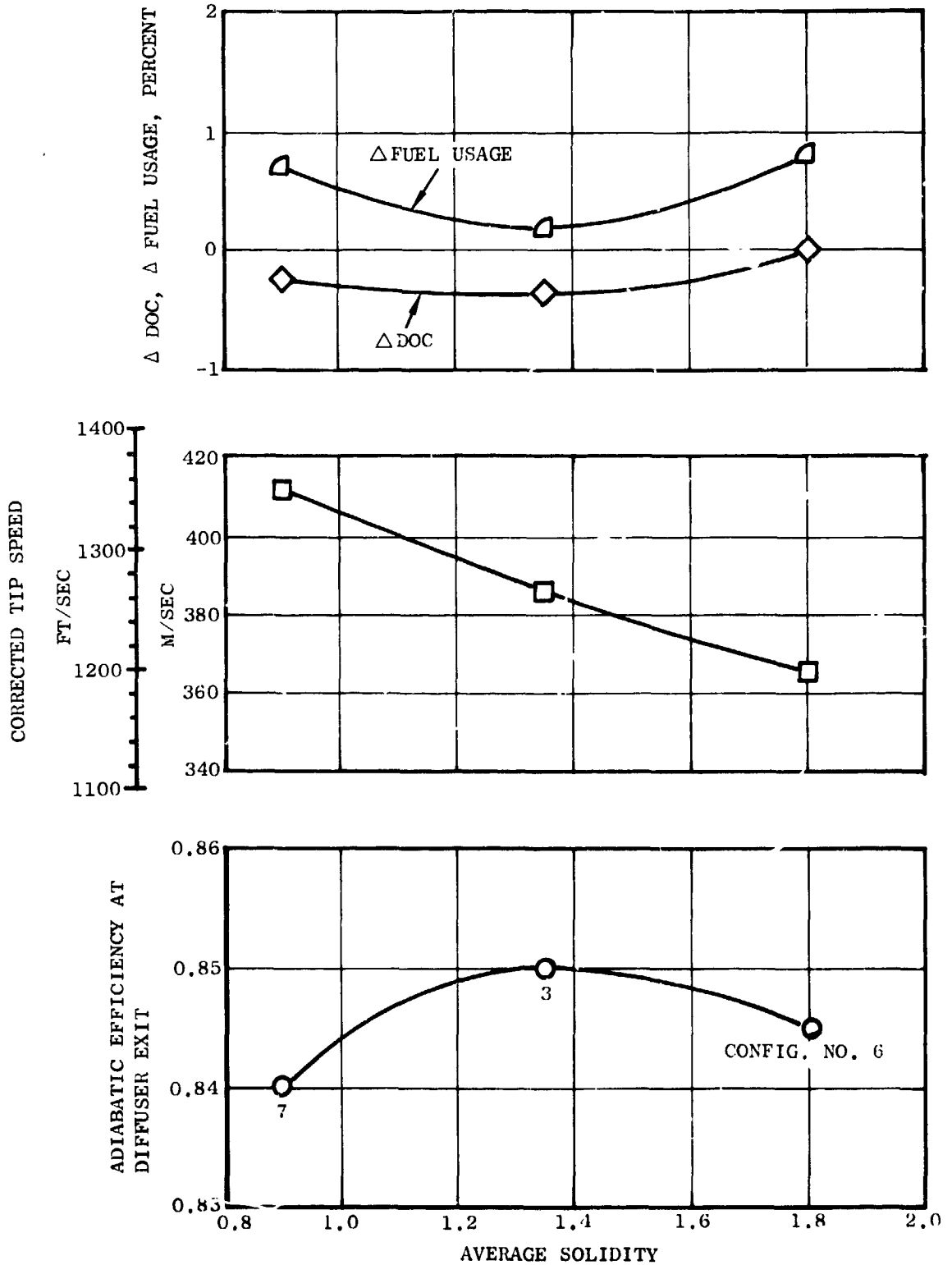

Figure 5 Variation in Direct Operating Cost, Fuel Usage, Tip Speed and Compressor Efficiency with Average Solidity

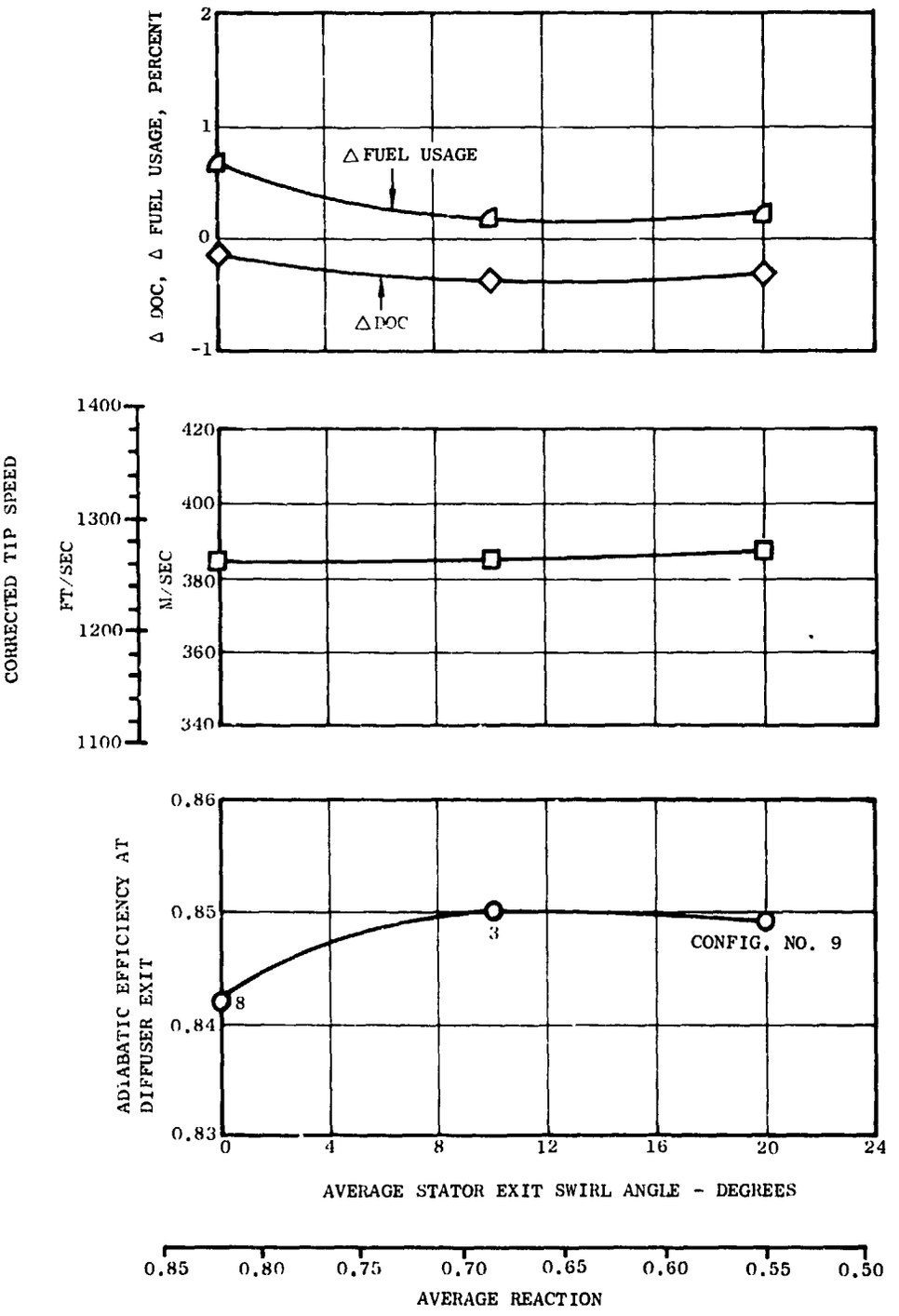

Figure 6 Variation in Direct Operating Cost, Fuel Usage, Tip Speed, and Compressor Efficiency with Average Stator Exit Swirl Angle

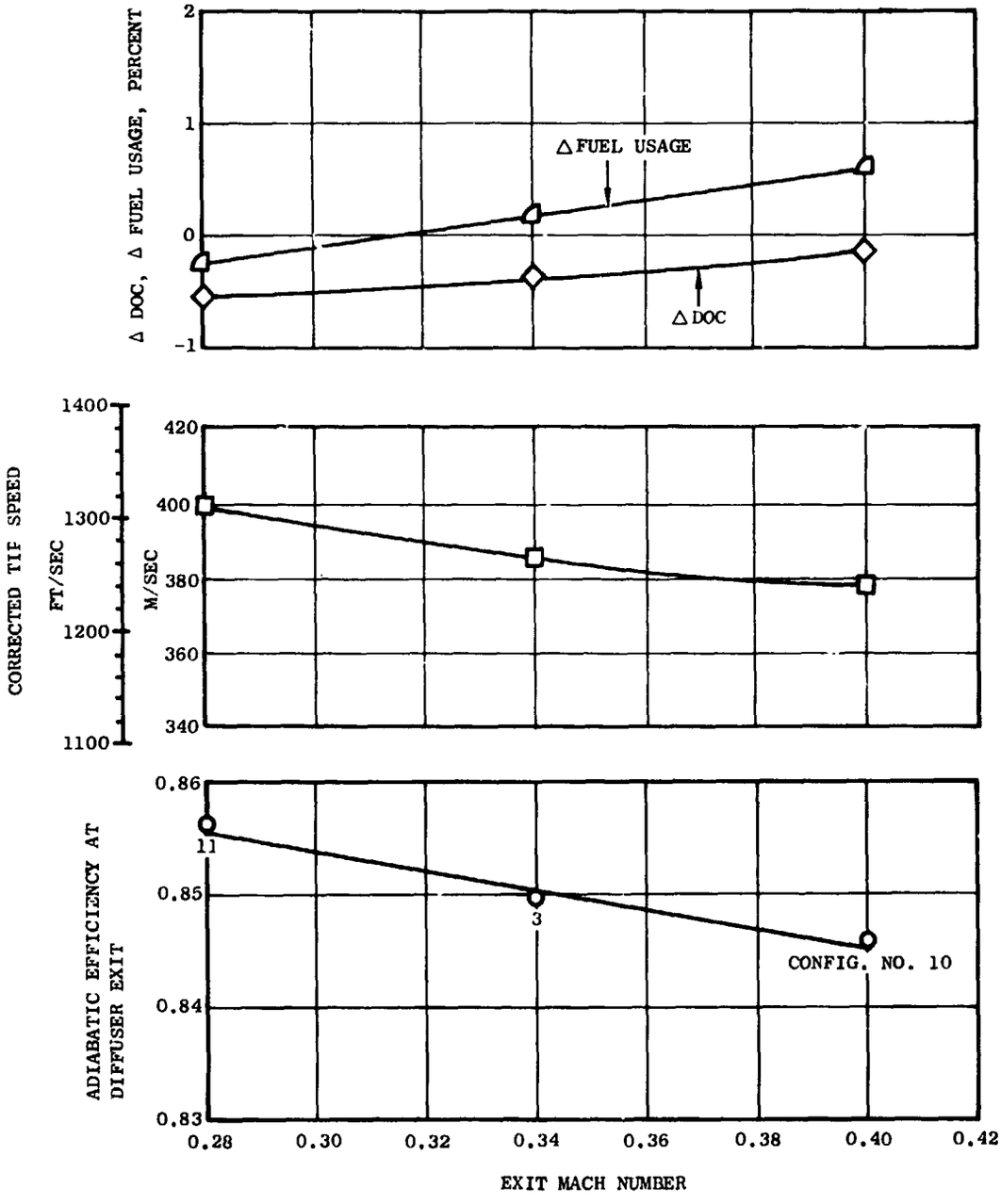

Figure 7 Variation in Direct Operating Cost, Fuel Usage, Tip Speed, and Compressor Efficiency with Exit Mach Number

The effects of variation in inlet corrected flow per unit annulus area are presented in Figure 8. These results clearly indicate that low inlet specific flow is desirable for the general class of designs considered.

The results of varying the inlet radius ratio are shown in Figure 9. Each design had a constant pitch radius type flowpath, but at a different radius level. The data show that high inlet radius ratio penalizes efficiency. The larger diameter of the high radius ratio design results in larger clearances and smaller blade heights, both of which increase end-wall losses. Cascade losses are not significantly reduced despite the reduction in tip speed that the higher radius ratio allows. The low inlet radius ratio design is longer, but has fewer airfoils, weighs less, and costs less than the nominal or high radius ratio designs. These factors, coupled with the higher efficiency, result in the lowest fuel usage and direct operating cost for the low inlet radius ratio design.

The direct operating cost and fuel usage data in Figure 9 present an interesting result. For the high inlet radius ratio compressor, the rpm decreased to the extent that an excessive high pressure turbine loading was encountered. As a result, the turbine flowpath diameter had to be increased to reduce the loading to a reasonable level. This flowpath change increased the low pressure turbine diameter as well, and increased the low pressure turbine efficiency by 0.7 point. This more than compensated for the reduced compressor efficiency, therefore decreasing fuel usage. The discontinuity in the curve in Figure 9 reflects this change in turbine flowpath diameter. However, the high radius ratio design had the largest weight and cost which caused an increase in the direct operating cost even though fuel usage decreased.

The use of different exit radius ratios and flowpath shapes is explored in Figure 10. Configuration 16 has a constant tip diameter and an exit radius ratio of 0.957, while Configuration 17 has a constant hub diameter and an exit radius ratio of 0.913. As the exit radius ratio is increased, the rpm and corrected tip speed are rapidly reduced because the work can be input at the larger average radius with a lower rpm. The cascade losses decrease as the wheel speed is reduced due to a reduction in shock and Mach-number associated losses. At the same time, as the exit radius ratio is increased, the blade heights become smaller, making the tip-clearance/blade-height ratio larger which, in turn, increases end-wall losses. As shown in Figure 10, there is an efficiency improvement as the exit radius ratio is increased from 0.913 to 0.934. This is due to the fact that the cascade losses decrease faster than the end-wall losses increase. For exit radius ratios above 0.934, the tip speed has become so low that no further improvement in cascade efficiency is realized, and the increasing end-wall losses dominate, thus reducing adiabatic efficiency. The low speed of the high exit radius ratio design required a turbine flowpath change similar to that needed for the high inlet radius ratio case described earlier. Resulting turbine efficiency changes are again responsible for the discontinuities in fuel usage and direct operating cost.

The effect of varying the number of stages in the compressor was also studied, and the results are shown in Figure 11. The interesting result is that the efficiency was not strongly affected by stage number, at least for the particular combination of stage parameters investigated. With fewer stages, a higher speed is required, of course. The cascade losses are nearly constant, but the end-wall losses decrease due to increased

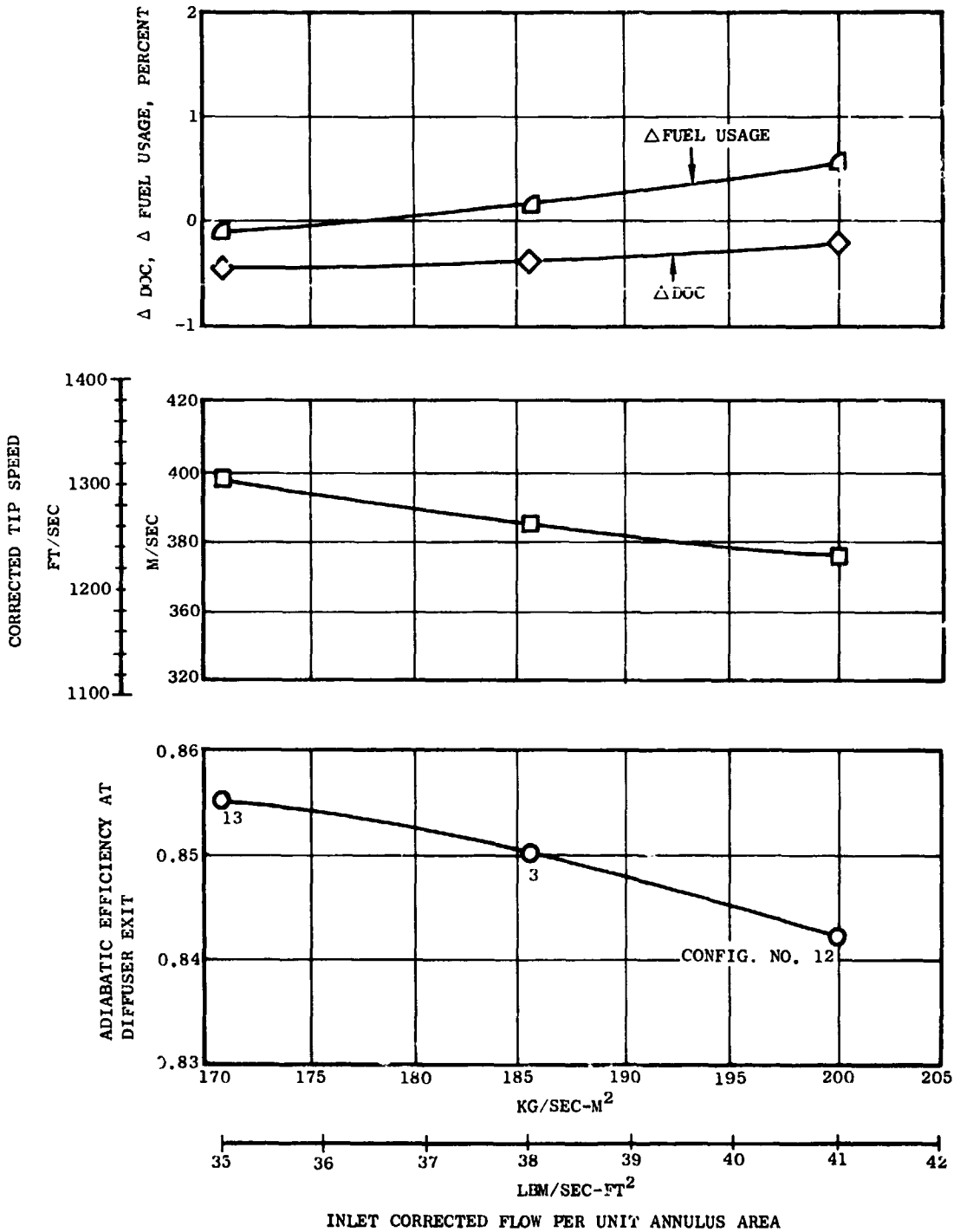

Figure 8 Variation in Direct Operating Cost, Fuel Usage, Tip Speed, and Compressor Efficiency with Inlet Corrected Flow Per Unit Annulus Area

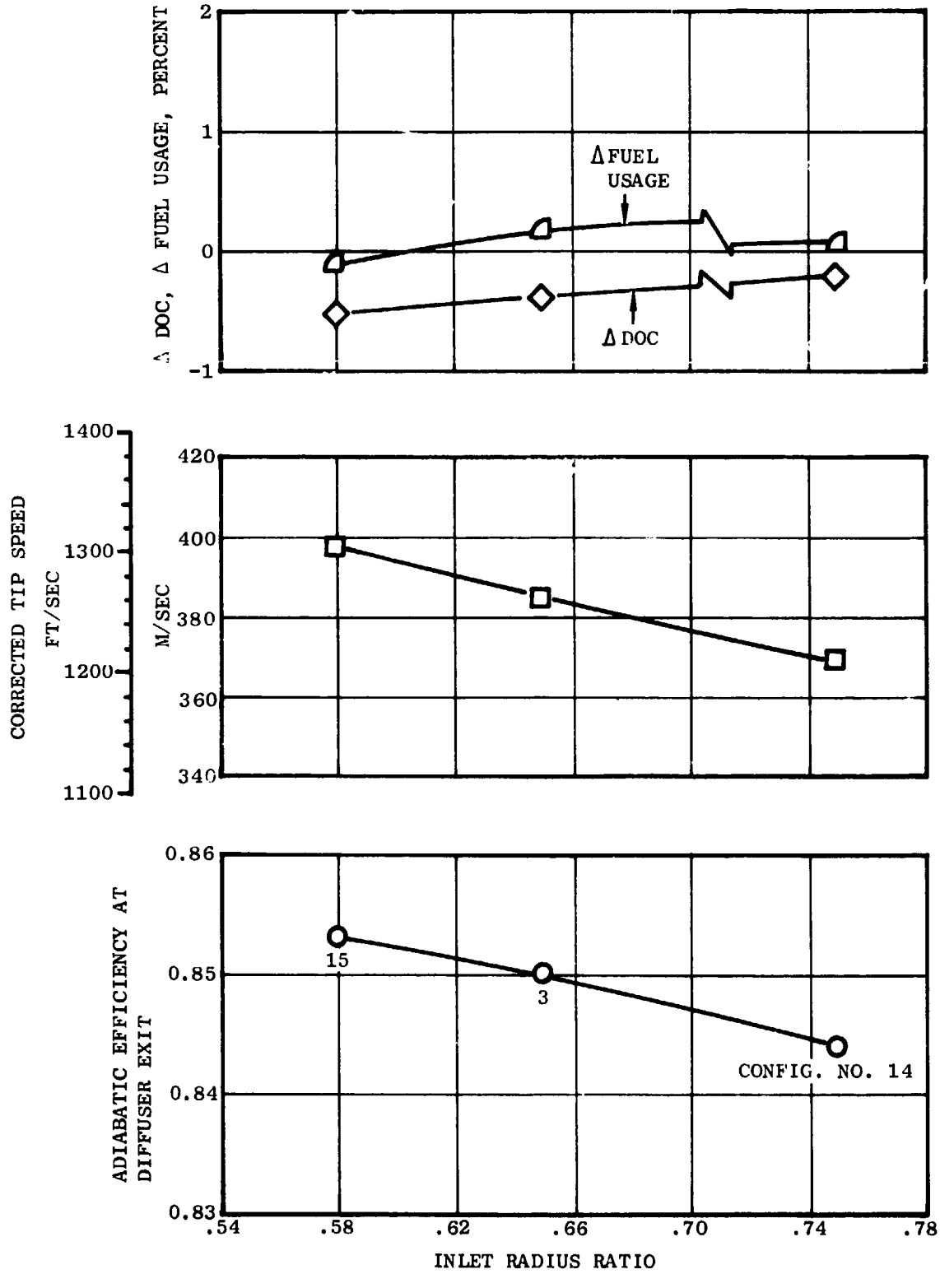

Figure 9 Variation in Direct Operating Cost, Fuel Usage, Tip Speed and Compressor Efficiency with Inlet Radius Ratio

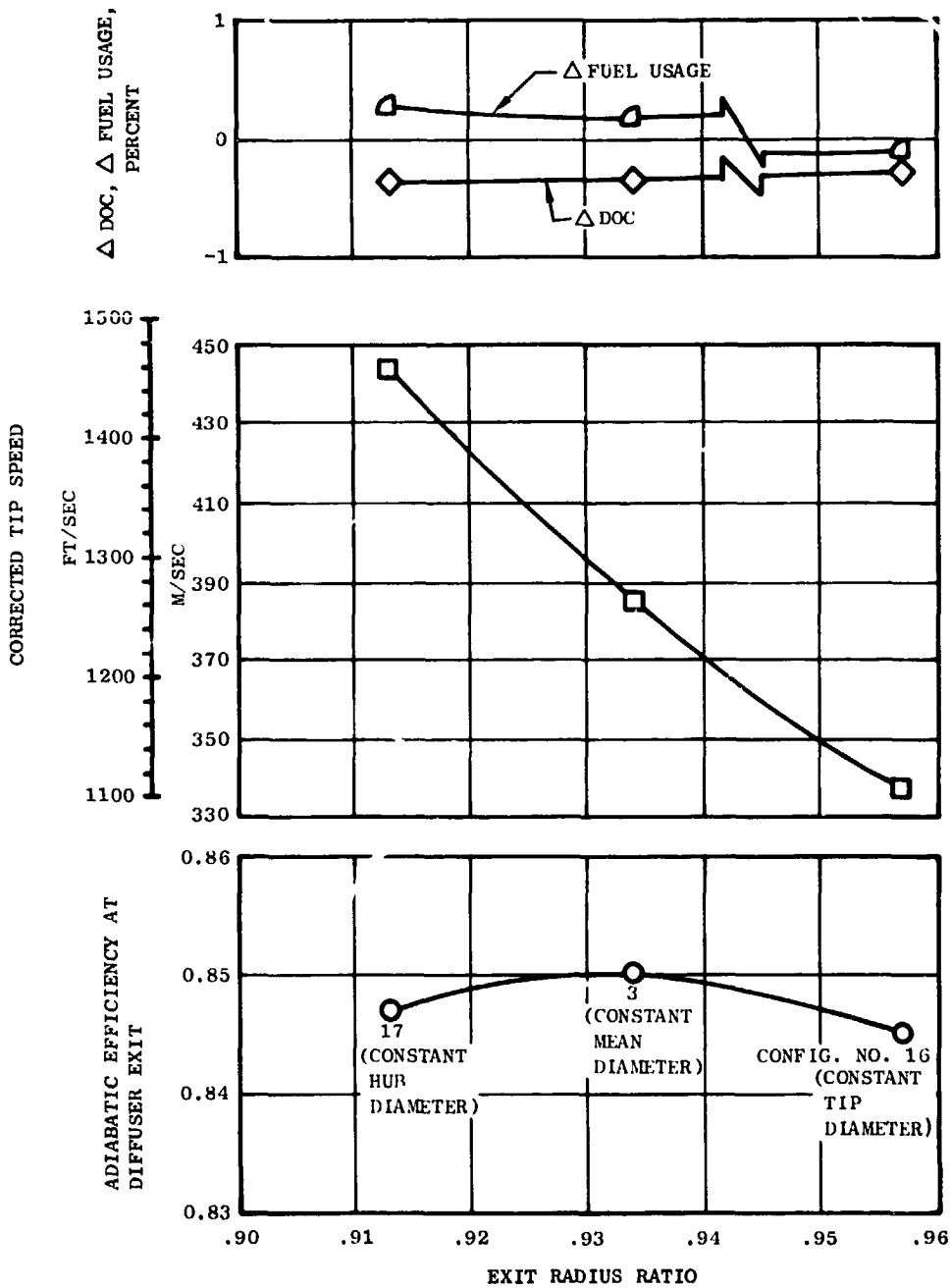

Figure 10 Variation in Direct Operating Cost, Fuel Usage, Tip Speed, and Compressor Efficiency with Exit Radius Ratio

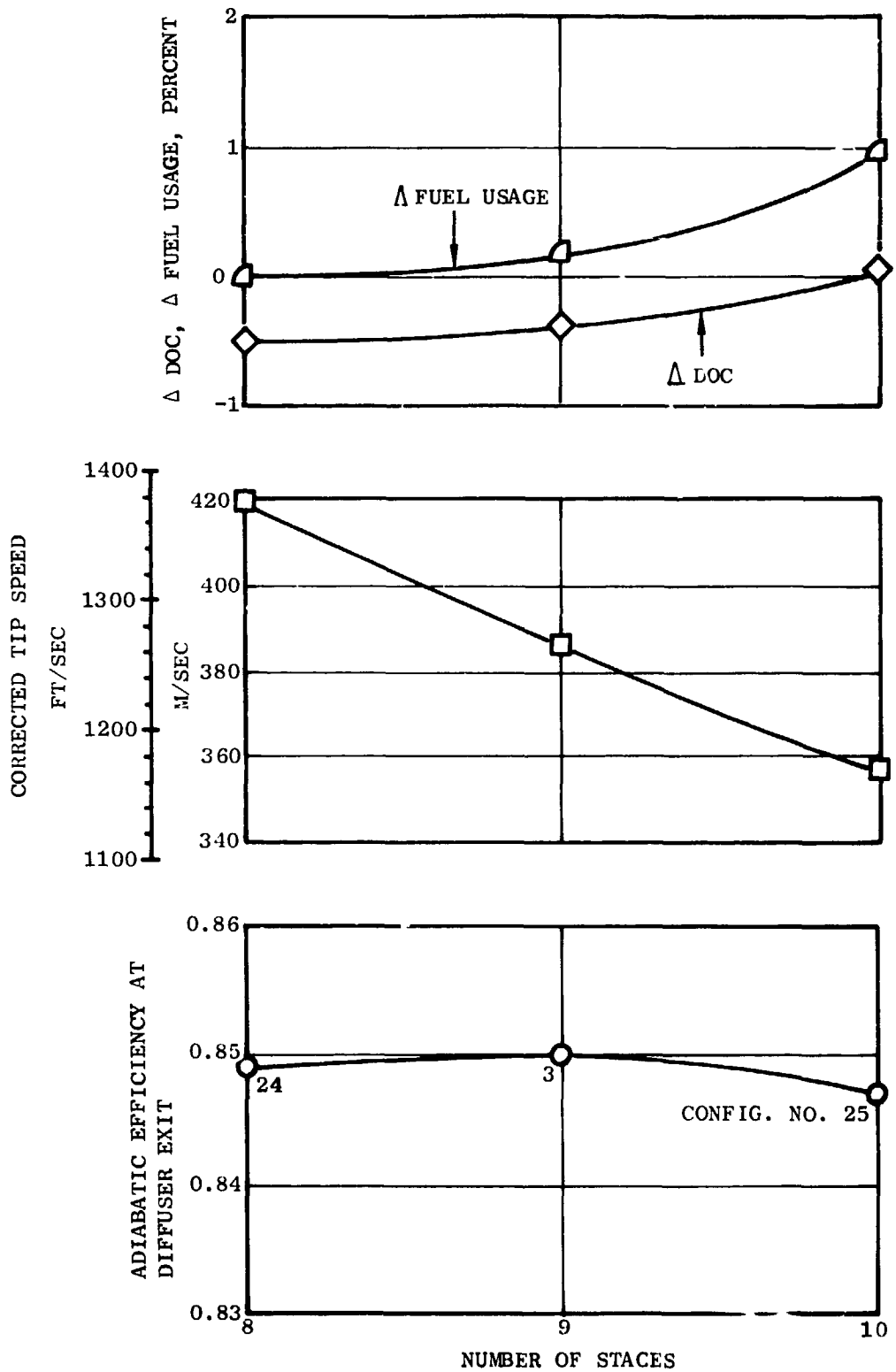

Figure 11 Variation in Direct Operating Cost, Fuel Usage, Tip Speed and Compressor Efficiency with Number of Stages

blade stagger angles (higher passage aspect ratios) as the speed increases. With fewer number of stages, rotative speed increases, thus increasing high pressure turbine efficiency and counteracting the slight decrease in compressor efficiency. The result is a slight improvement in fuel usage for the eight-stage compressor compared to the nine-stage. However, for the 10-stage compressor, the rotative speed has been significantly decreased, causing the high pressure turbine loading to increase and its efficiency to decrease. The reduced turbine and compressor efficiencies result in higher fuel usage for the 10-stage compressor compared with the nine-stage. The trend of the direct operating cost follows that of the fuel usage. It should also be noted that the rear rim speed of the eight-stage compressor is approaching the assumed mechanical limit of 381 m/sec (1250 ft/sec).

In summary, the findings of the one-parameter variation studies show the following trends, although it is recognized that for a different class of compressors, such as turbojets, different values of the optimum parameters might result:

1. Best efficiency is obtained when core compressors are designed with:
   (a) Medium average aspect ratios (1.3-2.0)
   (b) Medium average solidities (1.2-1.5)
   (c) Medium-to-high reactions (0.5-0.7)
   (d) Low exit Mach number (~0.28)
   (e) Low inlet flow/annulus area (171 kg/sec-m^2 (35 lbm/sec ft^2))
   (f) Low inlet radius ratio (i.e., minimum, practical value within physical and structural constraints)

2. High blade speed does not penalize performance until front stage tip Mach number is greater than about 1.4.

3. High rpm can increase turbine efficiency, often without reducing compressor efficiency.

4. Fewer stages are less expensive, but not necessarily lighter, and need not involve an efficiency penalty provided that tip speed does not become excessive.

5. Medium-to-high rear radius ratio can be beneficial, provided that it helps maintain the front stage relative tip Mach number below the level at which high shock losses are encountered.

These findings were used to guide the selections of design parameters for two series of high efficiency compressors, one group having a pressure ratio of 14 and the other group having a pressure ratio of 23. These designs will be discussed in a later section, Further Studies of High Efficiency Compressors.

Discussion of Other Screening Studies

Maximum Life Configurations - Configurations 19a and 19b, the Maximum Life designs, were based on Configuration 17, the nine-stage, constant hub radius, nominal loading, 14:1 pressure ratio design. Modifications to increase the rotor tip trailing edge thickness

and reduce blade speed were made in order to achieve longer blade erosion life. Configuration 17 was chosen as a starting point because its rear rim speed was low. Lower aspect ratios and high solidities reduced the tip speed required for 19 percent stall margin. Use of lower aspect ratios also increased the trailing edge thickness for a given thickness-to-chord ratio. A reduced exit Mach number was also used to increase rotor blade heights and, for a given aspect ratio and trailing edge thickness-to-chord ratio, to increase the blade trailing edge thickness. High solidity enabled the blade passage aspect ratios to be kept relatively high as the chord was increased, thus avoiding high end-wall losses. In Configuration 19a only the rotors were given longer chords and high solidities, and in Configuration 19b the stator chords and solidities were increased as well to give a further reduction in speed. As a result, the relative blade life of the limiting stage was increased from 2.87 in Configuration 17 to 6.22 for Configuration 19b, an improvement of over 200 percent. This increase was accomplished with a slight improvement in efficiency of 0.2 point and only moderate increases in cost and weight, as seen in Table II. The study showed that compressor life can be significantly increased without adversely affecting performance by proper design of the limiting stages.

Lightly Loaded First Stage Configuration - A nine-stage, 23:1 pressure ratio compressor was designed utilizing a front stage that was quite lightly loaded relative to its tip speed. This design, Configuration 23, was investigated in order to allow use of the double-oblique-shock type of rotor aerodynamic design reported in Reference 3 under NASA Contract NAS3-13498. This type of design could possibly result in a higher first stage efficiency than would be obtained if the first stage were loaded to its full capacity. Configuration 23 was obtained by zero-staging Configuration 24, a nominal loading eight-stage, 14:1 pressure ratio compressor. This procedure consisted of selecting an operating condition at 97 percent corrected speed as the match point for the lightly loaded fan stage, scaling the fan so that its tip diameter was compatible with the flowpath of the existing eight-stage design, and cutting off the hub portion of the zero stage so that an inlet corrected flow of 46.86 kg/sec (103.3 lbm/sec) was obtained. At this match condition, the corrected tip speed of the fan stage was 474 m/sec (1555 ft/sec), total pressure ratio was 1.64, and efficiency was estimated to be 0.85. The corrected flow and tip speed at the inlet to the rear block were approximately two percent lower than the original design values for this eight-stage compressor, so a new blade geometry definition, efficiency estimate, and stall margin check were made for these stages. The efficiency of the front stage reported in Reference 3 at the match point was 1.5 point better than predicted by the efficiency model, so the overall compressor efficiency was adjusted upward by 0.3 point to reflect this. The resulting overall adiabatic efficiency of 0.822, however, was not significantly better than expected from the trend of efficiency versus number of stages defined by the other 23:1 pressure ratio compressors studied. A summary of key design and performance parameters for Configuration 23 is contained in Table II. This table also allows a comparison with the other 23:1 pressure ratio configurations. This compressor is seen to be compact, light, and inexpensive; features which give the engine using it a low direct operating cost. The fuel usage, however, is not as good as the engine using the higher efficiency, conservative loading, 14-stage compressor (Configuration 20).

FURTHER STUDIES OF HIGH EFFICIENCY COMPRESSORS

The results of the parametric screening studies reported in the previous section were used to define two families of compressors with high efficiency potential: the Configuration 26 group with a total pressure ratio of 23; and, the Configuration 18 group with a total pressure ratio of 14. The approach used was to follow the trends seen in the one-parameter variations that led to higher efficiencies. These compressors, therefore, have low inlet and exit axial Mach numbers, medium blade aspect ratios and solidities, medium-to-high reaction ratios, low inlet radius ratios, and medium exit radius ratios. Aerodynamic design details of these configurations are presented in the following sections.

P/P = 23 Compressor Configurations

Aerodynamic design and performance parameters for the 23:1 pressure ratio high-efficiency compressors are presented in Table III. A number of different compressor designs were evaluated in an attempt to fine-tune the selection of parameters to yield the best combination of high efficiency, low fuel usage, and low direct operating cost. The number of stages ranged from nine to 14, and the corrected tip speeds required ranged from 451 m/sec (1480 ft/sec) to 541 m/sec (1775 ft/sec). The diffuser exit adiabatic efficiency for Configuration 26a of 0.858 shown in Table III was 1.4 points better than the efficiency of Configuration 20, the best of the initial 23:1 pressure ratio configurations. The efficiency values listed in Table III and shown in Figure 12 decreased appreciably as the number of stages was reduced, mainly because tip speeds became very high and high rotor shock losses were encountered. End-wall losses remained about constant, and the overall adiabatic efficiency at the diffuser exit followed the trend of the freestream airfoil cascade efficiency.

Configurations 26b2, 26e, and 26d2 were evaluated in an effort to regain the efficiency that was lost as the number of stages was reduced. These configurations had the same number of stages used previously, but utilized flowpaths having larger exit radii which allowed the use of considerably lower tip speeds. The results presented in Table III and in Figure 12 show that an efficiency improvement of about 0.4 - 0.5 point was obtained in each case. This efficiency improvement came about because the significantly lower tip speeds reduced the Mach-number-associated losses. This effect overshadowed the end-wall loss increases caused by the larger tip-clearance-to-blade-height ratios that resulted from the larger exit radius ratios.

In order to further improve efficiency, the previous best nine-stage design, Configuration 26d2, was modified by decreasing the inlet radius ratio from 0.546 to 0.502, thus creating Configuration 26d5. This modification reduced the inlet tip diameter, and although the required rpm increased, the corrected inlet tip speed was reduced. The resulting reduction in Mach number losses brought about a 0.3 point improvement in adiabatic efficiency compared to Configuration 26d2.

Compressor mechanical design and aircraft/engine system economic analysis data are presented in Figures 13 and 14, respectively. As the number of stages is reduced, the rear rim speed increases, with the higher exit radius ratio designs having higher rear

Table III. Aerodynamic Summary of Configuration 26 Designs, Maximum Efficiency, 23:1 Pressure Ratio

Configuration Number Number of Stages	26a 14	26b 11	26c 10	26d 9	26b2 11	26e 10	26d2 9	26d5 9
Corrected Inlet Tip Speed, m/sec (fps)	451 (1480)	500 (1642)	522 (1712)	541 (1775)	457 (1500)	472 (1547)	491 (1610)	480 (1575)
Physical Rear Hub Speed, m/sec (fps)	301 (987)	340 (1116)	358 (1174)	382 (1252)	354 (1163)	366 (1200)	388 (1273)	393 (1290)
Physical Speed, rpm	13,155	14,596	15,218	15,767	13,333	13,751	14,301	14,436
Inlet Radius Ratio	0.488	0 488	0.488	0.546	0.488	0.488	0.546	0.502
Inlet Flow/Annulus Area, kgm/sec-m^2 (lb/sec-ft^2)	171 (35)	171 (35)	171 (35)	186 (38)	171 (35)	171 (35)	186 (38)	186 (38)
Inlet Tip Diameter, m (in.)	0.676 (26.6)	0.676 (26.6)	0.676 (26.6)	0.677 (26.6)	0.676 (26.6)	0.676 (26.6)	0.677 (26.6)	0.656 (25.8)
Exit Radius Ratio	0.910	0.913	0.915	0.915	0.930	0.931	0.934	0.934
Exit Tip Diameter, m (in.)	0.480 (18.9)	0.488 (19.2)	0.491 (19.3)	0.502 (19.8)	0.546 (21.5)	0.545 (21.5)	0.555 (21.8)	0.556 (21.9)
Length to Diffuser Exit, m (in.)	1 03 (40.7)	0.773 (30.4)	0.743 (29.2)	0.987 (23.1)	0.767 (30.2)	0.717 (29.2)	0.603 (23.7)	0.630 (24.8)
Number of Airfoils	2237	1781	1677	1651	2087	1925	1915	1839
Average Aspect Ratio	2.0	1.85	1.78	1.79	1.85	1.70	1.70	1.70
Average Solidity	1.30	1.34	1.34	1.40	1.34	1.46	1.49	1.49
Average Swirl, Degrees	17.1	15.3	14.7	13.7	15.3	14.7	13.7	13.7
Average Reaction	0.692	0.734	0.748	0.761	0.732	0.736	0.749	0.744
Stall Margin, %	17	17	18	20	17	18	20	18
Adiabatic Efficiency at Diffuser Exit	0.858	0.852	0.849	0.841	0.856	0.853	0.846	0.849
Compressor Weight, kg (lb)	294 (648)	257 (566)	253 (558)	242 (534)	271 (598)	269 (594)	258 (568)	252 (556)
\Compressor Price, % of STEDLEC Compressor Price	17.0	21.2	16.6	8.2	27.3	22.0	14.2	12.1
Minimum Blade Life, hr	6000	1700	1300	4000	4500	1900	4600	4600
\Engine Price*, % of STEDLEC Total Engine Price	7.1	1.8	4.5	3.7	5.5	5.0	4.0	3.9
\Fuel Usage*, %	-2.06	-2.11	-1.90	-1.52	-2.41	-2.26	-2.07	-2.27
\Direct Operating Cost*, %	0.92	0.46	0.48	0.51	0.33	0.11	0.23	0.11

*Trans-continental trijet aircraft mission.

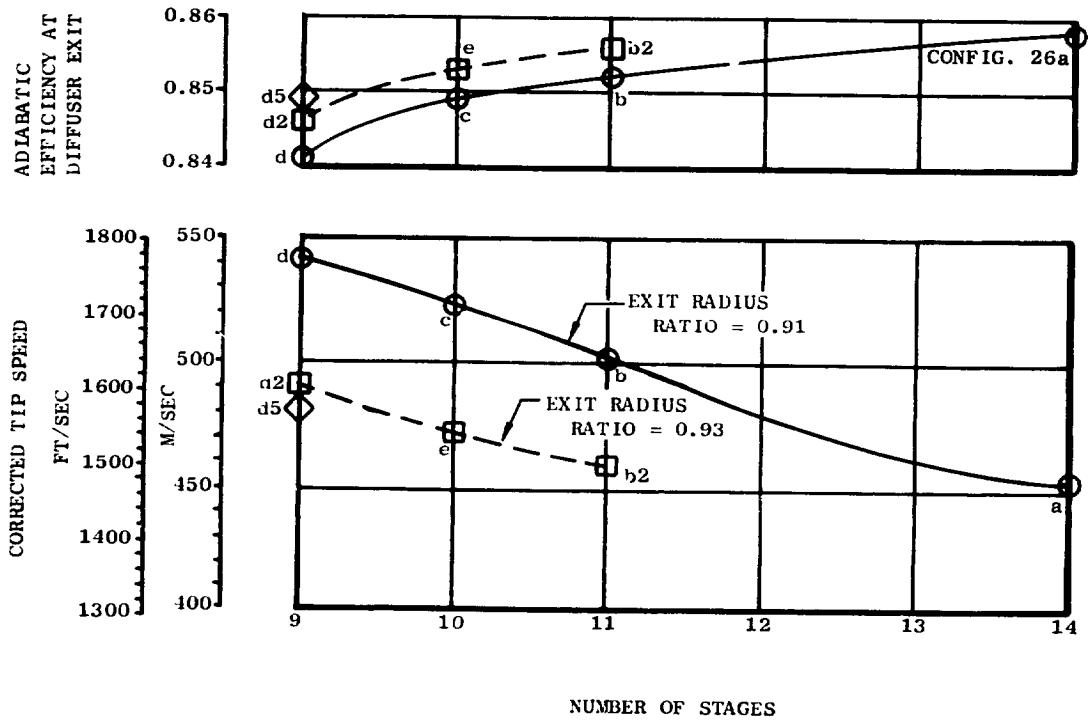

Figure 12 Adiabatic Efficiency and Corrected Tip Speed Versus Number of Stages for 23:1 Total-Pressure Compressors, Configuration 26

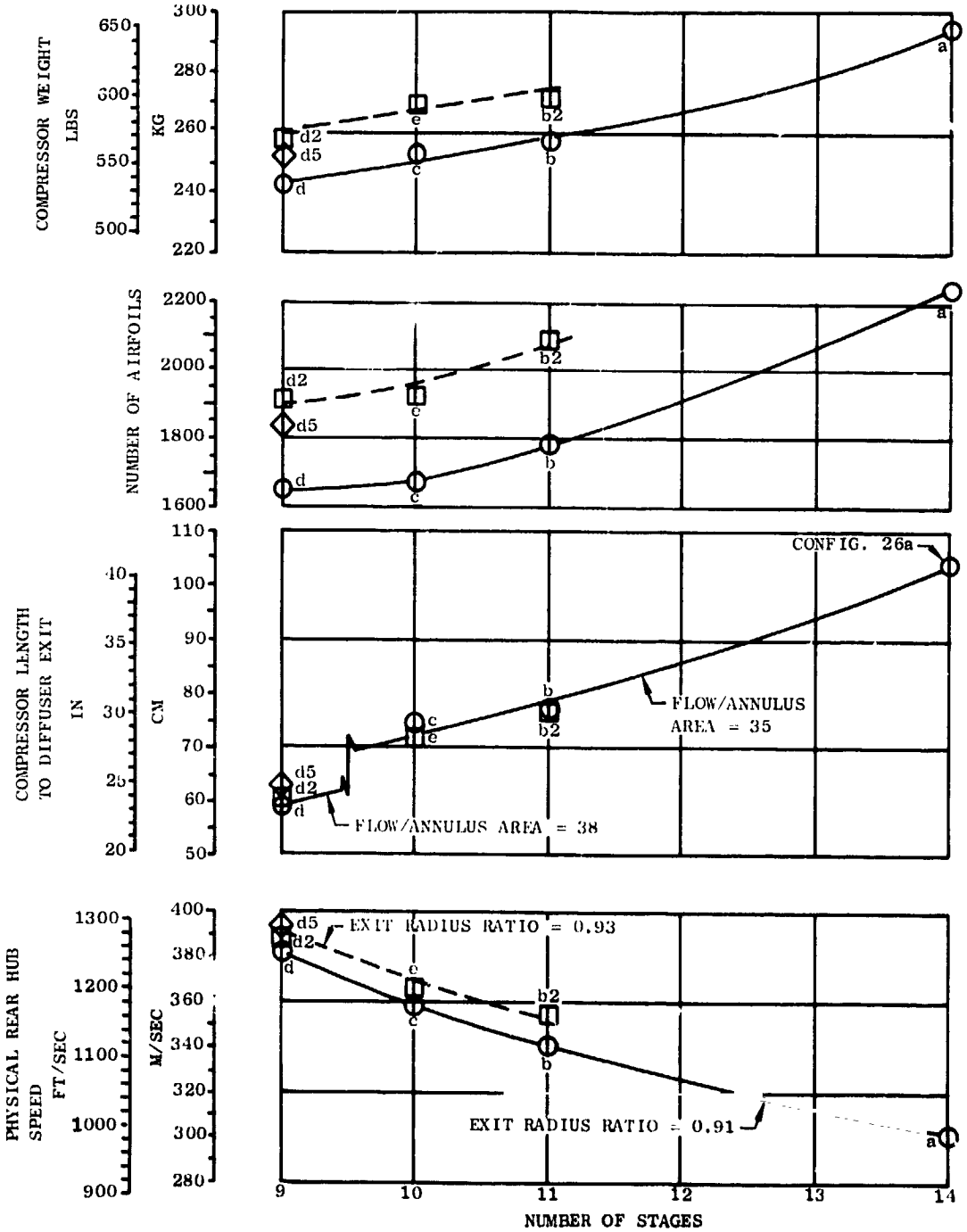

Figure 13 Compressor Physical and Mechanical Characteristics Versus Number of Stages for 23:1 Total-Pressure Ratio Designs, Configuration 26

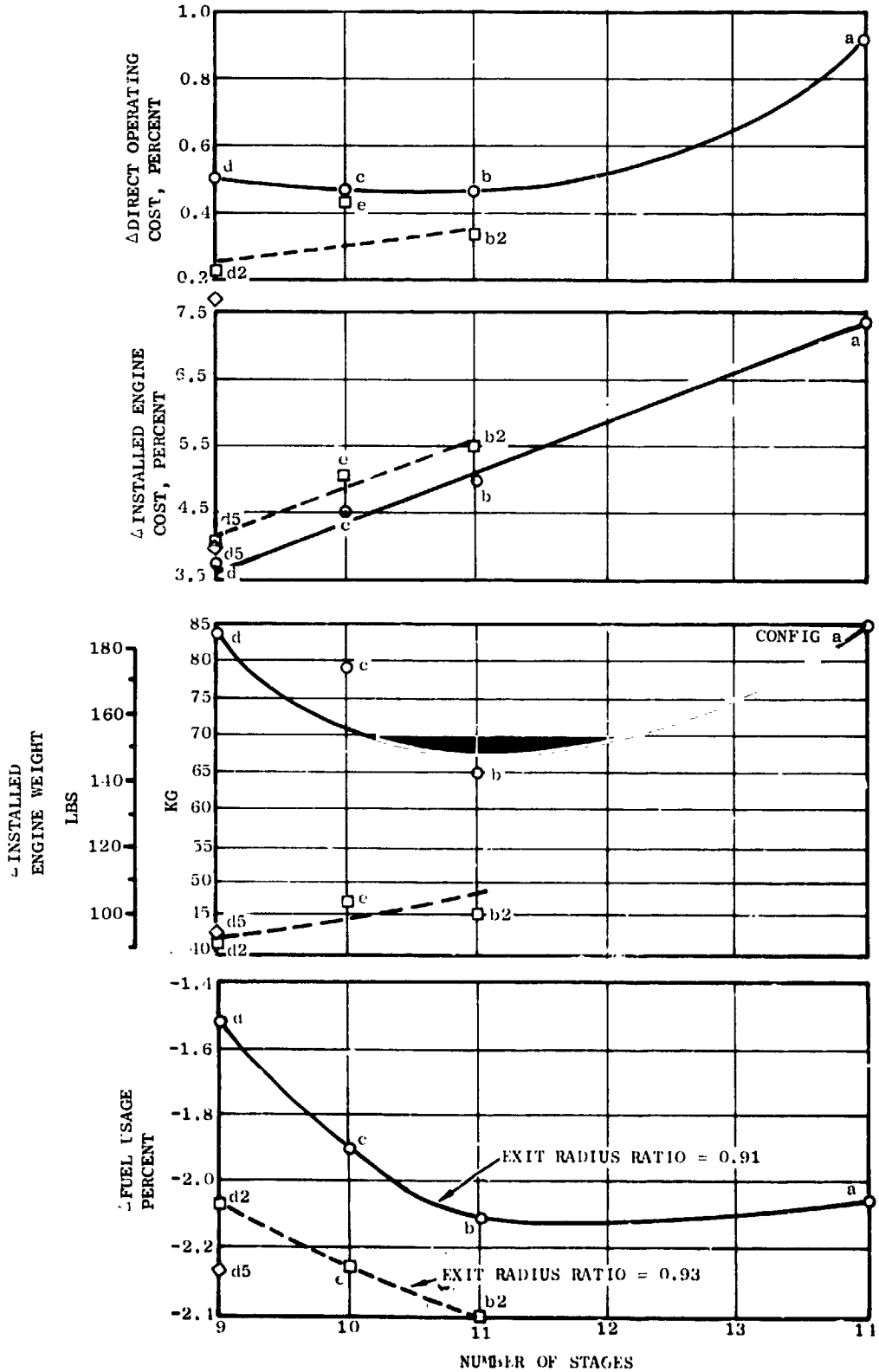

Figure 14 Engine Economic and Physical Characteristics Versus Number of Stages for 23:1 Total-Pressure Ratio Compressors, Configuration 26

rim speeds despite their lower rotative speeds. It should be noted that the originally assumed mechanical limit of 381 m/sec (1250 ft/sec) for the rear rim speed was relaxed for Configuration 26d5, for which the value of this parameter is 393 m/sec (1290 ft/sec). The compressor weight, length, and number of airfoils all decrease as the number of stages is reduced, which has the effect of reducing the engine cost. The overall engine installed weight remains relatively constant even though compressor weights are reduced by the use of fewer stages, because with fewer stages the rotative speeds have increased, requiring heavier turbines. The trend of fuel usage at a given exit radius ratio followed the trend of compressor efficiency, as expected, and the lighter engine weight and improved efficiency made possible by the use of a high rear radius ratio flowpath also reduced fuel consumption. The 11-stage design, Configuration 26b2, had the lowest fuel usage. Direct operating costs reflect both fuel usage and engine cost, and these combine to slightly favor the compressors with fewer stages.

P/P = 14 Compressor Configurations

Aerodynamic design parameters for the 14:1 pressure ratio high-efficiency compressors are presented in Table IV. As for the 23:1 pressure ratio designs, several designs differing in number of stages were evaluated in an attempt to select parameters that yielded high efficiency, low fuel usage, and low direct operating cost. The results of this effort are summarized in Table IV. The efficiencies are as high as 0.869, one point better than any of the 14:1 pressure ratio configurations that were identified in the initial parametric studies (Table II), and are within 0.5 point of the same level with as few as eight stages. As the number of stages is reduced, the corrected tip speed increases and the shock losses and Mach-number-associated losses increase. For the 12-stage, 10-stage, and nine-stage compressors, increases in cascade loss are offset by decreases in end-wall loss, resulting in nearly constant adiabatic efficiency. As the number of stages is reduced below nine, the increasing cascade losses caused by the increased tip speed dominate and the adiabatic efficiency decreases.

Mechanical design data and economic analysis data are also presented in Table IV. As the number of stages was reduced, the rear rim speed increased, and rim speeds above 381 m/sec (1250 ft/sec) were required for some configurations. No engine system data were given for the seven-stage compressor, Configuration 18f, because its extremely high rotative speed was judged to result in unacceptably high turbine stresses. The compressor length, number of airfoils, weight (except for Configuration 18f), and cost decreased as the number of stages was decreased, resulting in a decrease in engine cost. Overall engine weight varied less than compressor weight, partly because turbine weight increased with the higher speeds which were required as the number of compressor stages was reduced. Fuel usage was found to increase for fewer than 10 stages, due to declining compressor efficiency and increasing turbine cooling flows. The trend of direct operating cost shown in Table IV is due to both the trends of fuel usage and engine cost, resulting in minimum direct operating cost for an engine having a nine-stage core compressor.

Effect of State-of-the-Art Assumptions

The sensitivity of the predicted efficiency of the high-efficiency 23:1 pressure ratio designs to variations in the assumed level of aerodynamic and mechanical design technology was evaluated. In Figure 15, the upper curve of compressor efficiency versus number of

Table IV. Aerodynamic Summary of Configuration 18 Designs
Maximum Efficiency, 14:1 Pressure Ratio

Configuration Number Number of Stages	18a 12	18b 10	18c 9	18d 8	18f 7
Corrected Inlet Tip Speed, m/sec (fps)	387 (1270)	415 (1360)	437 (1435)	460 (1510)	489 (1604)
Physical Rear Hub Speed, m/sec (fps)	314 (1029)	348 (1143)	374 (1227)	398 (1306)	416 (1364)
Physical Speed, rpm	14,145	15,148	15,983	16,819	17,866*
Inlet Radius Ratio	0.566	0.566	0.566	0.566	0.566
Inlet Flow Annulus Area, kg sec-m^{-2} (lbm sec-ft^{-2})	171 (35)	171 (35)	171 (35)	171 (35)	171 (35)
Inlet Tip Diameter, m (in.)	0.583 (23.0)	0.583 (23.0)	0.583 (23.0)	0.583 (23.0)	0.583 (23.0)
Exit Radius Ratio	0.908	0.907	0.911	0.913	0.916
Exit Tip Diameter, m (in.)	0.465 (18.3)	0.485 (19.1)	0.491 (19.3)	0.495 (19.5)	0.485 (19.1)
Length to Diffuser Exit, m (in.)	0.737 (29.0)	0.604 (23.8)	0.536 (21.1)	0.470 (18.5)	0.443 (17.4)
Number of Airfoils	1899	1780	1626	1486	1211
Average Aspect Ratio	2.09	2.00	1.93	1.88	1.71
Average Solidity	1.20	1.34	1.37	1.40	1.44
Average Swirl, Degrees	16.0	14.4	14.0	14.1	13.3
Average Reaction	0.705	0.733	0.747	0.756	0.762
Stall Margin, %	17	17	20	21	17
Adiabatic Efficiency at Diffuser Exit	0.868	0.869	0.868	0.865	0.858
Compressor Weight, kg (lb)	224 (493)	208 (458)	198 (436)	191 (421)	197 (434)
ΔCompressor Price, % of STEDLEC Compressor Price	13.4	1.6	-5.2	-10.9	-12.9
Minimum Blade Life, hr	6500	5300	4900	3900	1200
ΔEngine Price†, % of STEDLEC Total Engine Price	1.3	0	-0.5	-1.1	----
ΔFuel Usage†, %	-0.73	-1.04	-0.95	-0.60	----
ΔDirect Operation Cost†, %	-0.17	-0.71	-0.78	-0.68	----

*Unacceptable because of turbine stress

†Transcontinental trijet aircraft mission

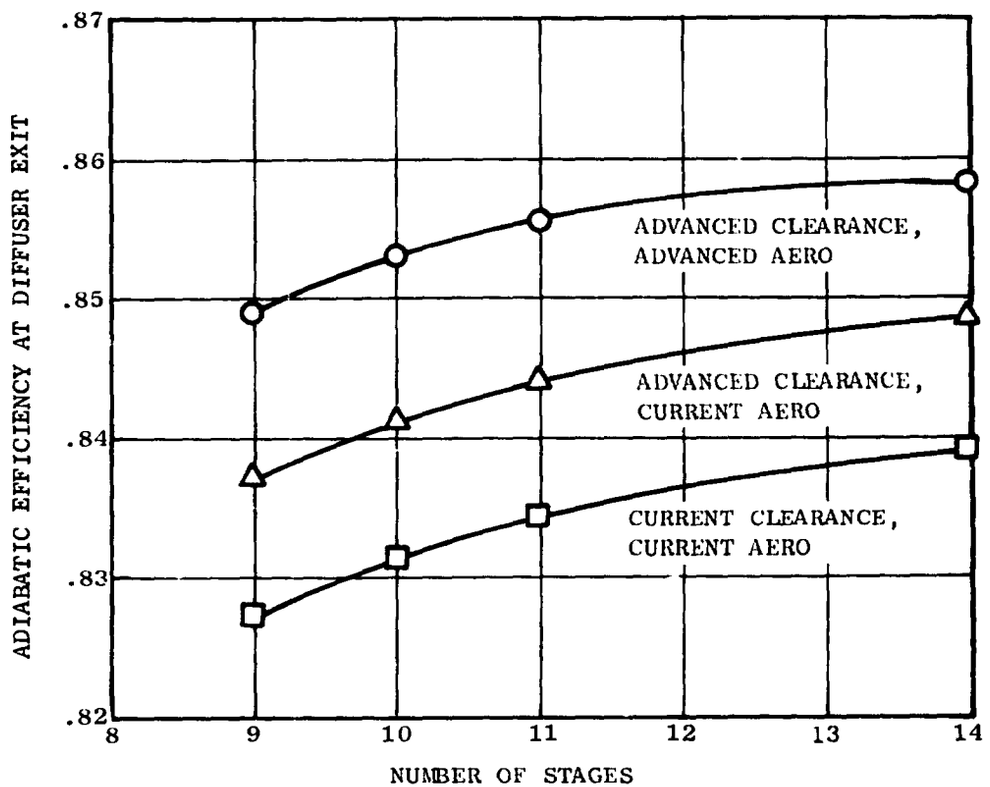

Figure 15 Effect of Technology Level Assumptions on Efficiency of 23:1 Total-Pressure Ratio Compressors

stages, labeled "advanced clearance, advanced aero", gives the efficiency for the advanced level of technology assumed throughout this study. The consequences of not reducing end-wall losses by the assumed 15 percent and not achieving the assumed improvement in rear stage rotor blade surface finishes, combined with a 15 percent increase in shock losses above the assumed "best current experiences" level, are shown in the middle curve labeled "advanced clearance, current aero" to result in about a one point reduction in predicted efficiency. A further reduction in efficiency of about one point is predicted if clearances cannot be reduced below current levels. It should be noted that all four compressors shown in the figure were affected nearly equally by changes in the level of technology assumed. It was thus concluded that, for this type of engine/aircraft system, the selection of the optimum number of core compressor stages should not be particularly dependent upon achieving specific advances in either aerodynamic or mechanical design technology. Although not shown in the figure, use of current technology clearances would result in approximately four to five points less stall margin than if advancement in clearance control were achieved.

Additional studies were conducted to determine if variations in assumed technology level would affect the choice of compressor rear radius ratio. The nine-stage 23:1 pressure ratio compressor was employed for this investigation. As shown by the upper curve in Figure 16, predicted efficiency is highest at an exit radius ratio of about 0.95 if advanced technology clearances and aerodynamics are assumed as was done throughout this study. This trend is caused by the large reduction in shock losses that accompanies the lower rotative speeds which result from the use of high exit radii. If current technology clearances are assumed, as in the middle curve of Figure 16, the larger rear stage clearance-to-blade height ratios that result from use of high exit radius ratios reduce the most favorable exit radius ratio to approximately 0.935. This value of exit radius ratio still appears to be about optimum if shock losses are assumed to be 15 percent higher than used throughout the study, as shown by the lower curve in Figure 16. It was concluded, therefore, that the exit radius ratio should be chosen to be in the 0.930 - 0.935 range in order to keep front stage tip speeds from becoming so high that overall efficiency would be compromised if low shock losses could not be achieved. Yet this radius ratio is not so high that failure to achieve significant clearance reductions below current levels might severely increase rear stage losses and reduce overall efficiency potential.

DETAILED STUDY OF THREE SELECTED COMPRESSORS

Three of the most promising compressors identified in the final screening studies were selected for further, more detailed, aerodynamic and mechanical design studies. These three configurations were the 11-stage and nine-stage 23:1 pressure ratio designs and the nine-stage 14:1 pressure ratio design, Configurations 26b2, 26d5, and 18c, respectively.

The two 23:1 pressure ratio designs were selected because engines employing these compressors had the lowest fuel usage, and because it was realized that a good 14:1 pressure ratio compressor could be derived from each of these designs by removal of the first stage. The 11-stage and nine-stage designs covered the range of stage numbers where overall unboosted engine system performance was best. Since the optimum number of stages was not clearly evident from the parametric study results, it was desired to study

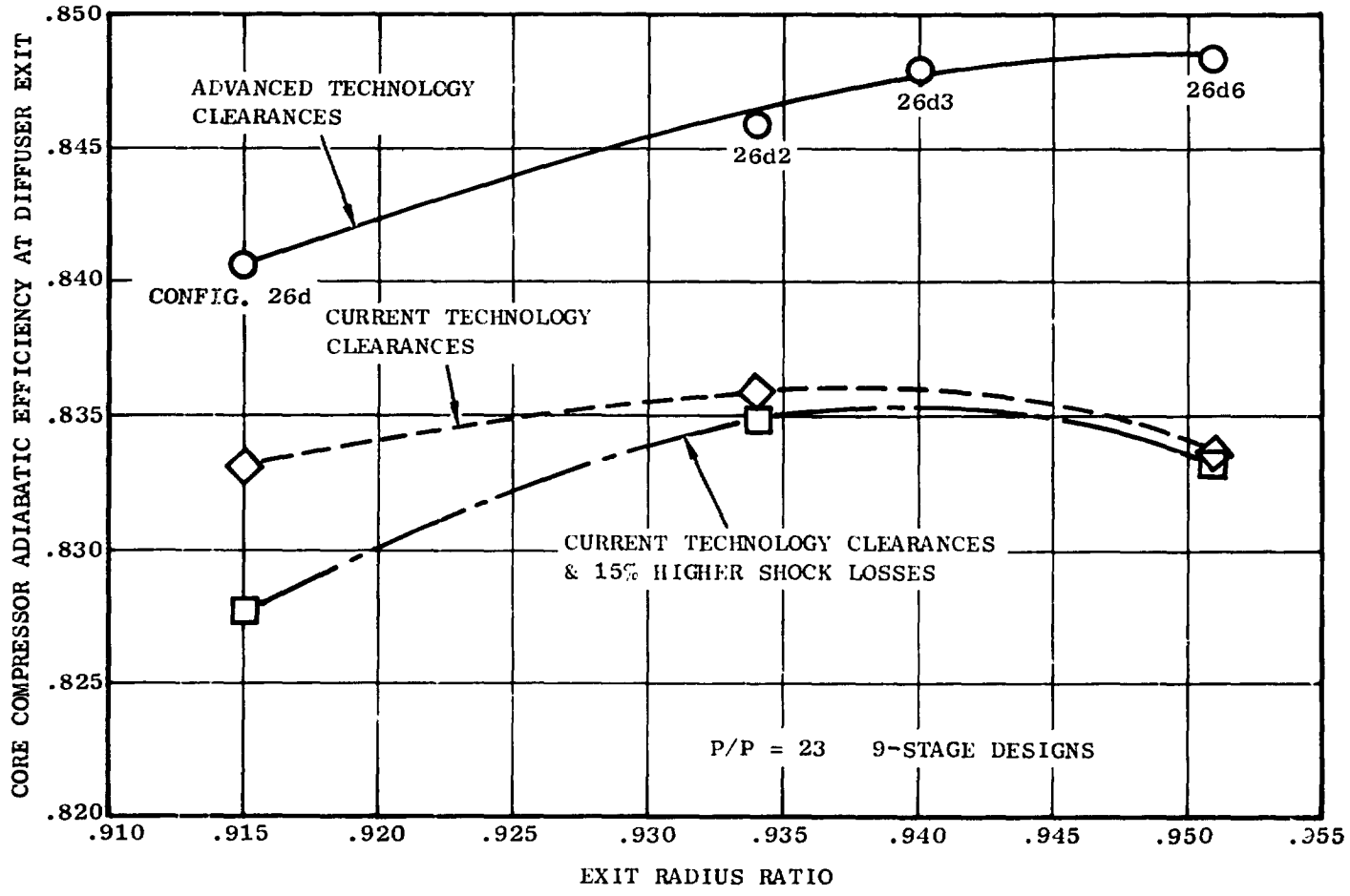

Figure 16 Compressor Efficiency as a Function of Exit Radius Ratio and Assumed Level of Technology for 9-Stage 23:1 Total-Pressure Ratio Designs

two cases that differed in this parameter to see if some subtle difference, perhaps not adequately identified in the parametric study, might be uncovered. For example, there was concern that the higher rotative speed of the nine-stage design might lead to bearing problems or to blade and disk stress problems. Part-speed stall margin and acceleration time could also be of concern for this configuration. On the other hand, the greater length of the 11-stage design might lead to bearing span, rotor deflection, or system vibration problems.

The nine-stage 14:1 pressure ratio compressor was selected for further study because the engine based upon this design had the lowest predicted direct operating cost of any configuration studied. It also had a fairly high rear rim speed and a very high rotative speed, thus providing mechanical design challenges in the areas of compressor disk stresses and turbine stresses and cooling.

The major aerodynamic design parameters for the three selected compressors, as well as a comparison of these parameters with the other configurations identified in the parametric studies, are presented in Table II. Cross-sections of the three designs, indicating the aerodynamic flowpaths and major mechanical design features of these configurations, are presented in a later section, Detailed Design Study.

The detailed aerodynamic design studies consisted primarily of an analysis of vector diagram parameters and aerodynamic loading levels in order to determine if any severe problems existed that might make it unlikely that the predicted stall margin or efficiency could be achieved. In addition to studies of design point operation, a combination of analytical and semi-empirical methods was employed to generate compressor performance maps that would represent estimated part-speed flow, efficiency, and stall line magnitudes.

Axisymmetric Flow Calculations

Calculation of circumferential average values of vector diagram parameters and fluid properties along nine design stream surfaces was performed using the General Electric Circumferential Average Flow Determination computer program. Flowpath annulus geometry, blade geometry, inlet temperature, and pressure at the engine maximum cruise thrust sizing point, flows, and rotative speed were input for the three selected configurations. These inputs were based upon data generated during the parametric screening studies using the pitchline analysis procedure. Stagewise distributions of average pressure ratio, stator exit flow angle, efficiency, and wall boundary layer blockage were also based on results from the screening study.

Nonconstant radial distributions of loss coefficient, stator exit flow angle, and total pressure were input so as to simulate the general characteristics of profiles actually measured in high speed compressors. This design approach gives an indication of the severity of blade end aerodynamic loading and incidence angles that will exist in the compressor, and allows the designer to select appropriate blade sections for these conditions.

After the axisymmetric flow analysis was completed, preliminary values of incidence angles, deviation angles, and camber and stagger angles were determined for each blade and vane row using General Electric correlations. In general, the analysis of each

configuration was carried sufficiently far to determine if major aerodynamic problem areas existed, but not so far as to represent a finished design.

Selected results of this analysis are presented in Figures 17 and 18. Mach numbers are seen to be moderate after the first one or two stages. The pitchline diffusion factor plots show that all three designs have highly loaded rear stators. Although these loadings are somewhat larger than usual and may require further design refinement in axial velocity ratios, swirl angles, and work input distributions, they are not believed to be so excessive as to present an unsolvable problem in achieving stall margin and efficiency goals.

De-Staged 23:1 Compressor

By examining the stagewise pressure distributions of the two 23:1 pressure ratio compressors, it was found that both designs had the potential of being useful as a building-block type compressor. For example, if the first stage of Configuration 26d5 were removed, an eight-stage, 13.9:1 pressure ratio compressor would result. If the last stage were removed, an eight-stage 18.3:1 pressure ratio compressor would be obtained. Similarly, the 11-stage design, Configuration 26b2, could form the basis of a 10-stage compressor with pressure ratios of either 14.5:1 or 18.9:1 by removing the first or last stage, respectively.

The results presented in Table V show that there would be little or no sacrifice in efficiency with the de-staged compressors when compared with the efficiency of Configuration 18c, the high efficiency 14:1 pressure ratio compressor. Another significant conclusion was that even though the de-staged compressors are heavier, cost more, and have more airfoils, they are still competitive with Configuration 18c on a direct operating cost and fuel usage basis. In fact, the direct operating cost and fuel usage of the eight-stage compressor and of Configuration 18c are nearly identical. This results because the lower speed of the de-staged compressor allows the turbine weight and cooling flow to be decreased without a significant sacrifice in turbine efficiency. Based on these results, it was concluded that a de-staged 23:1 pressure ratio compressor was competitive with the 14:1 pressure ratio compressor previously selected as an optimum design.

Off-Design Analysis

In addition to determining the estimated design point performance, a combination of semi-empirical and analytical methods was employed to generate performance maps for the 23:1 and 14:1 pressure ratio compressors. Stage characteristics were constructed consistent with stage design points and the estimated stall points. These stage characteristics were then employed in a stage stacking computer program capable of accounting for the effects of bleed and variable stators, and the performance was determined at several part-speed conditions for various bleed flows and stator schedules. The results of the study showed that sufficient part speed stall margin could be obtained with reasonable stator schedules and without the use of additional bleed flow, other than that normally needed for turbine cooling and aircraft cabin pressurization or air conditioning. It is expected that additional bleed flow will be required for engine starting.

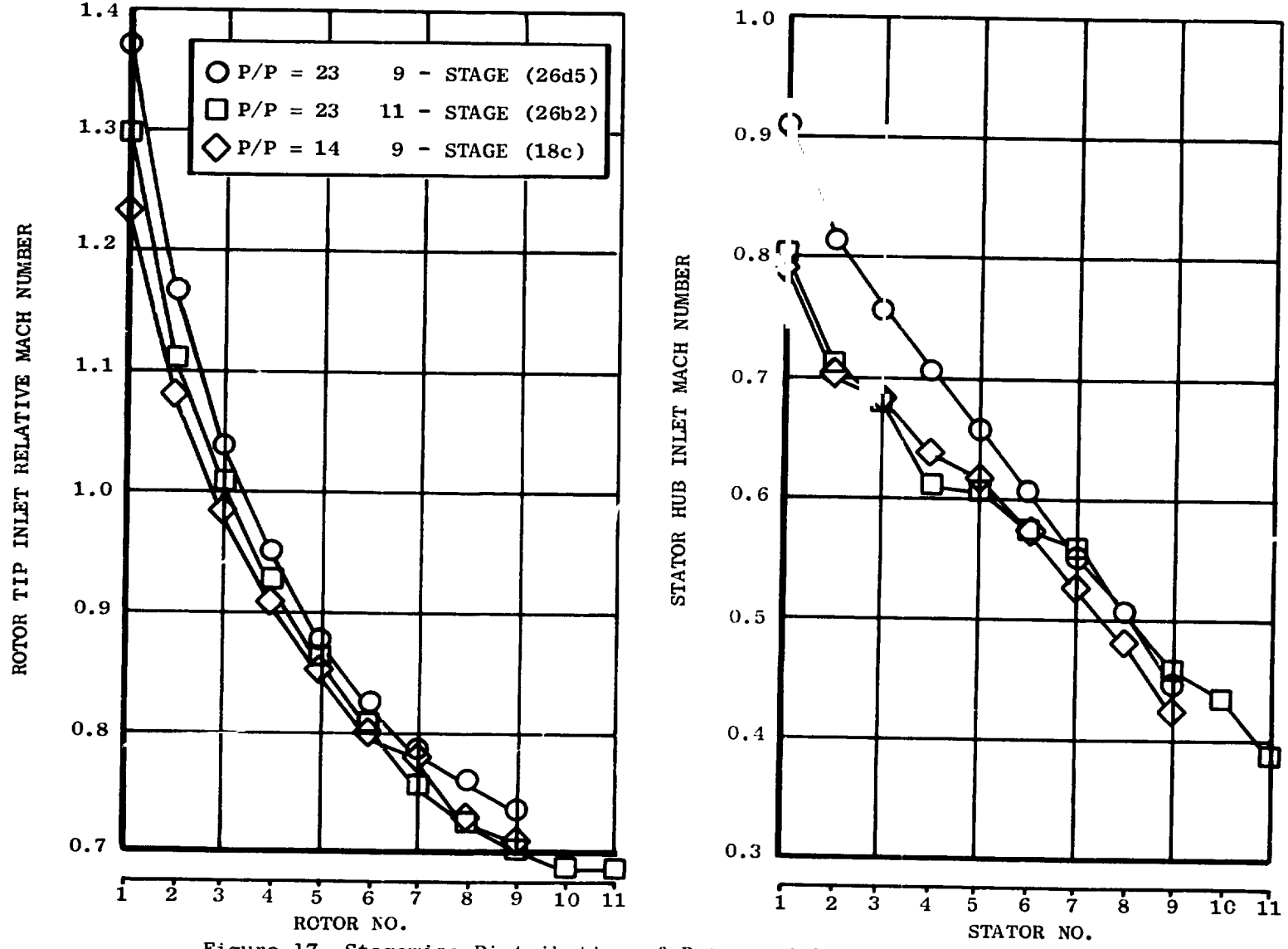

Figure 17 Stagewise Distribution of Rotor and Stator Mach Number for the Three Selected Compressors

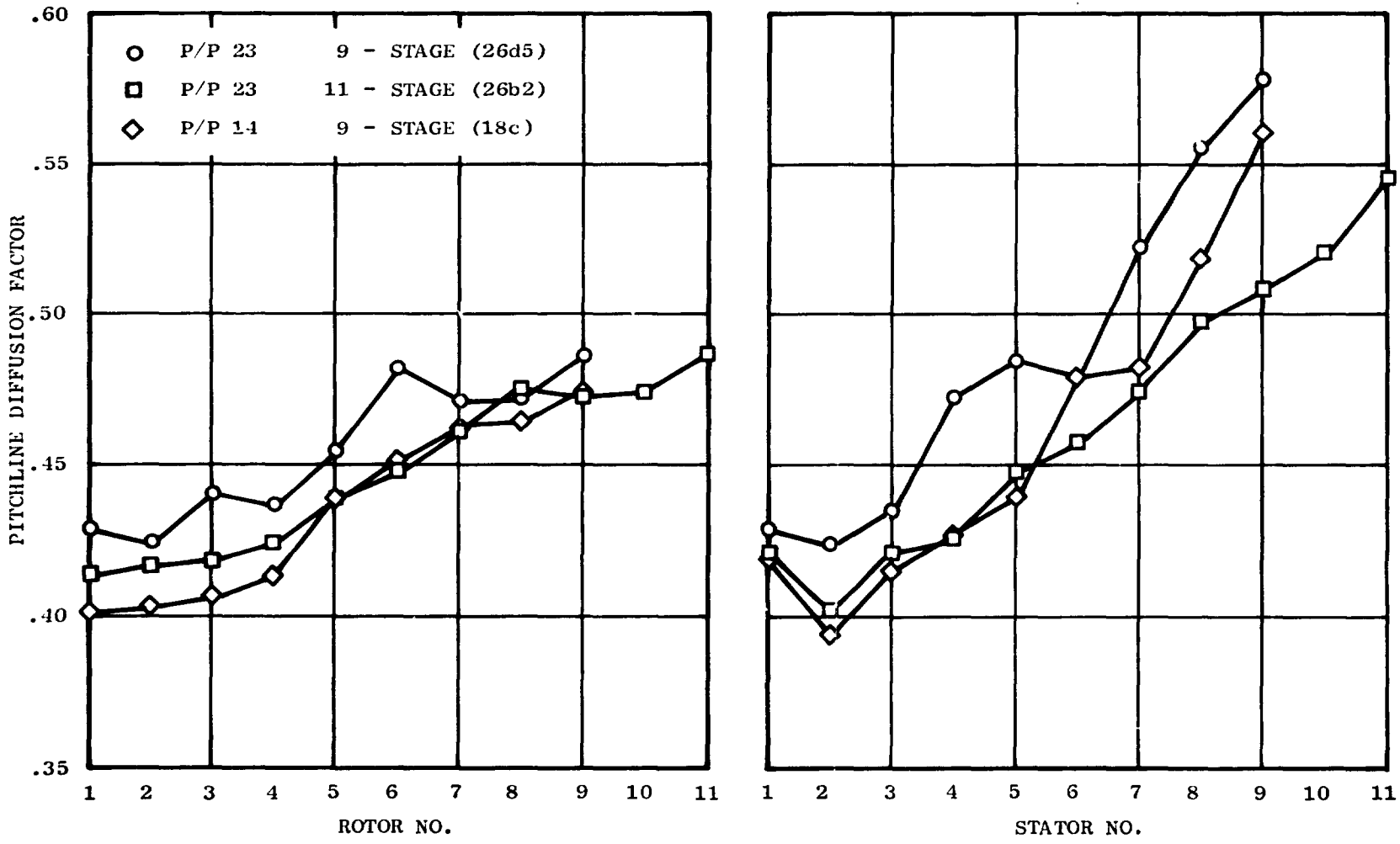

Figure 18 Stagewise Distribution of Rotor and Stator Pitchline Diffusion Factor for the Three Selected Compressors

Table V. Comparison of De-staged 23:1 Compressors with Configuration 18c.

Configuration	Stages 2 - 9 of Configuration 26d5	18c	Stages 2 - 11 of Configuration 26b2
Pressure Ratio	13.9	14.00	14.5
Corrected Flow, kg/sec (lbm/sec)	30.5 (67.3)	31.0 (68.4)	31.7 (69.9)
Number of Stages	8	9	10
Inlet Corrected Tip Speed, m/sec (ft/sec)	425 (1395)	437 (1435)	406 (1331)
Inlet Physical Tip Speed, m/sec (ft/sec)	476 (1562)	488 (1601)	453 (1488)
Exit Physical Hub Speed, m/sec (ft/sec)	393 (1290)	371 (1227)	354 (1163)
Physical Speed, rpm	14,436	15,983	13,333
Inlet Radius Ratio	0.656	0.566	0.624
Inlet Corrected Flow per Annulus Area, kg/sec m^2 (lbm/sec ft^2)	171.3 (35.7)	170.9 (35.0)	158.2 (32.4)
Inlet Tip Diameter, m (in)	0.6256 (24.63)	0.5832 (22.96)	0.6547 (25.12)
Exit Radius Ratio	0.936	0.911	0.930
Exit Mach Number	0.26	0.26	0.26
Exit Tip Diameter, m (in)	0.5588 (22.00)	0.4905 (19.31)	0.5358 (21.19)
Length, Rotor 1 Inlet to Outlet Guide Vane, m (in)	0.4112 (17.19)	0.5138 (20.23)	0.5860 (23.07)
Number of Blades and Vanes	1770	1626	2016
Adiabatic Efficiency at Outlet Guide Vane	0.871	0.875	0.876
Adiabatic Efficiency at Diffuser Exit	0.864	0.868	0.869
Compressor Weight, kg (lb)	217 (479)	198 (436)	235 (517)
\Compressor Price, % of STEDLEC Compressor Price	-1.2	-5.2	12.7
\Direct Operating Cost*, %	-0.75	-0.78	-0.54
\Fuel Usage*, %	-0.96	-0.95	-0.92

*Transcontinental trijet aircraft mission factors relative to STEDLEC baseline.

A 23:1 pressure ratio compressor performance map was constructed using the stage stacking results, combined with other General Electric experience, and is presented in Figure 19. It is seen that relatively low flows are delivered at part speeds. This is a desirable feature because it leads to high part-speed stall margin and reduced acceleration time from idle airflow to full airflow. The 14:1 compressor performance map is similar in character. In general, these performance maps indicate that sufficient part-speed stall margin and good part-speed efficiency are obtainable.

RECOMMENDED CONFIGURATION

The configuration for the Advanced Multistage Axial-Flow Compressor recommended as a result of this study program is a 10-stage compressor with a pressure ratio of 23:1. This compressor is a refinement of Configuration 26a that was developed during the screening studies. The two key issues that arose in selecting the recommended configuration were to determine which pressure ratio should be selected and how many stages should be selected.

The 14:1 pressure ratio compressors were driven by single-stage high pressure turbines and required booster stages to achieve the overall cycle pressure ratio. The 23:1 pressure ratio compressors had two-stage high pressure turbines and were unboosted. Results of the detailed design study showed smaller engine system economic differences between engine types than predicted in the parametric screening study. Engines using the 23:1 pressure ratio compressors had moderate fuel savings over those using the 14:1 compressors, although they had a slight direct operating cost penalty. In summary, there was no clear-cut advantage for either the boosted or the unboosted configuration based on the engine studies. The 23:1 pressure ratio compressor was selected primarily because it will provide technology directly applicable to either type of engine. If de-staged, as previously discussed, this compressor would form a good 14:1 pressure ratio compressor for a boosted engine and could be achieved without the extensive additional development that would be anticipated if the high pressure system pressure ratio were increased by adding a front stage.

The second issue to be decided was the number of stages to be recommended for the 23:1 pressure ratio compressor. In selecting the number of stages, certain key results of the detailed design studies showing the variation of performance and mechanical design factors with stage number were examined. Table VI lists comparative data for the nine-stage and 11-stage compressors studied in detail, and also presents estimated data for a lower speed, more refined version of the 14-stage Configuration 26a design. It can be noted in Table VI that the 14-stage compressor has better efficiency and acceleration time, but higher direct operating cost and fuel usage. Consequently, there is little benefit in selecting more than 11 stages. It is believed that a 10-stage compressor, when compared to the nine-stage, has the potential of achieving an overall core engine weight saving with better efficiency, faster acceleration time, and more acceptable development risk, all with little or no economic disadvantages. Selection of a 10-stage compressor, therefore, represents a reasonable compromise between the nine-stage and the 11-stage 23:1 pressure ratio compressors.

The flowpath of the recommended 10-stage compressor is shown in Figure 20. Comparisons of aerodynamic, mechanical, and economic parameters for the 9-stage, 10-stage, and 11-stage 23:1 pressure ratio designs are given in Table VII and reflect final weight and engine performance data at the completion of the detailed design studies. Final data for the nine-stage 14:1 pressure ratio design Configuration 18c is also given in the table.

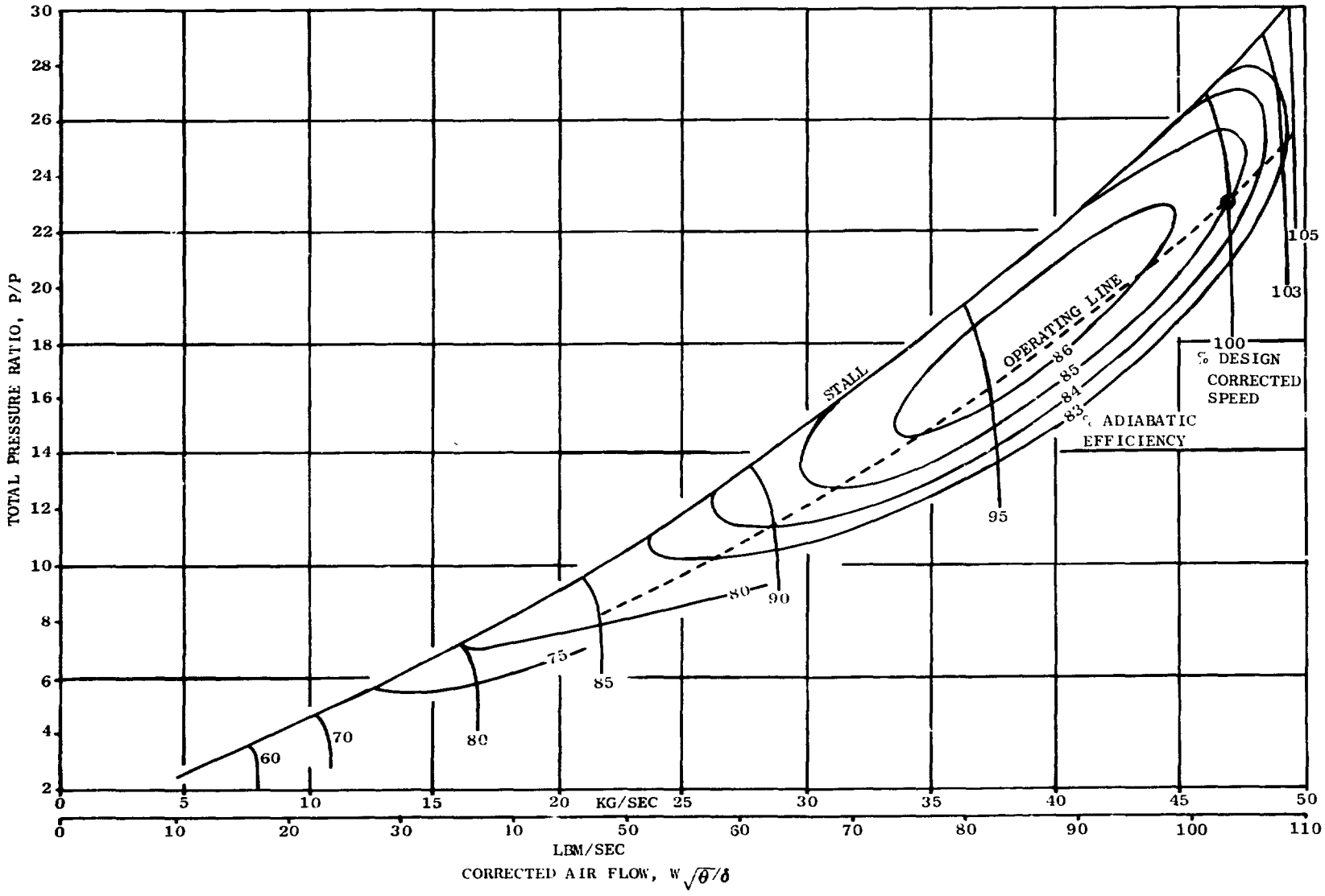

Figure 19 Estimated Performance Map for Recommended AMAC 23:1 Total-Pressure Ratio Compressor

Table VI. Detailed Design Study Results for 23:1 Total-Pressure Ratio Compressors

	9-Stg	11-Stg	14-Stg
Advanced Technology Efficiency, %	84.9	85.6	85.8
Current Technology Efficiency, %	82.7	83.4	83.9
Physical Speed, rpm	14,425	13,336	12,178
Turbine Efficiency, Δ points	+ 3.1	+ 3.0	+ 3.0
Rear Rim Speed, m/sec (ft/sec)	393 (1290)	355 (1164)	308 (1010)
Physical Rotor 1 Tip Speed, m/sec (ft/sec)	496 (1626)	472 (1549)	431 (1415)
Relative Accel Time	1.19	1.00	~0.9
Compressor Weight, kg (lb)	275 (606)	294 (648)	~338 ~(745)
Turbine Weight, kg (lb)	384 (847)	343 (757)	~316 ~(696)
ΔWeight (Compressor & Turbine) for 5% rpm Growth, kg (lb)	52 (114)	35 (78)	~32 ~(70)
Total Weight After Growth, kg (lb)	711 (1567)	673 (1483)	~685 ~(1511)
ΔCompressor Price, % of STEDLEC Relative to Base Compressor Price	12.2	27.4	~47
ΔDirect Operating Cost, *%	-0.40	-0.18	~0.45
ΔFuel Usage, *%	-1.93	-1.92	~-1.3

*Transcontinental trijet aircraft mission factors relative to STEDLEC baseline

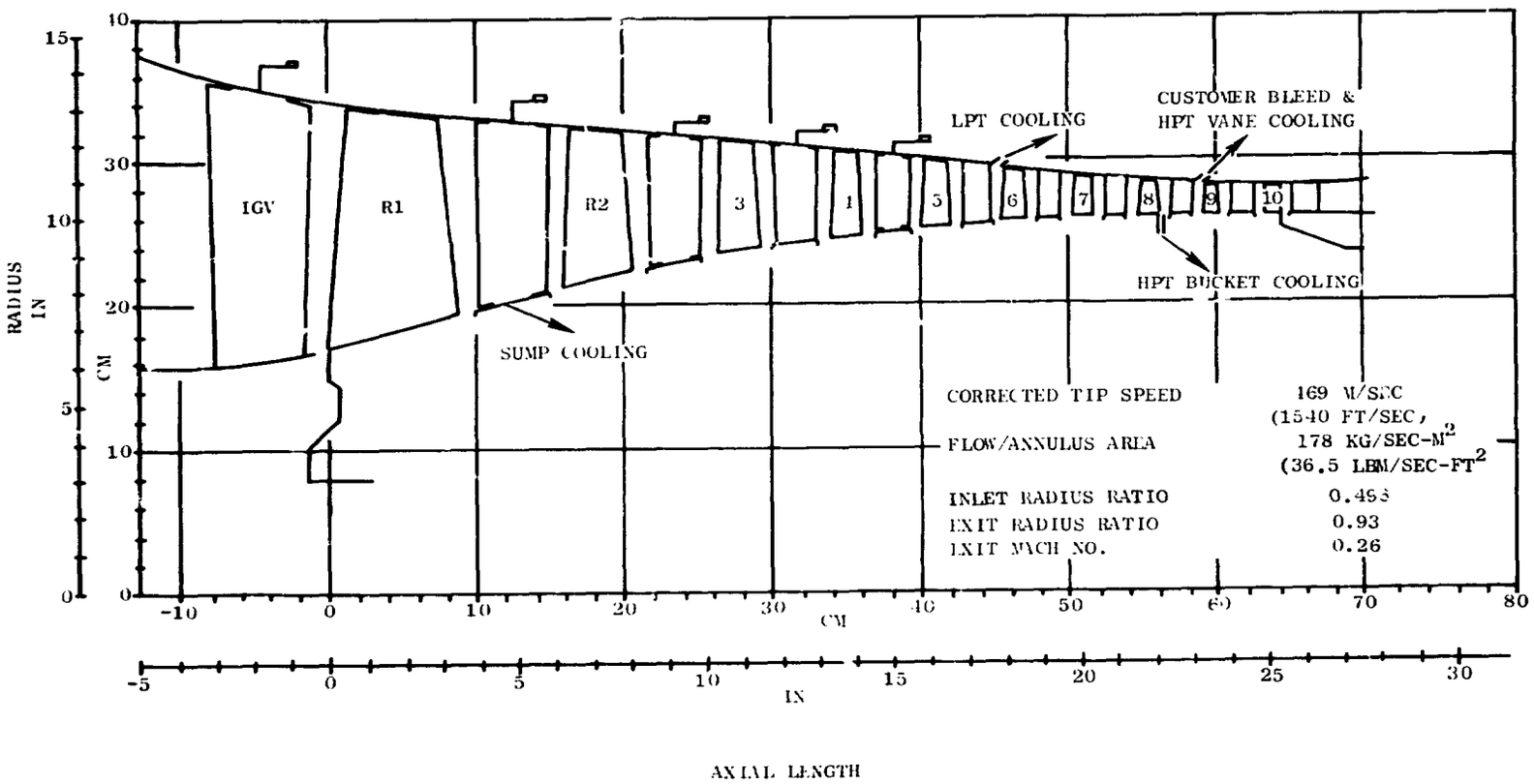

Figure 20 Flowpath of Recommended AMAC Compressor, Ten Stages, 23:1 Pressure Ratio, Configuration 26e2

Table VII. Comparison of Recommended 10-Stage AMAC Compressor With Final Data for Configurations 18c, 26b2 and 26d5.

Configuration Number	18c	26b2	AMAC	26d5
Total Pressure Ratio	14	23	23	23
Number of Stages	9	11	10	9
Corrected Inlet Tip Speed, m/sec (fps)	437 (1435)	457 (1500)	469 (1540)	480 (1575)
Physical Inlet Tip Speed, m/sec (fps)	488 (1601)	472 (1549)	485 (1590)	496 (1626)
Physical Rear Hub Speed, m/sec (fps)	374 (1227)	354 (1163)	370 (1214)	394 (1292)
Physical Speed, rpm	15,983	13,336	13,900	14,425
Inlet Radius Ratio	0.566	0.486	0.496	0.503
Inlet Specific Flow, kg/sec-m^2 (lb/sec-ft^2)	171 (35)	171 (35)	178 (36.5)	186 (38)
Inlet Tip Diameter, m. (in.)	0.5832 (22.96)	0.6761 (26.62)	0.6660 (26.22)	0.6563 (25.84)
Exit Radius Ratio	0.908	0.925	0.930	0.932
Exit Mach Number	0.26	0.26	0.26	0.26
Exit Tip Diameter, m (in.)	0.4912 (19.34)	0.5466 (21.52)	0.5456 (21.48)	0.5588 (22.00)
Length to OGV Exit, m (in.)	0.5169 (20.35)	0.7592 (29.89)	0.6614 (26.04)	0.5982 (23.55)
Length to Diffuser Exit, m (in.)	0.5387 (21.21)	0.7699 (30.81)	0.6900 (27.16)	0.6317 (24.87)
Number of Airfoils	1637	2035	1959	1810
Average Aspect Ratio	1.87	1.80	1.72	1.65
Average Solidity	1.39	1.39	1.40	1.48
Average Swirl, Degree	19.5	19.4	20.4	19.2
Average Reaction	0.714	0.715	0.695	0.701
Stall Margin, %	20	17	18	18
Adiabatic Efficiency at OGV Exit	0.875	0.863	0.860	0.856
Adiabatic Efficiency at Diffuser Exit	0.868	0.856	0.853	0.849
Compressor Weight, kg (lb)	225 (496)	294 (648)	269 (592)	275 (606)
Δ Compressor Price, % of STEDLEC Compressor Price	-5.1	27.2	18.0	12.2
Δ Engine Price*, % of STEDLEC Total Engine Price	-0.5	5.5	2.7	3.9
Δ Fuel Usage, %*	-1.02	-1.02	-1.99	-1.93
Δ Direct Operating Cost, %*	-1.02	-0.18	-0.35	-0.40

*Transcontinental trijet aircraft missions factors relative to STEDLEC baseline

MECHANICAL DESIGN STUDIES

Compressor mechanical design studies paralleled the aerodynamic design effort. An estimate was made of 1985 time period state of the art in the areas of clearance control, blade erosion resistance, achievable blade surface finish, and in the availability of materials and allowable stresses for blades, disks, and static structures. These assumptions were incorporated into preliminary design techniques used during the parametric screening study to estimate compressor weight, manufacturing cost, blade erosion life, and resulting blade replacement costs. Based upon the data generated in the parametric study, three compressor configurations were selected for further detailed mechanical study. This phase of the program was intended to determine if there were any structural problems that might lead to significant changes in the configuration, thereby affecting the efficiency, weight, or cost of the compressor. It also served to identify any problems which would require a major change in the engine layout, such as an additional frame at the compressor discharge.

COMPRESSOR MECHANICAL DESIGN TECHNOLOGY - 1985 STATE OF THE ART

Compressor mechanical design and development efforts at the General Electric Company have resulted in mechanical design innovations and techniques that have improved overall aerothermodynamic performance characteristics and provided significant advancements in the state of the art. The innovations included introduction of bore entry cooled compressor rotors, high strength low thermal mass disks, thermally shielded casing structures, low hysteresis variable stator mechanisms, removable casing liners with abradable rub coatings, and low loss, low heat generating seals. These innovations have provided improved clearance control and compressor efficiency and permitted higher rim speeds, higher stage pressure ratios, and higher compressor exit temperatures.

The 1985 state-of-the-art mechanical technology ground rules established for this study were based on application of these innovations, plus expected advancements in materials, manufacturing, and similar design disciplines. The following topics were specifically addressed: cooling and clearance control; blade surface finish; blade erosion; rear rim speed; inlet radius ratio; and system vibration as it relates to bearing placement.

Clearance Control

Realization of the full flow, pressure rise, and efficiency potential of any compressor is dependent upon maintaining small operating radial tip clearances. Recent experience at General Electric has indicated that significant future progress in compressor development, especially for subsonic turbofan applications, can be achieved by using advanced clearance

control features. These features include use of thermally shielded casing structures, cooled outer casing supports, use of advanced materials that would permit better matching of rotor and stator thermal growths, and use of internally cooled rotors. Analysis indicated that use of such clearance control techniques in the 1985 time period assumed for this study would enable compressors to operate with clearances approximately 25% smaller than those in current designs of the same type.

A tip clearance model was used to establish a base level of minimum running clearance-to-diameter for each stage in the compressor at the sea level takeoff operating condition where compressor physical speed, inlet temperature, and inlet pressure were highest. This minimum clearance was then adjusted to the altitude cruise operating condition where compressor performance was evaluated. This base level of clearance accounted for thermal and stress growths, rotor deflections from vibration or maneuvers, and manufacturing tolerances. Stage-to-stage differences in local temperature, materials, and type of rotor or stator construction were accounted for in the base clearance-to-diameter ratio established for each stage. Additional tip clearance was also provided as needed for each stage to allow for blade vibratory or stall deflections and for rotor/stator differential axial movement. This extra clearance was a function of rotor blade aspect ratio, blade height, and casing slope.

Airfoil Surface Finish

Airfoil surface finish has a significant impact on aerodynamics, especially in the latter stages of the compressor where Reynolds numbers are high. Recent advances in the field of electro-mechanical machining (ECM) have made it possible to forecast that a rotor blade airfoil surface finish of 0.25 micron (10 microinches) can be achieved and this level has been assumed for the rear stages in the analysis. Current capability is about 0.4 micron (16 microinches), and this base has been used for the forward stage rotor airfoils. Stator vane airfoil surface finishes have been maintained at the current level of 0.8 micron (32 microinches).

Blade Erosion

Blade erosion causes aerodynamic performance degradation, mechanical deterioration, potential engine loss due to foreign object damage, increased maintenance costs, and blade replacement costs. A new correlation of in-service data from commercial engines was developed to predict blade life and to identify key stages in the compressor where blade geometry could be adjusted to achieve increased life.

The erosion life estimations were based on data from the CF6-6 engine. A correlation was developed based on the consideration that blade erosion is a function of:

1. Time in hours or cycles on a wing position
2. Operating environment
3. Axial location in the compressor
4. Blade geometry
5. Blade tip speed
6. Blade material

Factors such as particle size, particle hardness and sharpness, and average impact angle were not considered explicitly in the analysis, but were assumed to be typical of those encountered by CF6 engines.

The erosion life estimation was based on rotor tip trailing edge thickness reduction. Blade life is assumed to be used up when a 50 percent reduction in trailing edge thickness occurs in the tip region.

Figure 21 depicts actual and predicted erosion lives for the CF6-6. Agreement is generally satisfactory, except for the rear stages where the actual life does not appear to be affected by the material change as would be predicted.

Rear Rim Speed

For compressor discharge temperatures and materials considered in this study, rear rim speeds are primarily limited by the increasingly severe weight penalties associated with an increasing rim speed. Therefore, for the purpose of the study, it was recommended that a rear rim speed of 380 m/sec (1250 ft/sec) not be exceeded unless the associated aerodynamic improvement offset the additional weight penalty. This limit was adhered to in the first phase of the screening study. However, it was subsequently relaxed, and the additional weight required was employed in the economic analysis.

Inlet Hub Radius

The effect of inlet hub radius on structure capability was studied to determine the minimum value that could be used. The level of torque to be carried by a fan shaft was estimated, and the corresponding size of the shaft thus dictated the minimum diameter of the stage 1 disk bore. As the inner flowpath diameter was decreased with the disk bore remaining fixed, a mechanically less efficient disk design resulted. Weight was added to overcome this inefficiency up to the point at which the design became untenable. For this study involving engines in the 147,000 n (33,000 pound) thrust size, the compressor flowpath inlet hub radius was restricted to a minimum value of 16.5 cm (6.5 in.).

System Vibration and Engine Bearing Layout

Current General Electric practice is to use two bearings to support the core rotor: one located at the front end of the compressor; and one located aft of the high pressure turbine. With this system, no core engine rotating parts are cantilevered. A more rigid rotor system is realized, and clearance changes due to maneuver loadings are minimized. A preliminary system vibration analysis was performed to determine if the two-bearing concept could be maintained for all the compressors to be studied. The analysis, which was later refined, indicated the two-bearing arrangement would be satisfactory.

Additional Mechanical Design Features

In addition to the above considerations, general ground rules were established for blade maximum thickness and edge thickness that were expected to lead to aeromechanically acceptable designs for the maximum, nominal, and conservative loading compressor configurations.

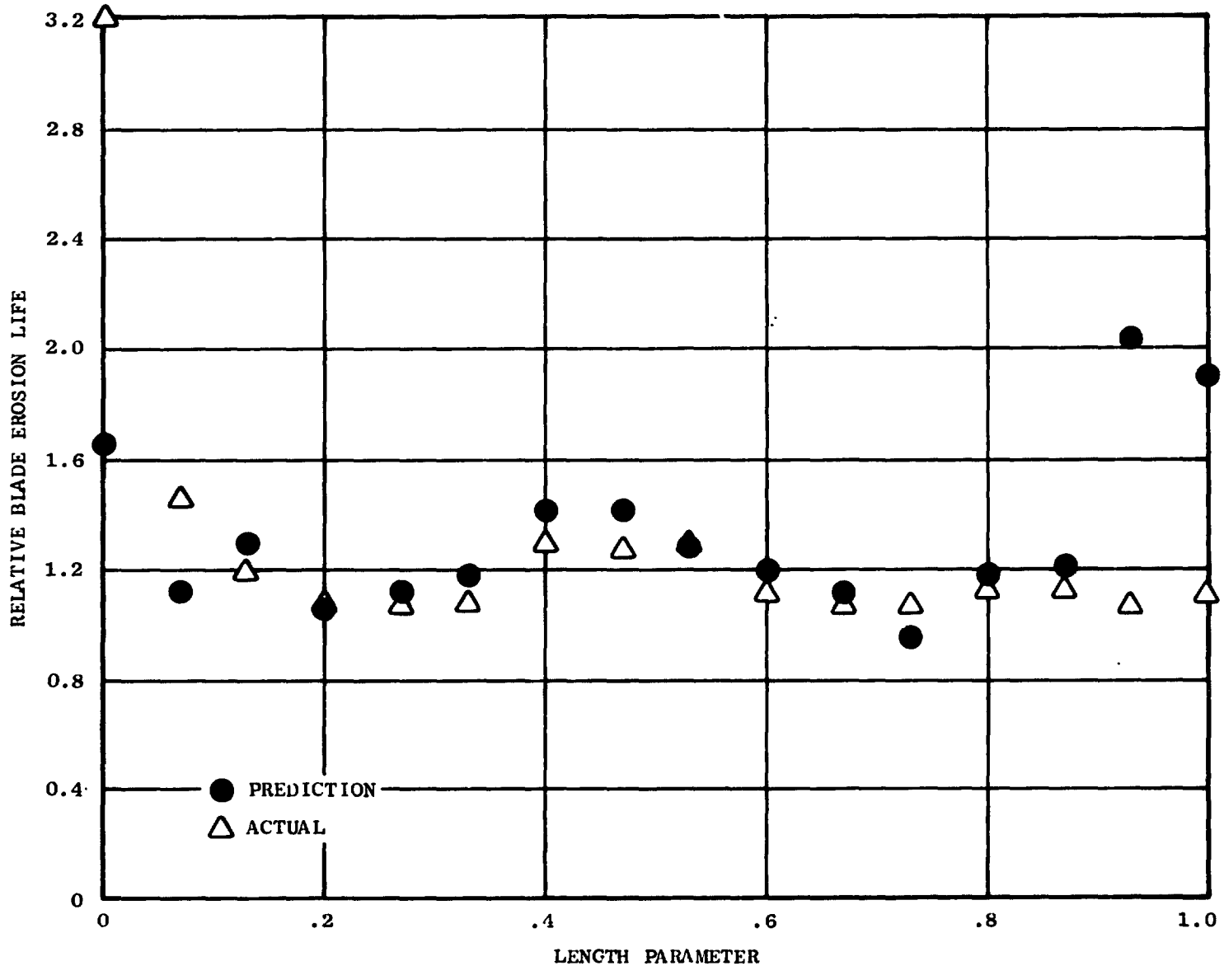

Figure 21 Comparison of Actual and Predicted Blade Erosion Life

Additional mechanical features were also assumed during the study in order to provide the potential for achieving the desired clearance control for aerodynamic performance, while providing a rugged, reliable, long life design. They included:

1. Casing liners with rub coatings
2. Shrouded stators with honeycomb interstage seals
3. Abrasive coated rotor spool interstage seal teeth
4. Horizontally split casings

Materials selected were 1985 state-of-the-art nickel- and titanium-base superalloy materials to permit high stress levels, while maintaining defect tolerances through increased fracture toughness. All components of the rotor were assumed to be designed using a selected combination of corrosion-resistant, high strength superalloys.

PARAMETRIC SCREENING STUDIES

The parametric screening studies were conducted to establish relative merits of the various configurations using a consistent set of assumptions. For the compressor rotor, the weight estimation assumptions included:

1. All spools would be fully inertia welded.
2. Disk temperature was assumed equal to stage exit temperature.
3. Disk size was set by equating average tangential stress to 0.02% yield strength.
4. Disk bore radii were set by manufacturing criteria for inertia welded spools.
5. Minimum disk web thickness was set at 0.165 cm (0.065 in.).
6. Spacers were 0.178 cm (0.070 in.) thick.

A computer program was developed utilizing these assumptions to: size the flowpath from the aerodynamic input; scale the rotor blade and disk rim weights; calculate the disk web thicknesses from the rim loads and allowable stress criteria; and calculate the disk, spacer, and shaft weights. The screening study initial costs for the rotor were based on the 250th unit cost for the F101 core compressor, quoted in 1974 dollars. The F101 compressor was chosen as a baseline because it is typical of an advanced, highly loaded, core compressor. Costs were scaled based on compressor weight, number of stages, number of blades, and included the effects of incorporating bore entry cooling.

Parametric studies of the compressor stator structure also utilized the F101 core compressor as the base for both weight and cost estimates. The mechanical configuration was assumed to be similar to that of the F101. The point where steel casing material had to be substituted for titanium was assumed to occur at approximately the same pressure and temperature as exists in the F101. Subsequent conceptual layouts of the selected candidate compressors validated the earlier cost and weight scaling assumptions.

Static component items scaled in the weight assessment studies included casings, liners, the radial support for the rear compressor case, airfoils, shrouds, lever arms, and actuation rings. Small components with minor influence upon the total assembly weight,

such as the variable stator actuator assembly, were assumed constant for all configurations. Scaling factors accounted for length, diameter, and quantity differences. Additional assumptions employed in the weight analysis included:

1. The inlet guide vanes and Stage 1 through 3 stator vanes were assumed to be variable with all remaining stages stationary. (For the detailed design study the number of variable stators required was related to the other compressor aerodynamic design variables using General Electric correlations.)

2. The required thickness of the forward compressor casing would be limited by manufacturing capability rather than compressor size and internal pressure.

3. The required thickness of aft casings is greatly influenced by stress limitations and, therefore, largely dependent upon pressure loading and size.

The base for stator cost projections was an estimate established by the General Electric Development Manufacturing Engineering Operation for the 250th unit of the F101 compressor in 1974 dollars. Individual component costs were ratioed by quantity and size differences to arrive at the individual component and total costs of the candidate compressors.

A tabulation of mechanical design data for all the compressors studied in the parametric screening study is presented in Table VIII.

DETAILED DESIGN STUDY

The mechanical layout of the three compressor configurations selected for detailed design study are shown in Figures 22, 23, and 24 for configurations 26b2, 26d5, and 18c, respectively. The major mechanical characteristics of each are also tabulated in these figures. These configurations were analyzed in detail to assure no problems existed that could not be eliminated by prudent application of current design practices. Specifically, these included blade stresses, blade natural frequencies, blade stability, dovetail stresses, disk stresses, stresses in related shafting and attaching shell structures, and system vibration characteristics.

The designs were based on achieving the objectives of high reliability, durability, safety, ease of maintenance and ease of assembly. Design requirements were consistent with those of current engines:

1. 15% margin over 2/rev excitation
2. Life - 36,000 cycles/36,000 hours
3. Material properties were average minus 3 sigma
4. Blade and disk dovetails stronger than the blade airfoil
5. Disk burst speed greater than 122% speed
6. No engine system critical speeds in the operating range
7. Blades designed to be "stall protected" from aeromechanical instabilities

Table VIII. Parametric Screening Study Mechanical Design Results.

Configuration Number	Pressure Ratio	Number of Stages	Corrected Rotor One Inlet Tip Speed m/sec (ft/sec)	Physical Rear Rim Speed m/sec (ft/sec)	Design Physical rpm	Δ Rotor Weight kg* (lb)	Δ Stator Weight kg* (lb)	Δ Total Weight kg* (lb)	Minimum Relative Blade Life†
1	14:1	12	415 (1360)	336 (1101)	15148	-12 (-28)	14 (32)	2 (4)	2.04
2		6	454 (1490)	381 (1250)	14411	26 (56)	-17 (-37)	9 (19)	2.83
3		9	385 (1263)	344 (1127)	13513	0 (0)	0 (0)	0 (0)	2.83
4			360 (1182)	321 (1053)	12646	31 (68)	8 (19)	39 (87)	4.83
5			407 (1335)	363 (1191)	14283	-16 (-36)	-4 (-8)	-20 (-44)	1.65
6			365 (1197)	326 (1068)	12807	3 (6)	5 (12)	8 (18)	3.17
7			411 (1349)	367 (1203)	14433	-4 (-9)	-6 (-13)	-10 (-22)	2.43
8			384 (1261)	343 (1124)	13491	1 (1)	0 (0)	1 (1)	2.83
9			388 (1272)	346 (1134)	13609	1 (2)	0 (0)	1 (2)	2.78
10			377 (1238)	338 (1109)	13245	1 (1)	0 (0)	1 (1)	3.04
11			399 (1309)	353 (1160)	14005	3 (5)	1 (3)	4 (8)	3.00
12			376 (1232)	339 (1113)	13351	-3 (-7)	-3 (-5)	-5 (-12)	2.74
13			398 (1305)	350 (1147)	13755	5 (11)	3 (6)	8 (17)	3.09
14			369 (1210)	352 (1156)	11273	21 (46)	12 (27)	33 (73)	3.17
15			397 (1304)	337 (1106)	14935	-7 (-17)	-6 (-13)	-13 (-30)	2.65
16			337 (1105)	359 (1179)	11822	14 (30)	7 (15)	21 (45)	2.57
17			444 (1457)	322 (1057)	15588	-8 (-17)	-7 (-1)	-14 (-31)	2.87
18a		12	387 (1270)	313 (1028)	14145	-2 (-5)	22 (48)	20 (43)	2.83
18b		10	415 (1360)	348 (1143)	15148	-4 (-9)	8 (17)	4 (8)	2.30
18c		9	437 (1435)	374 (1227)	15983	-6 (-14)	0 (0)	-6 (-14)	2.13
18d		8	460 (1510)	398 (1306)	16819	-4 (-9)	-9 (-20)	-13 (-29)	1.70
18e		8	492 (1614)	387 (1270)	17534	-5 (-11)	-9 (-19)	-14 (-30)	1.70
18f		7	489 (1604)	416 (1364)	17866	8 (17)	-15 (-33)	-7 (-16)	1.83
19a		9	442 (1451)	321 (1053)	15524	1 (2)	-5 (-10)	-4 (-8)	5.43
19b		9	428 (1405)	311 (1019)	15032	4 (9)	5 (10)	9 (19)	6.22
19c		9	435 (1428)	316 (1036)	15278	4 (7)	2 (5)	6 (12)	5.96
20	23:1	14	492 (1615)	315 (1034)	14356	4 (9)	70 (155)	75 (164)	2.00
21		7	491 (1610)	381 (1250)	11731	91 (199)	13 (30)	104 (229)	2.70
22		10	428 (1404)	357 (1171)	11355	50 (109)	33 (74)	83 (183)	2.57
23		9	474 (1555)	370 (1213)	14544	9 (20)	6 (14)	15 (34)	1.83
24	14:1	8	419 (1375)	374 (1226)	14676	2 (-6)	-9 (-19)	-11 (-25)	2.48
25	14:1	10	357 (1170)	318 (1043)	12517	6 (12)	9 (21)	15 (33)	3.39
26a	23:1	14	451 (1480)	301 (987)	13155	30 (66)	60 (132)	90 (198)	2.61
26b		11	501 (1642)	340 (1116)	14596	22 (47)	31 (69)	53 (116)	2.04
26c		10	522 (1712)	358 (1174)	15218	23 (50)	26 (58)	49 (108)	1.87
26d		9	541 (1775)	382 (1252)	15767	25 (54)	13 (30)	38 (84)	1.74
26e		10	472 (1547)	366 (1200)	13751	36 (78)	30 (66)	65 (144)	2.13
26b2		11	457 (1500)	354 (1163)	13356	30 (66)	37 (82)	67 (148)	1.96
26d2		9	491 (1610)	388 (1273)	14301	34 (74)	20 (44)	54 (118)	2.00
26d5		9	480 (1575)	394 (1292)	14447	30 (66)	18 (40)	48 (106)	2.00

*Relative to Configuration Number 3

†Based on GE CF6-6 Experience

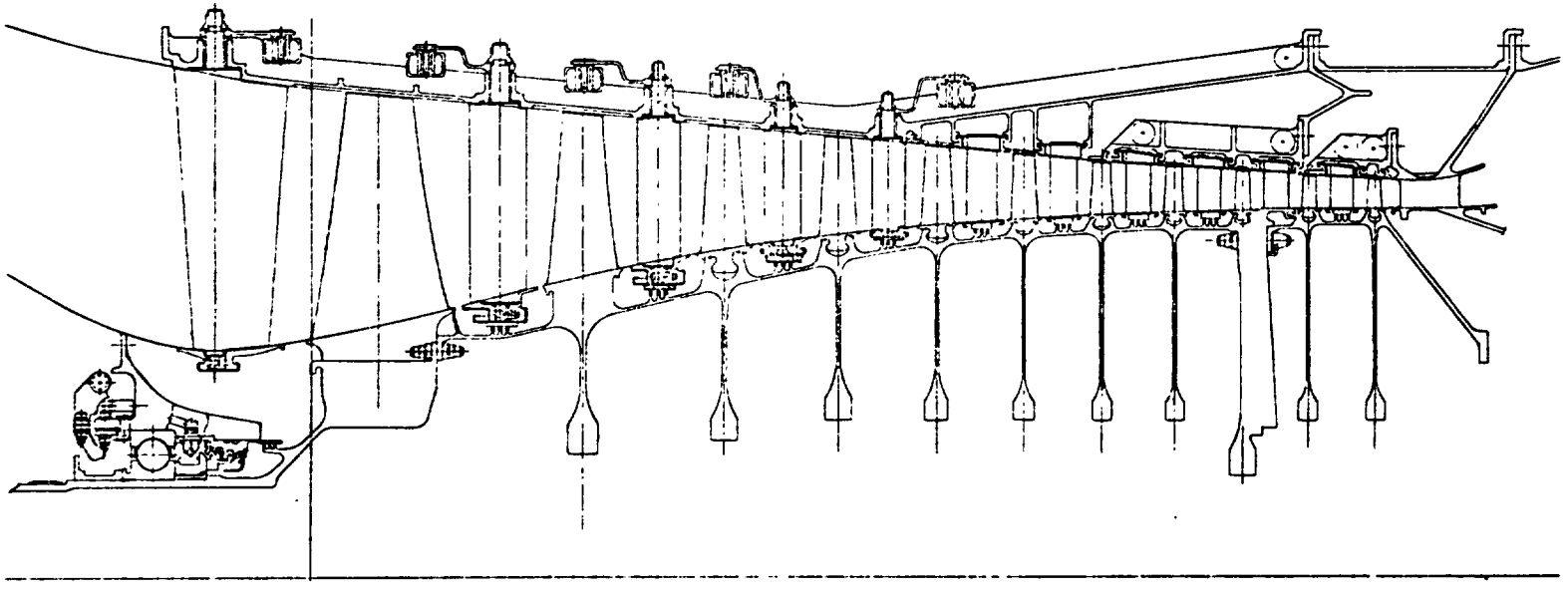

DESIGN RPM = 13336

INLET RADIUS RATIO = 0.486

R1 INLET TIP SPEED = 472 M/SEC
(1549 FT/SEC)

REAR RIM SPEED = 354 M/SEC
(1163 FT/SEC)

ROTOR WEIGHT = 142 KG
(313 LB)

COMPRESSOR WEIGHT = 294 KG
(648 LB)

Figure 22 Mechanical Layout of Configuration 26b2, Eleven Stages, 23:1 Pressure Ratio

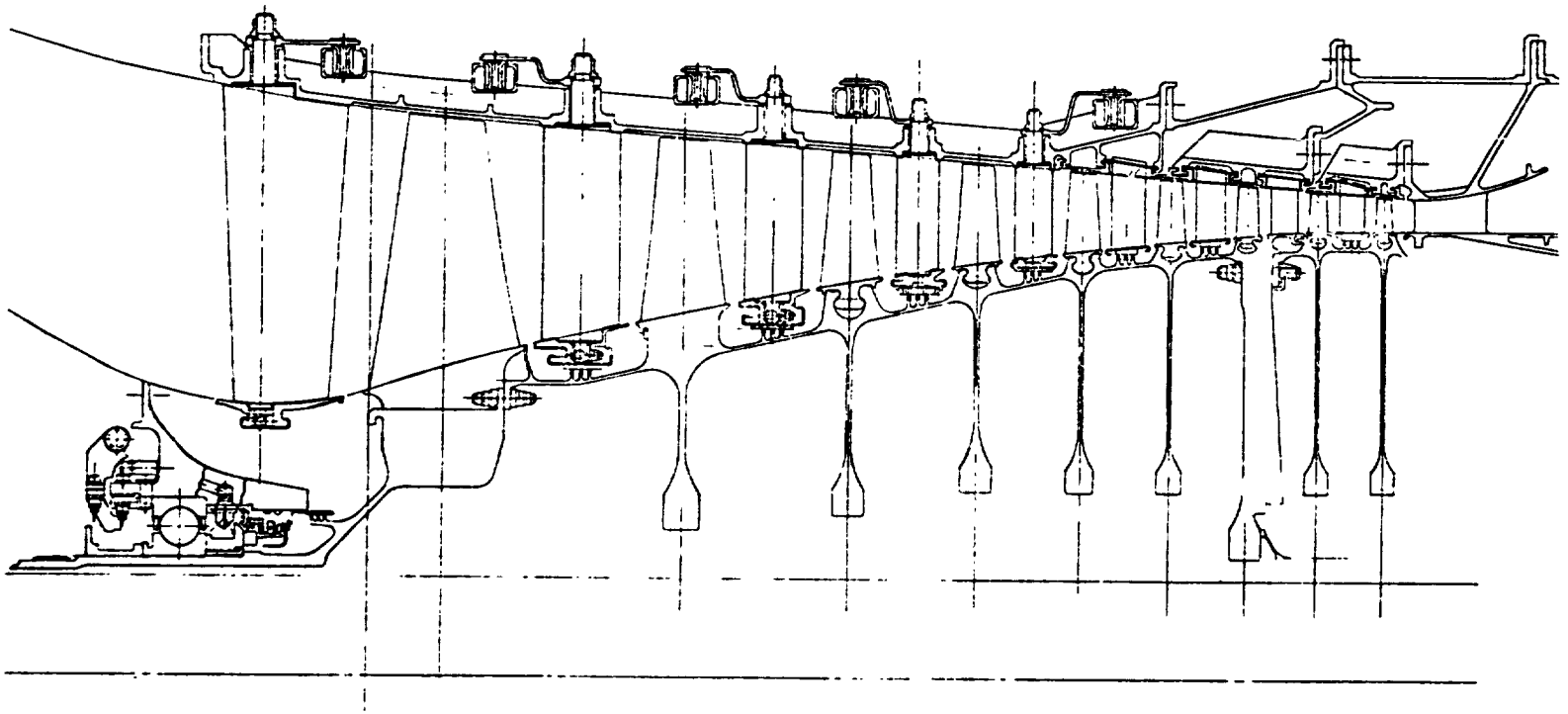

DESIGN RPM = 14,425

INLET RADIUS RATIO = 0.503

R1 INLET TIP SPEED = 496 M/SEC
(1626 FT/SEC)

REAR RIM SPEED = 394 M/SEC
(1292 FT/SEC)

ROTOR WEIGHT = 142 KG
(313 LB)

COMPRESSOR WEIGHT = 275 KG
(606 LB)

Figure 23 Mechanical Layout of Configuration 26d5, Nine Stages, 23:1 Pressure Ratio

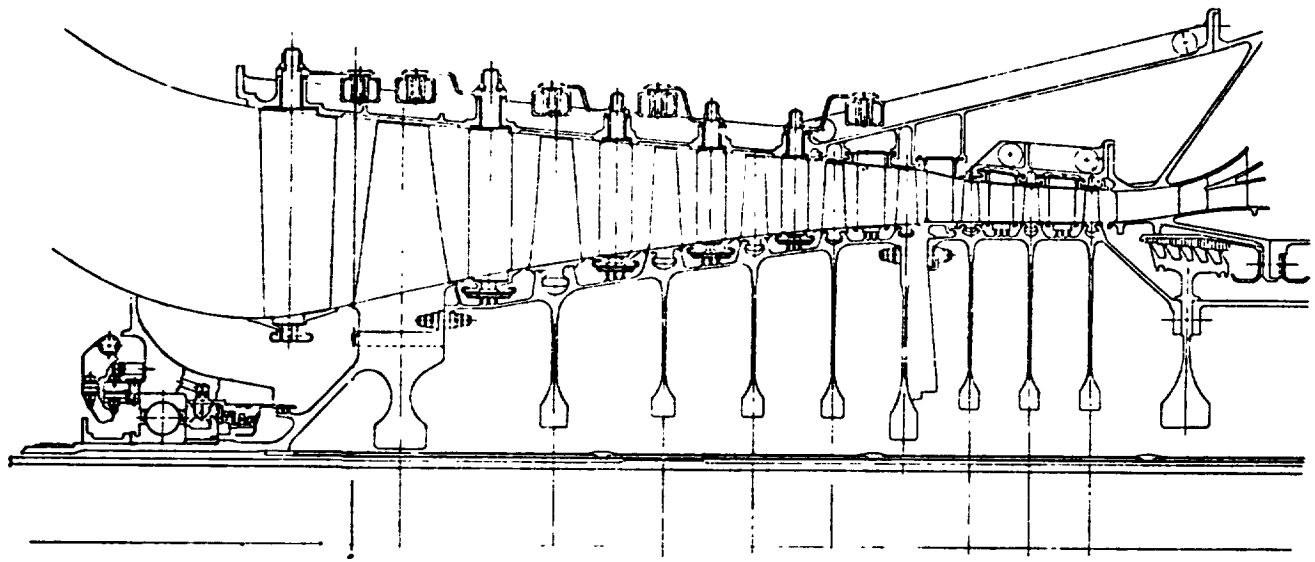

DESIGN RPM = 15983
INLET RADIUS RATIO = 0.566
R1 INLET TIP SPEED = 488 M/SEC
(1601 FT/SEC)

REAR RIM SPEED = 374 M/SEC (1227 FT/SEC)
ROTOR WEIGHT = 110 KG (243 LB)
COMPRESSOR WEIGHT = 225 KG (496 LB)

Figure 24 Mechanical Layout of Configuration 18C, Nine Stages, 14:1 Pressure Ratio

Blades and Vanes

The airfoils for the selected configurations were analyzed to determine their vibratory characteristics. Figure 25 shows Campbell diagrams for stages 1 and 9 of the 9-stage 23:1 pressure ratio design (Configuration 26d5). The diagrams are typical of the remaining stages of this compressor, and also of the other two configurations. In some instances, particularly in the first rotor, blade geometry might have to be adjusted to avoid resonances in the operating range. However, it was believed that only small changes to the chord or thickness would be required to increase blade flexural frequency enough to assure avoidance of resonances.

The aeromechanical stability of the rotor blades was also studied. The blading was checked to assure the blades were "stall protected"; i.e., the blades would stall prior to encountering blade aeromechanical instability. The analysis indicated that most rotors had adequate stability margin and that only small refinements to blade geometry would be required to achieve adequate stability margin on all rotors.

Table IX presents a summary of rotor blade mechanical design parameters for the three configurations.

Dovetails

The dovetails were analyzed to see if the blade and disk dovetails were stronger in fatigue than the airfoils. The dovetails were of conventional design (axial and/or circumferential straight line) with anti-fretting coatings to permit high levels of crush stress. No problems were uncovered in this area.

Disks and Structure

The disks were analyzed for basic stress levels and burst speed margins. Design allowables used were typical of advanced materials now in use. A summary of stage 1 and stage 9 disk mechanical design data for the three configurations is also given in Table IX. No untenable problems were found to exist in the stages analyzed.

System Vibration

A preliminary engine system vibration analysis was performed on the three compressor configurations recommended for further evaluation in order to evaluate potential vibration problems and to determine preference, if any, for one of the compressor configurations.

Analytical system vibration models of the three core compressors were established using the mechanical design information determined in the study. The engine system modeled was the NASA/General Electric STEDLEC Baseline Engine, with proper modifications to fit each compressor design. STEDLEC component weight estimates, and NASA/General Electric QCSEE or F101 component stiffnesses were used where applicable. The vibration analyses were conducted using the General Electric System Vibration and Static Analysis Program. The program was used to determine engine system critical frequencies, modal deflection patterns, and system response due to unbalance. These parameters were determined for critical frequencies of vibration which were synchronous with the core or synchronous with the low pressure rotor speed.

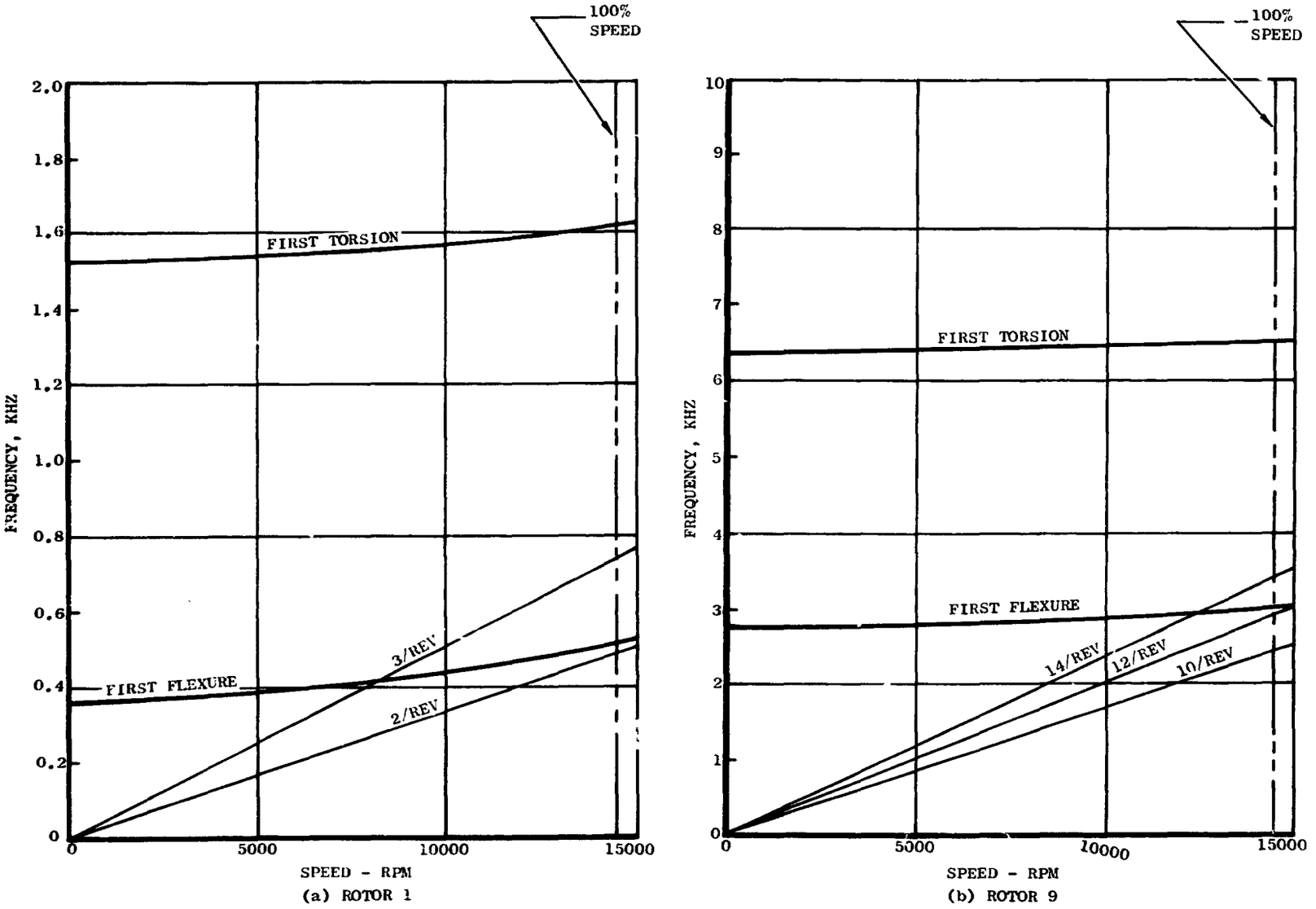

Figure 25 Campbell Diagrams for Rotors One and Nine, Configuration 26d5

Table IX. Rotor Blade and Disk Mechanical Design Summary.

	18c P/P = 14		26b2 P/P = 23		26d5 P/P = 23	
ROTOR BLADE	Stage 1	Stage 9	Stage 1	Stage 11	Stage 1	Stage 9
Number of blades	28	98	24	128	28	140
Material	Ti-8-1-1	1718	Ti-8-1-1	1718	Ti-8-1-1	1718
Average blade height, cm	11.6	2.26	1[illegible]0	2.03	14.6	2.00
(in.)	(4.569)	(0.891)	(6.280)	(0.799)	(5.765)	(0.788)
Chord (Tip), cm.	7 25	1.88	9.97	1.69	9.15	1.82
(in.)	(2.855)	(0.742)	(3.925)	(0.666)	(3.603)	(0.716)
Chord (Root), cm.	7.25	1.88	9.97	1.69	9.15	1.82
(in.)	(2.855)	(0.742)	(3.925)	(0.666)	(3.603)	(0.716)
Max thickness to chord ratio (Tip)	0.025	0.042	0 025	0.044	0.025	0.042
Max thickness to chord ratio (Root)	0.090	0.090	0.090	0.090	0.090	0.090
Solidity (Tip)	1.119	1.[illegible]93	1.143	1.252	1.238	1.446
Solidity (Root)	1.870	1.313	2.183	1.352	2.260	1.[illegible]58
Stagger (Tip)	62.6	63.1	64.2	61.0	61.5	64.1
Stagger (Root)	30.3	56.7	20.9	55.2	20.9	57.8
Camber (Tip)	8.5	7.0	7.1	10.0	8.7	10.2
Camber (Root)	39.7	19.2	50.3	2[illegible].1	37.3	17.0
Root Stress MPa	397	183	411	130	441	151
(KSI)	(57.5)	(26.5)	(59.6)	(18.9)	(64.0)	(22.1)
ROTOR DISK						
Material	Ti-17	R95	Ti-17	R95	Ti-17	R95
Bore Temperature ° C	216	499	216	510	216	199
(° F)	(420)	(930)	(420)	(950)	(420)	(930)
Mat'l Prop						
.2% Yield Stress at Bore Temperature MPa	765	1138	765	1138	765	1138
(KSI)	(111)	(165)	(111)	(165)	(111)	(165)
Ultimate Tensile Strength at Bore Temperature, MPa.	945	1189	945	1189	945	1189
(KSI)	(137)	(216)	(137)	(216)	(137)	(216)
.2% Plastic Creep (36,000 hrs), MPa	724	965	724	965	724	965
(KSI)	(105)	(140)	(105)	(140)	(105)	(140)
Stresses @ Design Pt.						
Bore Stresses, MPa.	631	938	631	903	634	945
(KSI)	(92)	(136)	(92)	(131)	(92)	(137)
Average Tangential Stress, MPa.	---	641	---	593	---	669
(KSI)	---	(93)	---	(86)	---	(97)
Web Effective Stress, MPa.	---	738	---	703	---	724
(KSI)	---	(107)	---	(102)	---	(105)

A possible core compressor excitation of the low pressure system (fan) shaft was found to be the most significant vibratory mode. This response sensitivity of the shaft to core rotor excitation is characteristic of two-spool engine systems using two main frames. Operating experience has shown that vibration problems have not resulted, because current state-of-the-art balancing techniques have been quite effective in holding vibration levels within safe limits. No severe core bending modes were found in the operating speed range of the core, and the system vibration spectrum for the low pressure rotor excited modes was found to be free of problems for all three compressor configurations.

For the three compressor configurations evaluated, no preference could be established based solely on the system vibration analysis. The low pressure system shaft excursions resulting from core rotor excitation are not expected to present a vibration problem for any of the three core compressor configurations.

Blade Erosion

Blade erosion estimates were revised for the three compressor configurations based on the final blade geometry data. In some instances, trailing edge thicknesses were made slightly thicker to attain a goal of 20 percent improvement in blade life over the current CF6-6 compressor rotor. For the recommended compressor configuration, a 50 percent improvement was specified.

Revised Compressor Weight Estimates

At the completion of the detailed design study, when all parts in the compressors had been sized so as to be structurally adequate, a final revised estimate of compressor weight was made. This was done partly as a check on the accuracy of the preliminary estimating method used in the parametric screening study, and also to account for detailed refinements in blade chord and thickness that had been made for structural or erosion life reasons during the detailed study. The revised weights were approximately 10 percent greater than given by the preliminary method for all three configurations. Since the change in estimated weight was essentially the same for each configuration, it was concluded that the relative merits of the various designs studied would not be affected.

RECOMMENDED CONFIGURATION

Configuration 26e2, recommended for design, manufacture, and test, is a 10-stage compressor with a 23:1 pressure ratio. This configuration was not studied in detail, since its mechanical design parameters were roughly midway between those of the nine- and 11-stage designs that had been studied. However, preliminary weights and costs were generated along with estimates for erosion life. Table X lists the estimated erosion lives of the compressor blades. Other compressor characteristics for the recommended configuration are listed below.

Pressure Ratio	23:1
No. of Stages	10
Design Speed (rpm), Uncorrected	13,900
Inlet Radius Ratio	0.496
Rotor One Inlet Tip Speed m/sec (ft/sec), Uncorrected	485 (1590)
Rear Rim Speed m/sec (ft/sec), Uncorrected	370 (1214)
Compressor Weight kg (lb)	269 (592)

Table X. Configuration 26e2 Compressor Erosion Summary.

Stage	Solidity	Chord		Tip Speed		Trailing Edge Thickness		Relative Blade Life*
		cm	(in)	m/sec	(ft/sec)	cm	(in)	
1	1.23	9.28	(3.65)	464	(1521)	0.093	(0.037)	3.66
2	1.26	5.36	(2.11)	448	(1469)	0.080	(0.032)	3.32
3	1.32	3.76	(1.48)	437	(1434)	0.056	(0.022)	2.42
4	1.36	3.05	(1.20)	426	(1397)	0.046	(0.018)	2.02
5	1.38	2.67	(1.05)	418	(1372)	0.040	(0.016)	1.82
6	1.41	2.38	(0.94)	410	(1345)	0.036	(0.014)	1.72
7	1.42	2.11	(0.83)	404	(1324)	0.032	(0.013)	1.54
8	1.43	1.97	(0.77)	398	(1305)	0.030	(0.012)	2.70
9	1.44	1.90	(0.75)	393	(1290)	0.028	(0.011)	2.96
10	1.45	1.93	(0.76)	392	(1285)	0.029	(0.011)	3.02

*Relative to CF6-6 average blade life experience.

ENGINE SYSTEM STUDIES

METHODS AND GROUNDRULES

Since the relative merit of each of the advanced compressor configurations is influenced by the performance of other engine components and by installation effects, engine systems studies were performed in order to arrive at the net impact of each configuration on typical aircraft mission performance. Aircraft mission merit factors used to measure performance were direct operating cost (DOC), return on investment (ROI), and fuel consumed (WF). Since DOC and ROI include the effects of fuel consumption on aircraft economics, they were considered to be the primary indicators in determining the relative merit of each compressor configuration.

Factors considered in the study (in addition to compressor performance) were:

1. Effect of engine performance, weight, and price on typical aircraft mission performance
2. Installation (including pylon) weight, price, and drag as influenced by engine length
3. Engine performance, expressed as specific fuel consumption, as influenced by engine type (boosted or unboosted)
4. Number of required high pressure turbine stages as influenced by core compressor pressure ratio
5. High pressure turbine weight, price, efficiency, and cooling flow requirements as influenced by core compressor rotational speed
6. Low pressure turbine efficiency and cooling flow requirements as influenced by engine type (boosted or unboosted)

The methods and ground rules used in evaluation of each of the above factors are described in detail in the following sections.

Aircraft Mission Analysis

The mission analysis procedure used in the study was identical to that used in prior NASA STEDLEC studies (Reference 2). Two baseline aircraft were defined: a domestic 3-engine trijet aircraft with a design range of 5550 km (3000 nm) and a total gross weight of

101,200 kg (223,000 lb); and an international 4 engine quadjet aircraft with a design range of 10,180 km (5500 nm) and a total gross weight of 145.200 kg (320,000 lb). Both aircraft were sized for 200 passenger capacity and appropriate fuel reserves. A parametric aircraft sizing procedure was used with varying wing loading and engine thrust to arrive at the minimum aircraft gross weight consistent with mission requirements. Other aircraft performance ground rules that were influential in aircraft sizing were a takeoff balanced field length, a sea level takeoff thrust per engine of approximately 88,900n (20,000 lb), and a minimum rate of climb of 1.52 m/sec (5 ft/sec) at the nominal cruise altitude of 10,600 m (35,000 ft) and 0.8 Mach number. Advanced technology aircraft features, such as a high aspect ratio wing (AR = 12), a high average cruise lift coefficient ($C_L \approx 0.52$), low cruise drag, and a high cruise lift/drag ratio ($L/D \approx 17$), were assumed.

Finally, each of the aircraft was exercised on an average mission of 1300 km (700 nm) for the trijet and 3700 km (2000 nm) for the quadjet using a load factor of 55 percent to determine the impact of engine performance quantities such as specific fuel consumption, weight, price, and maintenance cost on aircraft merit factors (DOC, ROI, and WF). Fuel costs were assumed to be 7.9 cents/ℓ (30 cents/gal) for the trijet and 11.9 cents/ℓ (45 cents/gal) for the quadjet.

Engine maintenance costs for each component, other than costs for compressor blade erosion, were estimated by using a component Parts Index* based on CF6-6 service experience. This index, together with the component initial price, then established total maintenance material costs accrued by each component. Summing the component maintenance costs and spreading them over the aircraft service life then determined the average hourly maintenance material costs. In addition to material replacement costs, maintenance labor costs equal to 2/3 of the material costs were added, again based on CF6 service experience. These costs were spread over a 15 year aircraft service life with average yearly utilizations of 3020 flight hours and 3840 flight hours, respectively, for the domestic and international range aircraft.

Compressor blade erosion life was handled separately from other engine maintenance costs. Average compressor erosion blade life and blading prices as defined in previous sections were used to compute engine maintenance costs due to blade erosion. Blade replacement costs associated with erosion were based on reworking or replacing all blade rows whose erosion life would have been used up before the next compressor maintenance. The time between compressor maintenance was determined by the stage having the minimum erosion life. Based on experience, the assumption was made that the compressor would be available for maintenance work approximately at these intervals l[illegible]use of other required engine work not resulting from compressor blade erosion. Th[illegible]re, the erosion costs did not include the labor involved in an engine removal and tear[illegible].

Installation Effects

A typical mixed flow installation as shown in Figure 26 was used for this study. Aircraft accessories were mounted inside the pylon to permit utilization of a cylindrical cross section, minimum-drag nacelle. Since the variations in booster, core compressor, and

*Parts Index = number of times a part is replaced during the life of the engine.

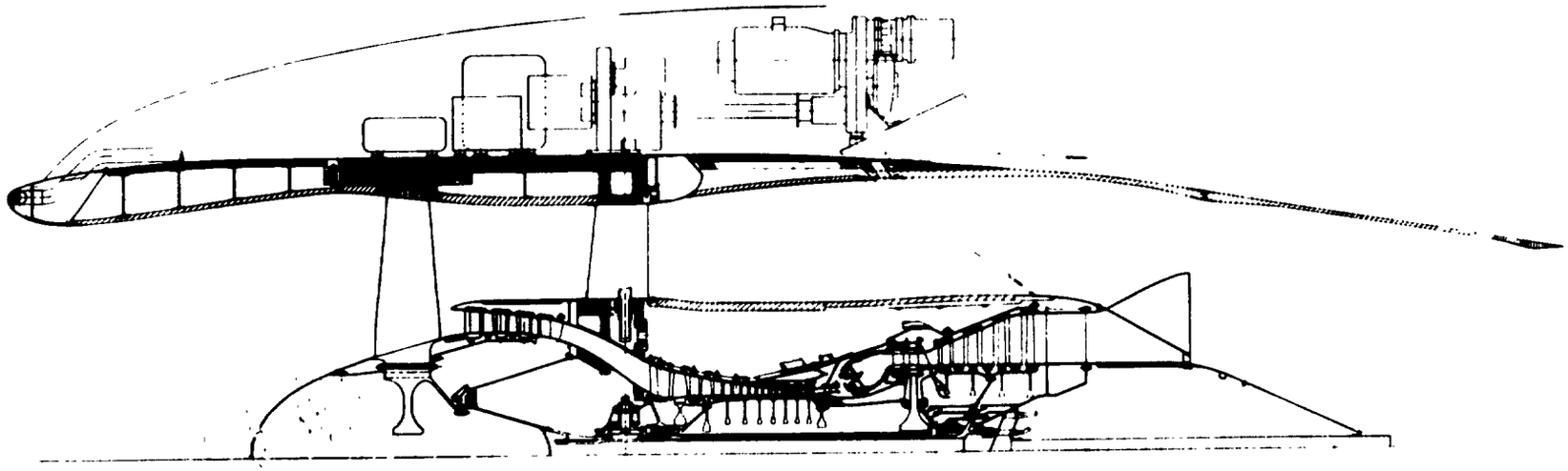

Figure 26 Typical Mixed Flow Installation Used for the Study

high pressure turbine staging inherent in this study could affect engine and installation length, the impact of engine length changes on installed drag was determined. The computed drag change with engine length assumed the nacelle inlet and exhaust sections were unaffected by engine length; only the center cylindrical portion of the nacelle was varied. The net effect of nacelle length, diameter ratio, nacelle surface area, and pylon surface area was then represented in terms of installation drag.

Engine Performance

Nominal engine cycles were established for both the boosted (14:1 pressure ratio core compressor) and unboosted (23:1 pressure ratio core compressor) engine types as shown in Table XI. The boosted engine cycle and nominal components were identical to those defined in the prior NASA-STEDLEC study (Reference 2), while a new unboosted cycle was defined to provide a basis for evaluation of the 23:1 pressure ratio core compressors. Note that the unboosted cycle retained the same overall cycle characteristics (overall pressure ratio = 38, T_4 = 1371° C (2500° F) @ max climb) as those of the boosted engine and was sized for the same fan corrected airflow. A two-stage, high pressure turbine was used for the unboosted cycle, since the turbine pressure ratio requirement was higher than practical for a single stage.

Since these cycles were established for nominal component performance levels, and component performance was an inherent variable of this study, cycle derivatives (influence coefficients) were determined to provide a basis for evaluating component performance changes. For ease of evaluation, the influence coefficients were established at constant engine thrust; i.e., fan and core compressor size were varied in order to maintain constant core engine energy extraction and constant use as component performance levels were changed. The net effects on required fan and core compressor size and on specific fuel consumption could then be determined.

Turbine Performance Effects

The basic factors that arise in considering the turbine performance effects are:

1. High pressure turbine staging effects as influenced by core compressor pressure ratio

2. High pressure turbine efficiency and cooling flow requirements as influenced by core compressor rotational speed selection

3. Low pressure turbine efficiency and cooling flow requirements as influenced by core compressor pressure ratio

The high pressure turbine efficiency variation with stage loading was based on a General Electric correlation of the observed performance of a number of specific designs. The two-stage turbine for the 23:1 pressure ratio core was assessed as having an efficiency potential of 2.6 points greater than the single-stage turbine for the 14:1 pressure ratio

Table XI. Boosted Versus Unboosted Cycle Comparison.

Mixed Flow - Nominal Components

Power Setting	Boosted (STEDLEC)			Unboosted		
	Maximum Climb	Maximum Cruise	Take-Off	Maximum Climb	Maximum Cruise	Take-Off
Altitude/Mach No., m (ft)	10.7k/0.8 (35K/0.8)	10.7k/0.8 (35K/0.8)	0/0 (0/0)	10.7k/0.8 (35K/0.8)	10.7k/0.8 (35K/0.8)	0/0 (0/0)
\Temperature relative to Standard Day, °C (°F)	10 (+18)	10 (+18)	15 (+27)	10 (+18)	10 (+18)	15 (+27)
Bare Engine Thrust, n (lb)	38,900 (8740)	35,600 (8010)	147,000 (33160)	38,600 (8670)	35,500 (7990)	149,000 (33600)
Relative Specific Fuel Consumption	1.004	1.00	------	0.9879	0.9833	------
Overall Pressure Ratio	38	36	30	38	36	30
High Pressure Turbine Inlet Temperature, °C (°F)	1371 (2500)	1326 (2420)	1427 (2600)	1371 (2500)	1326 (2420)	1427 (2600)
Bypass Ratio	6.9	7.1	7.5	7.0	7.2	7.6
Corrected Fan Flow, kg/sec (lbm/sec)	568 (1253)			568 (1253)		
Fan Pressure Ratio	1.71			1.71		
Boost Pressure Ratio	2.75			1 67 (Fan Hub)		
Core Compressor Pressure Ratio	14			23		
Corrected Core Compressor Flow, kg/sec (lbm/sec)	31.0 (68.4)			46.8 (103.2)		
No. High Pressure Turbine Stages	1			2		
High Pressure Turbine Pressure Ratio	3.8			4.4		
No. Low Pressure Turbine Stages	1+1/2			4+1/2		
Low Pressure Turbine Pressure Ratio	5.68			4.9		

core compressor. This performance differential was based upon the observed performance of typical cooled designs and is due to a number of factors, two of which are reheat effects and cooling effects, with the two-stage turbine showing a performance advantage from both effects.

Turbine cooling variations with staging and stage loading were computed with the aid of other correlations of General Electric data. Ground rules were selected to be consistent with achievable cooling systems and the availability of advanced materials and to provide a consistent basis for computing cooling flow trends. Use of these correlations and ground rules, together with turbine velocity diagram calculations to define a gas path heat load parameter, provided the required estimates of cooling flow variation with turbine loading.

The low pressure turbine efficiency and cooling flow requirements were established in a similar manner. The low pressure turbine for the 23:1 pressure ratio compressor required less cooling air than that used with the 14:1 pressure ratio compressor by virtue of the reduced inlet temperature. The major impact was in the first stage blading, which was uncooled for the turbine used with the 23:1 pressure ratio compressor. This reduction in cooling air impacted turbine efficiency, since less expansion energy in the downstream stages was available. Hence, with the 23:1 pressure ratio compressor, the low pressure turbine had a slightly reduced efficiency potential.[1]

Detailed turbine weight and price estimates were made for the turbine configurations used with the nominal 14:1 and 23:1 pressure ratio compressors, and empirical scaling relationships were used to evaluate the effect of rotational speed changes or these nominal values.

A maximum turbine rotational speed of approximately 17,000 rpm was established for both the 14:1 and 23:1 pressure ratio compressors. This limit was established based on mechanical feasibility of the turbine rotor blades and blade attachments in the 147,000 n (33,000 lb) thrust engine design size.

PARAMETRIC SCREENING STUDY

As previously discussed, a series of preliminary compressor aerodynamic designs was carried out in which key parameters were varied systematically. The results of this parametric screening study were used to evaluate the different compressor configurations in typical aircraft missions.

A nominal single-stage high pressure turbine and a compatible low pressure turbine flow path were established for the core engine having a 14:1 pressure ratio compressor as shown in Figure 27. This turbine flowpath was found suitable for all of the 14:1 pressure ratio core compressor configurations with the exception of Configurations 14 and 16. The relatively low rpm of these compressors exceeded the allowable single-stage loading limit, and for these two cases, the turbine diameter was increased to bring the high pressure turbine stage loading within acceptable limits. This also resulted in a less heavily loaded, more efficient, low pressure turbine.

---

(1) Chargeable cooling air is assumed to completely bypass the turbine in the cycle calculations. The adjustment to turbine efficiency accounts for the fact that some work is done by the chargeable cooling air.

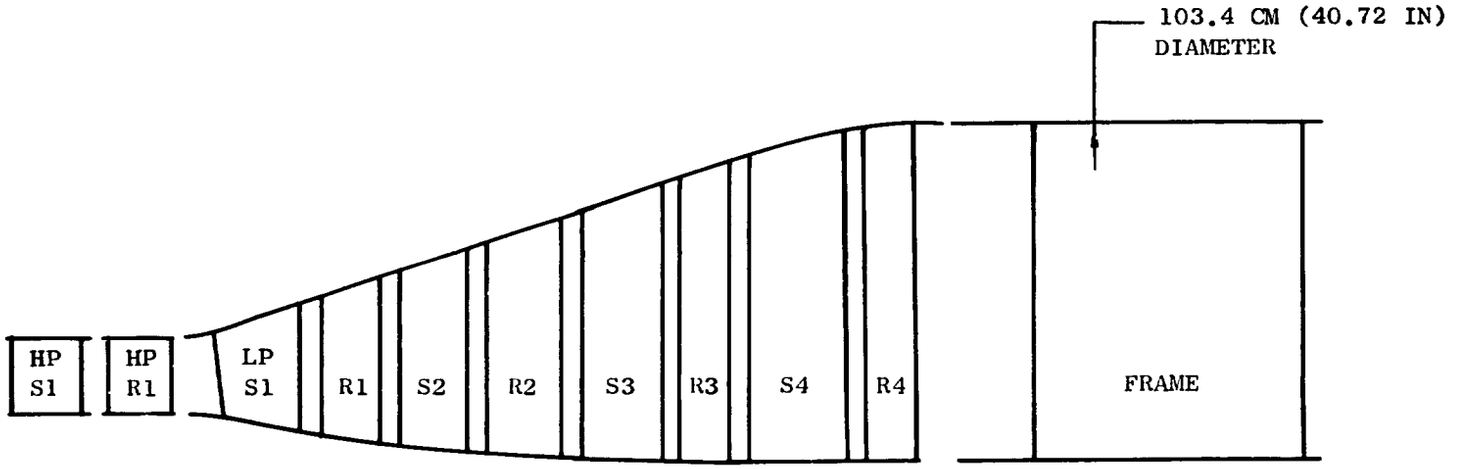

HP TURBINE

DELTA ENTHALPY = 488 KJ/KG (210 BTU/LB)

AV. PITCH DIAMETER = 75.5 CM (29.72 IN)

LP TURBINE

DELTA ENTHALPY = 456 KJ/KG (196.15 BTU/LB)

SPEED = 4460 RPM

AV. PITCH DIAMETER = 80.5 CM (31.7 IN)

WORK COEFFICIENT = 1.61

Figure 27 Nominal Turbine Flowpath for 14:1 Pressure Ratio Advanced Compressor

Similarly, a nominal two-stage high pressure turbine and matching low pressure turbine flow path was established for the core engines having a 23:1 pressure ratio compressor (Figure 28). Since the rotational speed variation was less than that of the 14:1 pressure ratio compressor, this flowpath was found to be suitable for all the 23:1 pressure ratio core compressors.

A summary of the component and engine weight and price variations, installation effects, and maintenance costs in the design size for each of the compressor configurations is presented in Table XII. It can be seen that the high pressure turbine weight variation far exceeds that of the compressor and is generally of an opposite sign. In terms of component and engine price variation, the compressor has the dominant effect, while turbine price is relatively insensitive to compressor configuration. Installation effects include the pylon, and maintenance cost data include parts and labor, as previously discussed. Although not shown in Table XII, an interesting result of the analysis was that the compressor efficiency variation, as listed in Table II, was far greater than the variation in turbine efficiency. Turbine cooling flow and intercompressor duct pressure loss variations were also fairly small. Thus, bare engine fuel consumption trends tended to be dominated by variations in core compressor performance.

Component performance levels that established the bare engine fuel consumption and the data contained in Table XII represent the total input to the aircraft system evaluation. The data given in Table XII are for the design size engine. Two final scaling steps were required on engine and installation weight and price to obtain the data presented in the last four columns of Table II. The first scaling step was required to adjust the core engine and the installation weight and price for the noted component performance differences, while the second scaling step was required to adjust the weight and price data to the engine size appropriate for the mission. The missions were 88,900 n (20,000 lb) sea level static take-off thrust and 93,300 n (21,000 lb) thrust for the trijet and quadjet, respectively.

The overall results of the engine system analysis have been summarized previously in Table II. Data in Table II are given only for the domestic transcontinental range trijet aircraft mission, since the trends seen for this case were typical of the international range mission as well. All aircraft system performance data given in Table II include the economic effects of compressor blade erosion.

REFINED SCREENING STUDY

The trends of compressor efficiency and engine system merit factors versus compressor design parameters established during the parametric screening study were used to define two families of high-efficiency compressors for further study. These families were the 14:1 pressure ratio Configuration 18 series for use in boosted engines and the 23:1 pressure ratio Configuration 26 series for use in unboosted engines. Because of the high efficiencies of these compressors, engines were obtained having superior economic and fuel usage ratings compared to those studied in the earlier parametric screening study. In addition to using design parameters shown to give high compressor efficiency, considerable attention was also devoted in this phase of the study to determining the effects that the number of compressor stages had on overall engine system performance and economics.

Table XII. Summary of Component Weight, Price, Installation, Maintenance and Specific Fuel Co... Pressure Ratio Compressors (Design Size Engines).

Compressor Configuration	Number Stages	ΔCompressor Weight kg (lb)	ΔHigh Pressure Turbine Weight kg (lb)	ΔLow Pressure Turbine Weight kg (lb)	ΔInstallation Weight kg (lb)	ΔTotal Installed Engine Weight (1),(3) kg (lb)	ΔCompressor Price %	ΔHigh Pressure Turbine Price %
Base	9	0	0	0	0 (0)	0 (0)	0	0
1	12	-4 (-8)	29 (63)	0	21 (47)	46 (102)	0.1	0
2	6	3 (7)	14 (31)	0	-30 (-66)	-13 (-28)	-0.3	0
3	9	0	-5 (-12)	-5 (-12)	0 (0)	-11 (-24)	-0.1	0
4	9	34 (75)	-11 (-24)	0	31 (68)	54 (119)	0.8	0
5	9	-25 (-56)	12 (26)	0	-17 (-37)	-30 (-67)	-0.3	0
6	9	3 (6)	-9 (-20)	0	-1 (-3)	-8 (-17)	0.4	0
7	9	-15 (-34)	15 (32)	0	0 (-1)	-1 (-3)	-0.6	0
8	9	-5 (-11)	0 (0)	0	-1 (-2)	-6 (-13)	-0.1	0
9	9	-5 (-10)	1 (3)	0	1 (3)	-2 (-4)	0	0
10	9	-5 (-11)	-4 (-8)	0	2 (4)	-7 (-15)	0	0
11	9	-2 (-4)	7 (16)	0	0 (0)	5 (12)	-0.1	0
12	9	-11 (-24)	-2 (-4)	0	-4 (-8)	-16 (-36)	-0.1	0
13	9	2 (5)	4 (8)	0	6 (13)	12 (26)	0	0
14	9	28 (61)	-11 (-24)	10 (22)	-22 (-48)	5 (11)	1.0	0
15	9	-19 (-42)	24 (53)	0	18 (40)	23 (51)	-0.5	0
16	9	15 (33)	-4 (-8)	10 (22)	-5 (-11)	16 (36)	0.5	0
17	9	-20 (-43)	39 (85)	0	5 (11)	24 (53)	-0.5	0
18A	12	14 (31)	10 (21)	0	28 (62)	52 (114)	0.9	0
18B	10	-2 (-4)	29 (63)	0	15 (34)	42 (93)	0.1	0
18C	9	-12 (-26)	49 (108)	0	8 (17)	45 (99)	-0.4	0
18D	8	-19 (-41)	77 (170)	0	0 (0)	59 (129)	-0.8	0.1
19A	9	-9 (-20)	37 (82)	0	11 (25)	40 (87)	-0.2	0
19B	9	3 (7)	26 (58)	0	20 (45)	50 (110)	0	0
19C	9	0 (0)	32 (69)	0	20 (44)	51 (113)	-0.1	0
24	8	-17 (-37)	19 (41)	0	-8 (-17)	-6 (-13)	-0.6	0
25	10	10 (21)	-12 (-27)	0	10 (21)	7 (15)	0.5	0
26B2	10	25 (55)	-2 (-4)	0	0 (0)	23 (51)	0.9	0
"De-staged" 26D5	8	8 (17)	15 (32)	0	-18 (-40)	4 (9)	-0.2	0
"De-staged" 20	14	69 (152)	167 (368)	-18 (-39)	29 (65)	145 (319)	1.8	5.8
21	7	98 (217)	95 (210)	-18 (-39)	-47 (-103)	26 (58)	2.1	6.5
22	10	78 (171)	88 (195)	-18 (-39)	-23 (-50)	23 (50)	2.1	6.7
23	9	10 (22)	176 (388)	-18 (-39)	-14 (-31)	51 (113)	0.3	5.8
26A	14	84 (186)	127 (280)	-18 (-39)	41 (91)	132 (291)	2.9	6.2
26B	11	47 (104)	179 (395)	-18 (-39)	10 (21)	115 (254)	1.4	5.8
26B2	11	62 (136)	132 (290)	-18 (-39)	9 (19)	81 (179)	1.9	6.0
26C	10	44 (96)	212 (468)	-18 (-39)	6 (13)	141 (311)	1.1	5.8
26D	9	33 (72)	257 (567)	-18 (-39)	-20 (-43)	150 (330)	0.6	5.9
26D2	9	48 (106)	166 (365)	-18 (-39)	-17 (-38)	76 (167)	1.0	5.8
26D5	9	43 (94)	172 (380)	-18 (-39)	-10 (-21)	85 (187)	0.9	5.9
26E	10	60 (132)	144 (318)	-18 (-39)	3 (6)	86 (190)	1.6	6.0

(1) A Δweight of -103 kg (-227 lb) was applied to the unboosted engine weights in addition to the above component Δweights to obtain the Δtotal engine weight. This was done to account for the fact that these engines did not have booster stages whereas the base configuration did.

(2) A Δprice of -3% was applied to the unboosted engine price in addition to the above component prices to obtain the Δtotal engine price. This was done for the same reasons as discussed in footnote (1).

(3) These totals are for design size engines.

Specific Fuel Consumption Data for the 14:1 and 23:1

ompressor Price %	ΔHigh Pressure Turbine Price %	ΔLow Pressure Turbine Price %	ΔInstallation Price %	ΔTotal Installed Engine Price (2),(3) %	ΔCompressor Blading Maintenance Costs $/Flight Hour	Δ All Other Engine Maintenance Costs $/Flight Hour	ΔBare Engine Specific Fuel Consumption at Cruise, %	ΔInstalled Drag, Drag/Thrust, %
0	0	0	0	0	0	0	0	0
0.1	0	0	0.4	0.5	-1.52	+0.03	-0.7	+0.12
-0.3	0	0	-0.6	-0.9	-1.98	-0.11	+3.7	-0.16
-0.1	0	0	0	-0.1	-1.85	-0.03	+0.2	0
0.8	0	0	0.6	1.4	-2.30	+0.27	+1.6	+0.19
-0.3	0	0	-0.3	-0.6	-0.25	-0.09	+0.5	-0.10
0.4	0	0	0	0.4	-1.67	+0.12	+0.8	0
-0.6	0	0	0	-0.6	-2.02	-0.18	+0.6	0
-0.1	0	0	0	-0.1	-1.85	-0.03	+0.6	0
0	0	0	0	0	-1.83	-0.02	+0.2	+0.01
0	0	0	0	0	-1.82	-0.01	+0.5	+0.01
-0.1	0	0	0	-0.1	-1.92	-0.04	-0.3	0
-0.1	0	0	-0.1	-0.2	-1.77	-0.05	+0.6	-0.02
0	0	0	0.1	0.1	-1.90	+0.01	-0 2	+0.02
1.0	0	0.1	-0.4	0.7	-1.58	+0.31	+0.2	-0.11
-0.5	0	0	0.4	-0.1	-1.97	-0.14	-0.3	+0.10
0.5	0	0.1	-0.1	0.5	-1.50	+0.18	-0.1	-0.04
-0.5	0	0	0.1	-0.4	-1.95	-0.14	+0.2	+0.02
0.9	0	0	0.6	1.5	-1.60	+0.29	-1.0	+0.16
0.1	0	0	0.3	0.4	-1.58	+0.0[illegible]	-1.2	+0.09
-0.4	0	0	0.2	-0.2	-1.67	-0.10	-1.1	+0.04
-0.8	0.1	0	0	-0.7	-1.57	-0.23	-0.7	0
-0.2	0	0	0.2	0	-1.60	-0.08	0	+0.06
0	0	0	0.4	0.4	-2.30	-0.02	+0.1	+0.12
-0.1	0	0	0.4	0.3	-2.32	-0.01	+0.2	+0.11
-0.6	0	0	-0.1	-0.7	-1.87	-0.18	0	-0.04
0.5	0	0	0.2	0.7	-1.90	+0.15	+0.8	+0.06
0.9	0	0	0	0.9	-1.27	+0.27	-0.9	0
-0.2	0	0	-0.3	-0.5	-1.36	-0.04	-0.8	-0.10
1.8	5.8	0.3	0.6	5.5	-1.38	+5.05	-1.8	+0.18
2.1	6.5	0.3	0.9	5.0	-1.50	+6.00	+3.5	-0.24
2.1	6.7	0.3	-0.5	5.6	-1.50	+6.30	-0.4	-0.13
0.3	5.8	0.3	-0.3	3.1	-1.28	+4.20	-0.6	-0.09
2.9	6.2	0.3	0.8	7.1	-1.43	+6.02	-2.6	-0.25
1.4	5.8	0.3	0.2	4.7	-1.37	+4.88	-2.3	+0.06
1.9	6.0	0.3	0.2	5.4	-1.32	+4.73	-2.5	+0.05
1.1	5.8	0.3	0.1	4.3	-1.40	+4.65	-2.2	+0.01
0.6	5.9	0.3	-0.4	3.4	-1.47	+4.36	-1.7	-0.10
1.0	5.8	0.3	-0.3	3.8	-1.40	+4.21	-2.0	-0.10
0.9	5.9	0.3	-0.2	3.8	-1.60	+4.36	-2.3	-0.06
1.6	6.0	0.3	0	4.9	-1.43	+5.15	-2.3	+0.01

tion to the
unt for the
did.

component
scussed

FOLDOUT

PRECEDI

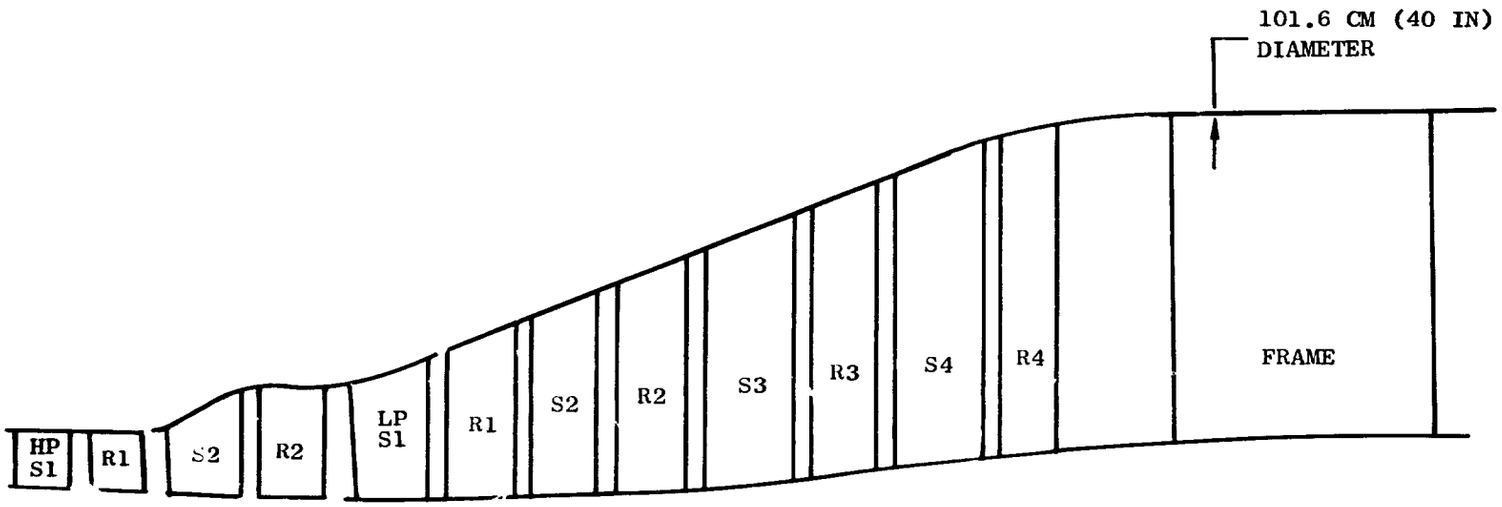

HP TURBINE

DELTA ENTHALPY = 548 KJ/KG (235.6 BTU/LB)

AV. PITCH DIAMETER = 63 CM (24.8 IN)

LP TURBINE

DELTA ENTHALPY = 399 KJ/KG (171.7 BTU/LB)

SPEED = 4460 RPM

AV. PITCH DIAMETER = 73.7 CM (29 IN)

WORK COEFFICIENT = 1.69

Figure 28 Nominal Turbine Flowpath for 23:1 Pressure Ratio Advanced Compressor

For both series of engines, the variation of core compressor efficiency with number of compressor stages was the major component performance trend affecting engine uninstalled performance. As shown previously in Figures 12 and 15, core compressor efficiency varied by about one point over the range of number of stages studied, with the lowest efficiencies being for the designs with the fewest stages and the highest speeds. High pressure turbine efficiency, however, was essentially constant for all configurations within each series, since rotative speeds were sufficiently high in all cases that aerodynamic loading effects in the turbine were negligible. Although the unboosted 23:1 pressure ratio core compressors had polytropic efficiencies that were slightly lower than those of the 14:1 pressure ratio compressors, the higher efficiency of the two-stage turbine used to drive the unboosted compressors more than offset this condition. As seen in Figure 29, the resulting uninstalled specific fuel consumption data show that the unboosted engines had an advantage over the boosted engines and that, in general, the compressors with the fewest stages gave the poorest fuel consumption.

As is also shown in Figure 29, both engine types have similar installed drag values. The trend toward reduced drag at low number of compressor stages is a consequence of reductions in overall engine length. For a given engine type the improvement in installed drag obtained as the number of compressor stages was reduced nearly offsets the increase in bare engine specific fuel consumption.

Uninstalled engine weight and cost trends versus number of compressor stages are shown in Figure 30 for the 147,000 n (33,000 lb) thrust engine size. The engine weight for the unboosted engines was greater than for the boosted engines primarily because of the use of a two-stage high pressure turbine. The fact that the turbine weight increased rapidly with rotative speed was responsible for the increase in bare engine weight as the number of compressor stages was reduced. Bare engine cost was reduced as the number of compressor stages was reduced, however.

Weight and cost trends for engine installation items (such as the nacelle, pylon, and thrust reverser) are shown in Figure 31. Both weight and cost for engine installation were reduced as the number of compressor stages, and thus engine length, was reduced. The reduction in installation weight nearly counteracted the increase in bare engine weight with fewer compressor stages shown in Figure 30. For unboosted engines, for example, the minimum bare engine weight is obtained by using the best 11-stage compressor, Configuration 26b2. If the best 9-stage compressor (Configuration 26d5) were used, this minimum bare engine weight would be exceeded by 23 kg (50 lbs). However, the installation-related weight of the engine with the nine-stage compressor is 18 kg (40 lb) less than that of the engine with the 11-stage compressor, thus nearly offsetting the bare engine weight penalty resulting from use of the nine-stage compressor.

The final significant variable in the engine systems evaluation was maintenance cost. Although compressor blading maintenance cost due to erosion did decrease slightly as the number of compressor stages was reduced, the cost difference was not significant because each configuration was designed to have a similar blade life. Remaining engine maintenance costs increased slightly with an increase in number of compressor stages due to a corresponding increase in the number of stator hub seals, abradable rotor tip

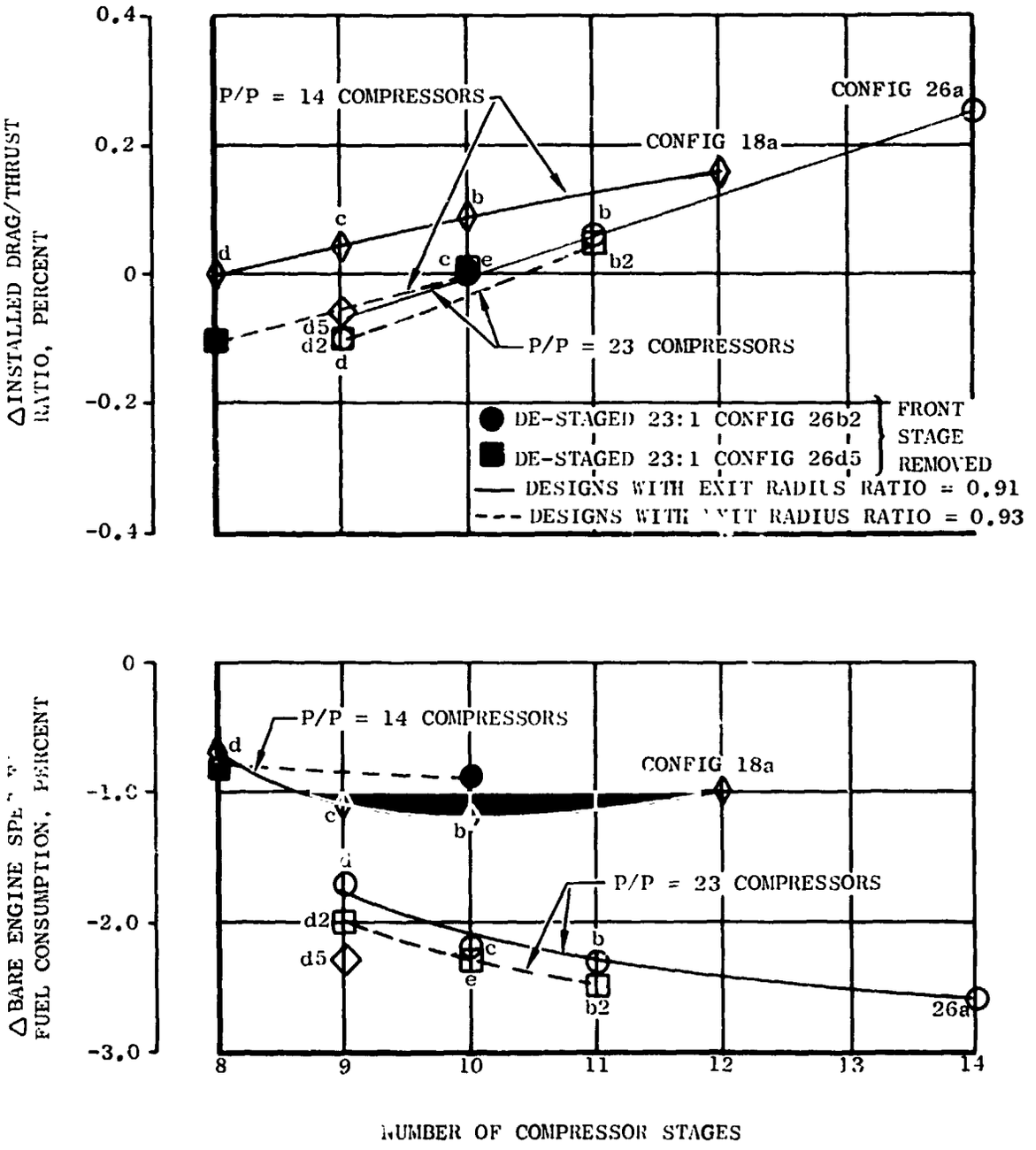

Figure 29 Effect of Number of Compressor Stages on Bare Engine Specific Fuel Consumption and Installed Drag

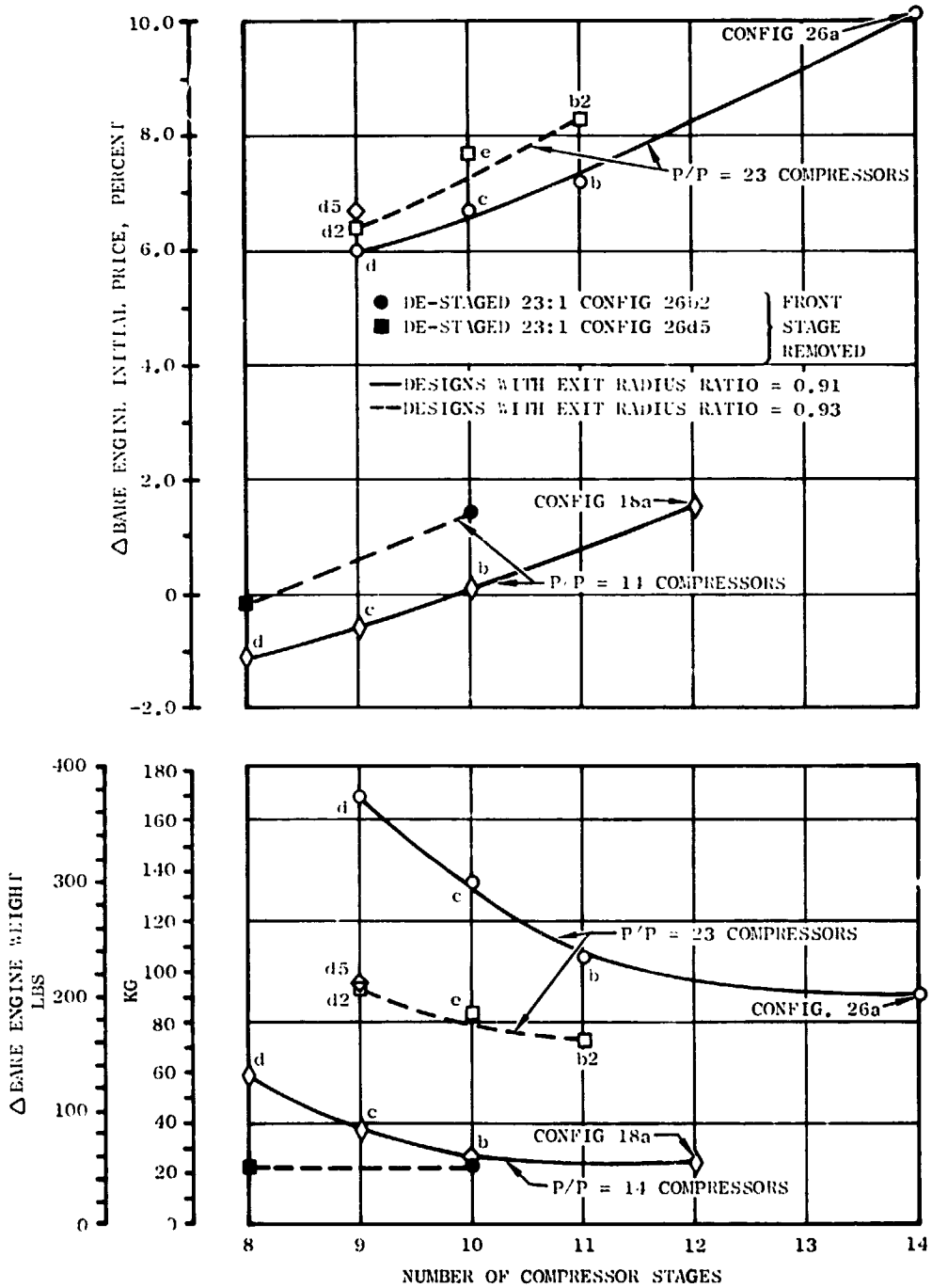

Figure 30 Effect of Number of Compressor Stages on Bare Engine Weight and Price (Design Size)

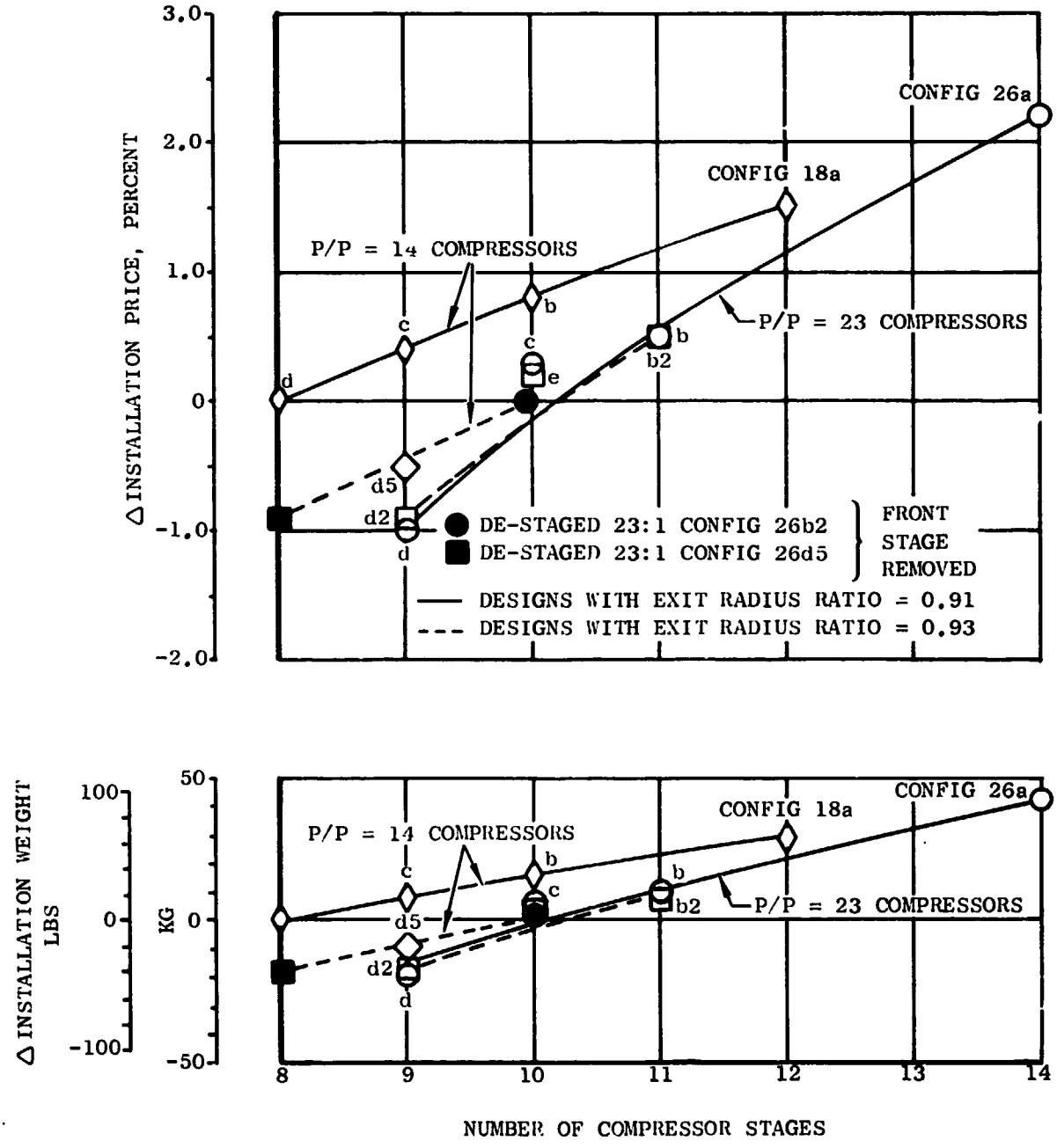

Figure 31 Effect of Number of Compressor Stages on Installation Weight and Price (Design Size)

liners, etc., that would be required. This trend was accounted for by the direct relationship of maintenance costs with engine initial price. The unboosted engine maintenance costs were significantly higher than those for the boosted engine due to the additional high pressure turbine stage.

Economic and fuel usage results for engines using the high-efficiency compressors defined in the refined screening study have been presented previously in Figure 14. As discussed in a previous section, Further Studies of High Efficiency Compressors, the principal results were that the unboosted engines had the lowest fuel consumption, while the boosted engines had the best economic merit factors. It was also found that no strong preference could be seen for a particular number of compressor stages for either engine type, as several compressors could be found in each case that gave near-optimum performance. Direct operating cost considerations slightly favored use of the fewest possible compressor stages, but fuel usage considerations favored selection of a less highly loaded compressor. In order to cover the spectrum of engine types and a range of near optimum number of stages for a given pressure ratio, the nine-stage 14:1 pressure ratio compressor and the nine-stage and 11-stage 23:1 pressure ratio compressors (Configurations 18c, 26d5, and 26b2, respectively) were selected for further detailed design studies.

DETAILED DESIGN STUDY

Three of the most promising compressors, identified in the refined screening study discussed above, were selected for more detailed design studies. Compressor aerodynamic and mechanical design refinements were made to each configuration,and the turbines used in each engine were evaluated as well. Finally, revised engine merit factors were computed which reflected the results of these detailed studies. All three of the turbines were examined in more detail, but only the turbine for the 9-stage 14:1 pressure ratio compressor, Configuration 18c, was changed. The high pressure turbine diameter was reduced slightly from that used in the screening study in order to better match the high rotational speed of this configuration. Turbine velocity diagram data and performance estimates were then made for the turbines of the three engine configurations. The principal result obtained from the turbine detail design analysis was that an increase in cooling flows was required for the two-stage high pressure turbines compared to those used in the screening study.

Component weight, relative price data, and relative maintenance costs for the three selected configurations were reevaluated using the same methods as discussed in the previous section, Parametric Screening Studies. The unboosted engine component and maintenance costs were determined to be slightly lower relative to the boosted engine than was determined in the screening study.

A summary of final engine characteristics for the three selected compressors is presented in Table XIII. Data are also given for the 10-stage 23:1 pressure ratio compressor recommended for further development, plus a de-staged version of this compressor having nine stages and a 14:1 pressure ratio. Configuration 18c was selected as the reference configuration for this comparison, since it had the best direct operating cost and return on investment of all the configurations studied. While the unboosted engines enjoyed a specific fuel consumption and fuel usage advantage over the boosted engines, they were at

Table XIII. Summary of Engine Characteristics and Engine Evaluation Results (with Erosion Effects).

Note: Design Size Engine Installed Thrust at Max Climb = 36,900 n (8300 lb)

Engine Characteristics (Design Size Engine)

					"De-Staged"
Compressor	18C	26b2	26d5	26e2	26e2
Number of Compressor Stages	9	11	9	10	9
Compressor Pressure Ratio	14	23	23	23	14
Bare Engine Thrust (F_N) n (lb) (36k/0.80/+18° Max Climb)	38,900 (8740)	38,900 (8740)	38,900 (8740)	38,900 (8740)	38,900 (8740)
Installed Drag/F_N at Max. Climb, %	5.0	5.1	5.0	5.0	5.0
Δ Installed Specific Fuel Consumption,% (35k/0.80/+18° Max Cruise)	Base	-1.1	-1.1	-1.1	+0.1
Bare Engine Weight, kg (lb)	2009 (4430)	2073 (4570)	2109 (4650)	2068 (4560)	1978 (4360)
Installation Weight, kg (lb)	1406 (3100)	1419 (3130)	1397 (3080)	1406 (3100)	1383 (3050)
Δ Bare Engine Price, %	Base	6.0	4.0	3.0	1.0
Δ Installation Price, %	Base	1.0	0.0	0 0	-0.4

Engine Evaluation Results (Mission Size Engine Used in Transcontinental Trijet Aircraft)

Δ Direct Operating Cost, %	Base	0.84	0.62	0.66	0.03
Δ Return on Investment, %	Base	-0.24	-0.16	-0.17	0.0
Δ Fuel Usage, %	Base	-0.90	-0.91	-0.97	-0.02
Δ Installed Specific Fuel Consumption, % (35k/0.80/+18° Max Cruise)	Base	-1.06	-1.09	-1.05	0.13
Δ Total Weight kg (lb)	Base	42(92)	48(106)	-31(69)	-34(-75)
Δ Total Price, %	Base	4.1	2.2	3.0	0.80
Δ Compressor Blade Maint. Cost, $/FL Hr.	Base	-0.04	-0.31	-0.20	-0.10
Δ Total Maint. Cost $/FL Hr.	Base	3.45	2.90	3.18	0.24

an economic disadvantage. These results were consistent with those of the screening study; however, the differences between the boosted and unboosted engines were reduced as a result of the more detailed analysis. The direct operating cost advantage of the boosted engines was due to lower engine price and maintenance costs, while weight and compressor blading erosion effects were negligible. The fuel usage advantage of the unboosted engines was due primarily to the specific fuel consumption advantage attributed to the higher efficiency of the two-stage high pressure turbine.

ENGINE SYSTEM MERIT FACTORS SENSITIVITY STUDY

Since there is some unavoidable degree of uncertainty in the estimated performance levels of the various components, sensitivity studies were conducted to determine the effect of variations in component performance, weight, and cost on the engine evaluation results. Several conclusions were drawn from the sensitivity studies. The first conclusion related to the engine evaluation's sensitivity to compressor efficiency: Changes in compressor efficiency of two to three points would be required in order to change the relative ranking of the configurations. Since the compressor efficiency model is expected to predict the efficiency potential of each configuration to within ± 1.0 point, it is not expected that the trend of the engine evaluation results would be influenced by uncertainties in compressor efficiency. The second conclusion was relative to the effect of high pressure turbine efficiency on the boosted versus unboosted engine comparison. It was found that a relative shift in the attainable efficiency of the single versus two-stage high pressure turbine of about three points was required to change the trend of the direct operating cost or return on investment results, while an approximate 1.5 point shift was required to change the trend of the fuel usage results. The result was that the single-stage high pressure turbine efficiency would have to be about six points lower than that of the two-stage configuration to eliminate the direct operating cost and return on investment advantage of the boosted engine. Conversely, the single-stage turbine efficiency would have to be within 1.5 points of that of the two-stage high pressure turbine for the boosted engine fuel usage to approach that of the unboosted engine. The third conclusion was relative to the impact of fuel cost, engine weight, and compressor price on the evaluation results. It was found that fuel costs of 18.5 and 21.1 cents per liter (70 and 80 cents per gallon), with all other costs held at 1974 levels, were required for the single-stage and two-stage turbines, respectively, to eliminate the economic advantage of the boosted engine. Similar lack of sensitivity to uncertainties in engine weight and compressor price were obtained. Therefore, it was concluded that anticipated uncertainties in these parameters would not be expected to change the trend of the results.

ENGINES USING THE RECOMMENDED COMPRESSOR CONFIGURATION

An improved version of the 10-stage 23:1 pressure ratio compressor identified in the refined screening study, Configuration 26e2, was selected as the design recommended for further development. A layout of an unboosted engine using this recommended compressor is shown in Figure 32. Weight, price, and performance factors used in the evaluation of this engine and of a boosted engine using a de-staged version of this compressor are also presented in Table XIII, along with the engine evaluation results. These results are compared to the results for the boosted engine using the nine-stage, Configuration 18c, compressor. The data indicate that an unboosted engine using the recommended compressor would have a direct operating cost comparable to one using the nine-stage compressor, Configuration 26d5, and a slightly lower fuel usage than engines using either the nine-stage or 11-stage compressors that were examined in the detailed design study phase of the program.

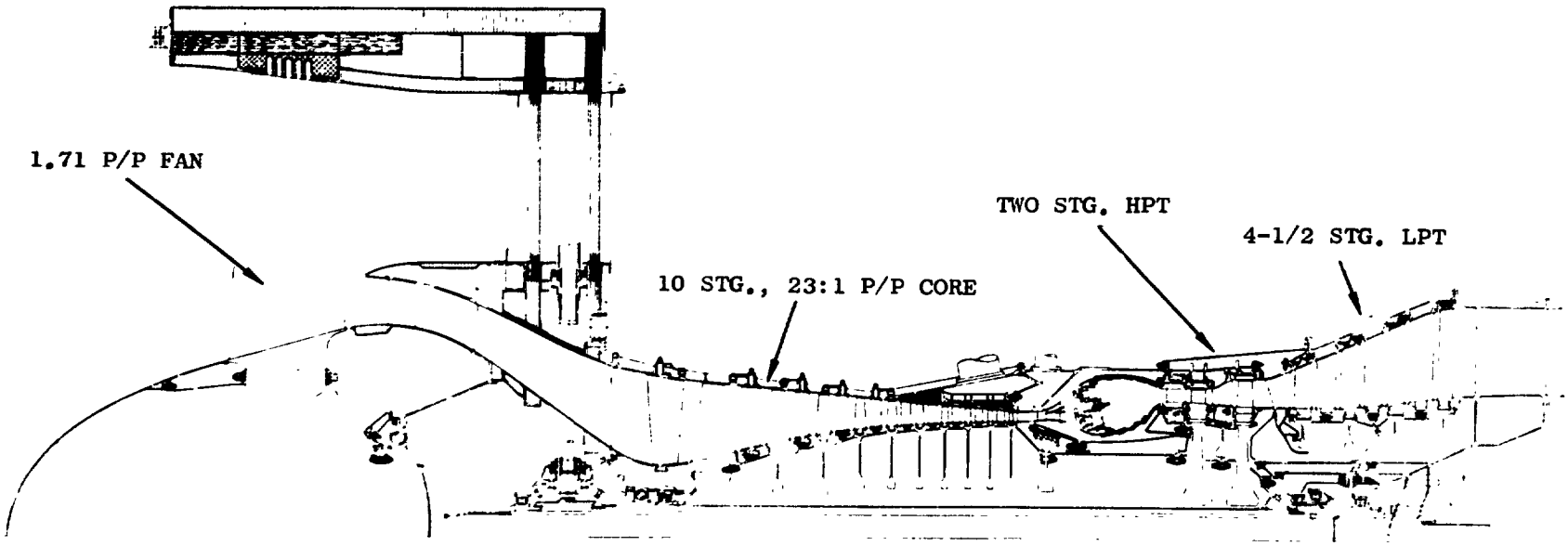

Figure 32 Layout of Engine Incorporating Recommended AMAC Compressor, Configuration 26e2

CONCLUSIONS AND RECOMMENDATIONS

PARAMETRIC SCREENING STUDY FINDINGS

The Parametric Screening Study effort identified a number of factors leading to high core compressor efficiency for the general class of compressors considered:

1. Low inlet radius ratio is beneficial.

2. Medium levels of stator exit swirl, 10° - 16°, lead to high efficiency.

3. Low inlet and exit axial Mach numbers improve overall compressor efficiency.

4. Shock losses do not significantly penalize overall efficiency for first rotor tip Mach numbers below about 1.4.

5. Use of fewer stages does not significantly penalize overall efficiency until increases in speed raise first rotor tip Mach numbers above about 1.4.

6. High exit radius ratio can be beneficial for efficiency provided it aids in reducing an excessively high tip speed. The optimum exit radius ratio is likely to increase as the number of compressor stages is reduced.

7. Medium aspect ratios give best overall efficiency. Low values cause increased end-wall losses, while high values require either high tip speed or more stages to maintain stall margin.

The effects of the advanced technology assumptions made for this study were:

1. Relative ranking of compressors is not greatly affected even if "current" rather than "advanced" technology is assumed.

2. "Advanced" aerodynamic and mechanical technology assumed in this study is responsible for a 2.0 - 2.5 point increase in predicted efficiency compared to "current" technology compressors.

Other findings of the parametric screening studies related to the overall engine system were:

1. Fewer stages give less expensive and shorter compressors, but core engine weight does not necessarily decrease and engine acceleration time may increase.

2. Blade erosion life can be improved significantly with virtually no performance penalty if low-life stages are identified and improved. Erosion itself has only a small effect on average engine economics, provided it does not become the reason that an engine must be removed prematurely from the airplane for overhaul.

3. Boosted engines have better direct operating cost but poorer fuel usage than unboosted engines, mainly because boosted engines use less expensive, but less efficient, single-stage high pressure turbines compared to the two-stage turbines in unboosted engines. While the magnitudes of these differences are relatively small, they persist despite any reasonable variations in aircraft mission, turbine efficiency, turbine cost, fuel cost, and compressor cost assumptions.

DETAILED DESIGN STUDIES

Aerodynamic design analysis results were:

1. No severe aerodynamic design problems were identified in any of the three cases studied that might invalidate the estimates of their performance potential.

2. The nine-stage, 23:1 pressure ratio compressor configuration had higher rotor and stator inlet Mach numbers and higher diffusion factors than the 11-stage 23:1 pressure ratio configuration or the nine-stage 14:1 pressure ratio configuration, and thus would be more difficult to develop.

3. Off-design studies of the 23:1 pressure ratio compressor designs indicated that a part-speed stall margin of about 25 percent could be achieved without using bleed in the normal engine operating range, although starting bleed probably would be needed.

Mechanical design analysis results were:

1. No severe mechanical problems were discovered in any configuration. The high rear rim speeds, low inlet radius ratios, two-bearing rotor layout, and medium front rotor blade aspect ratios all were specifically examined and found to be acceptable. Final weight estimates were somewhat higher than in the screening studies, but the estimated weights increased about equally for all three configurations and did not change the relative ranking of the compressors.

RECOMMENDED CONFIGURATION

A 23:1 pressure ratio design was recommended for further development because:

1. It provides an engine having the lowest fuel usage.

2. Lower pressure ratio versions could be derived from this configuration by removing front or rear stages, and the resulting compressors would still be near-optimum for use in boosted engines having excellent economic ratings.

A 10-stage 23:1 pressure ratio compressor was selected as the configuration with the best combination of advantages: high efficiency, low operating cost, low fuel usage, and acceptable development risk.

REFERENCES

1. Koch, C.C. and Smith, L.H., Jr.; "Loss Sources and Magnitudes in Axial-Flow Compressors," Transactions of ASME Journal of Engineering for Power, Vol. 98, Series A, No. 3, July 1976, Page 411

2. Neitzel, R.E., Hirschkron, R., and Johnston, R.P.; "Study of Turbofan Engines Designed for Low Energy Consumption," NASA CR-135053, 1976

3. Ware, T.C., Kobayashi, R.J., and Jackson, R.J.; "High-Tip-Speed, Low-Loading Transonic Fan Stage, Part 3 - Final Report," NASA CR-121263, February, 1974